Equable climates

EPS 231 Climate dynamics
Eli Tziperman

Including slides from Dorian Abbot

56 to 34 Myr ago: Eocene

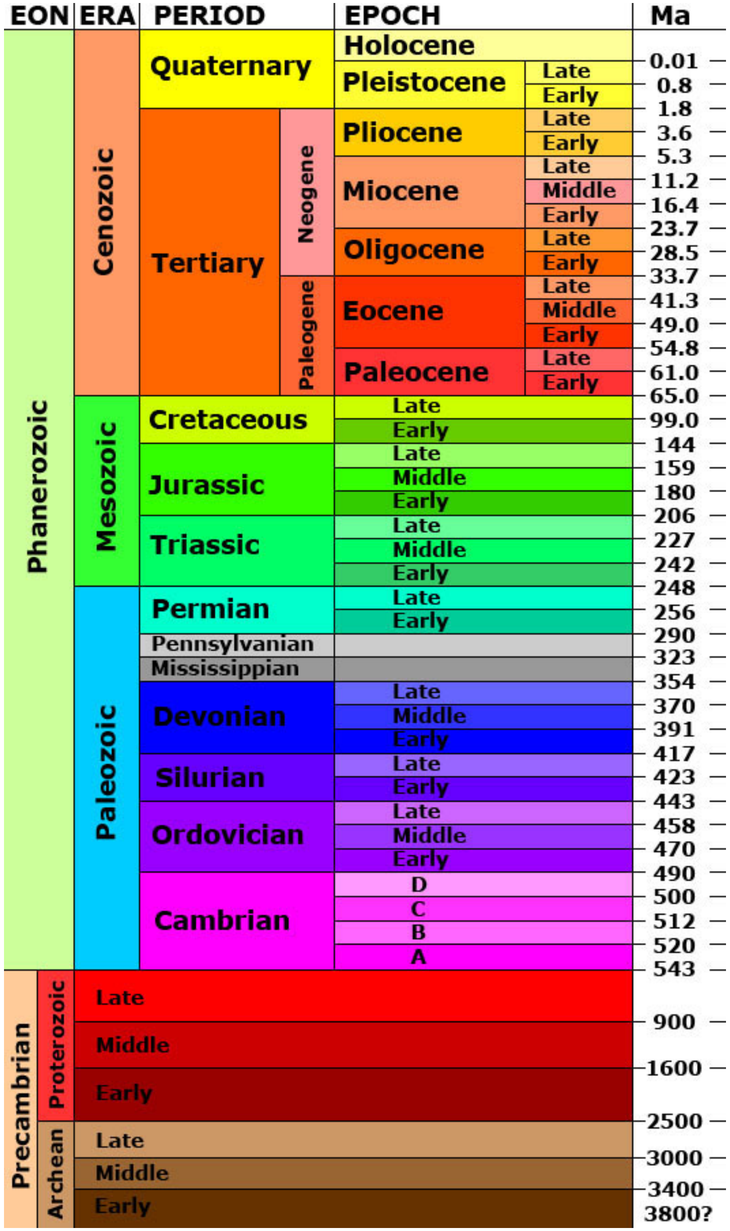

EON	ERA	PERIOD		EPOCH		Ma
Phanerozoic	Cenozoic	Quaternary		Holocene		0.01
				Pleistocene	Late	0.8
					Early	1.8
		Tertiary	Neogene	Pliocene	Late	3.6
					Early	5.3
				Miocene	Late	11.2
					Middle	16.4
					Early	23.7
			Paleogene	Oligocene	Late	28.5
					Early	33.7
				Eocene	Late	41.3
					Middle	49.0
					Early	54.8
				Paleocene	Late	61.0
					Early	65.0
	Mesozoic	Cretaceous		Late		99.0
				Early		144
		Jurassic		Late		159
				Middle		180
				Early		206
		Triassic		Late		227
				Middle		242
				Early		248
	Paleozoic	Permian		Late		256
				Early		290
		Pennsylvanian				323
		Mississippian				354
		Devonian		Late		370
				Middle		391
				Early		417
		Silurian		Late		423
				Early		443
		Ordovician		Late		458
				Middle		470
				Early		490
		Cambrian		D		500
				C		512
				B		520
				A		543
Precambrian	Proterozoic	Late				900
		Middle				1600
		Early				2500
	Archean	Late				3000
		Middle				3400
		Early				3800?

Warm climates 146–34 Myr

Gradual cooling over past 55 Myr

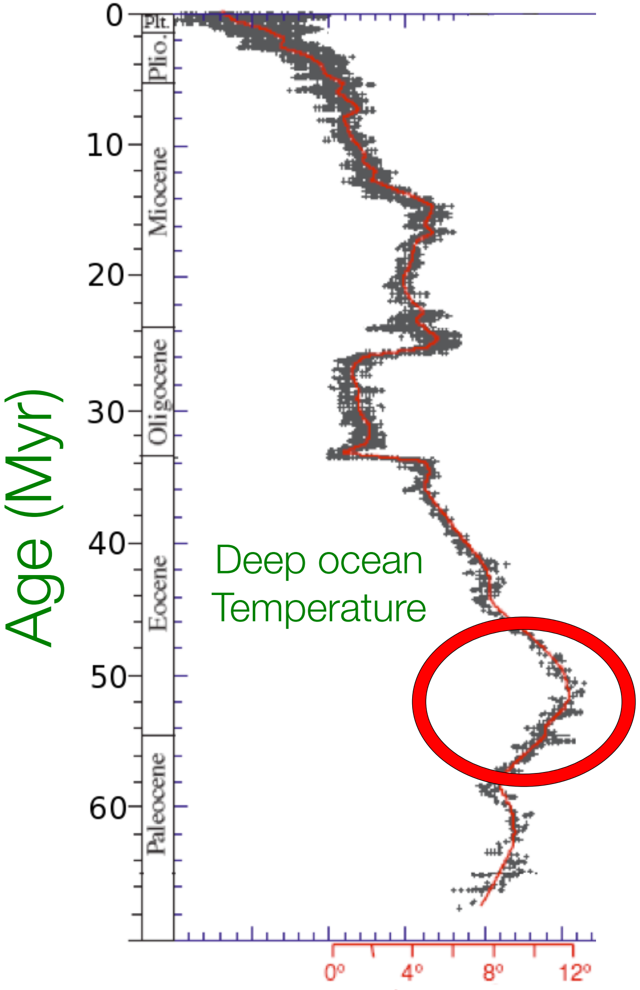

[Zachos et al., 2001]

Equable Climates

Frost-intolerant species in high-latitude continental climate regions

Cretaceous Coastal Environment

Hadrosaurus - **Cretaceous**

Artist: Karen Carr

Cretaceous Marine Environment

Artist: Karen Carr

Eobasileus - Eocene

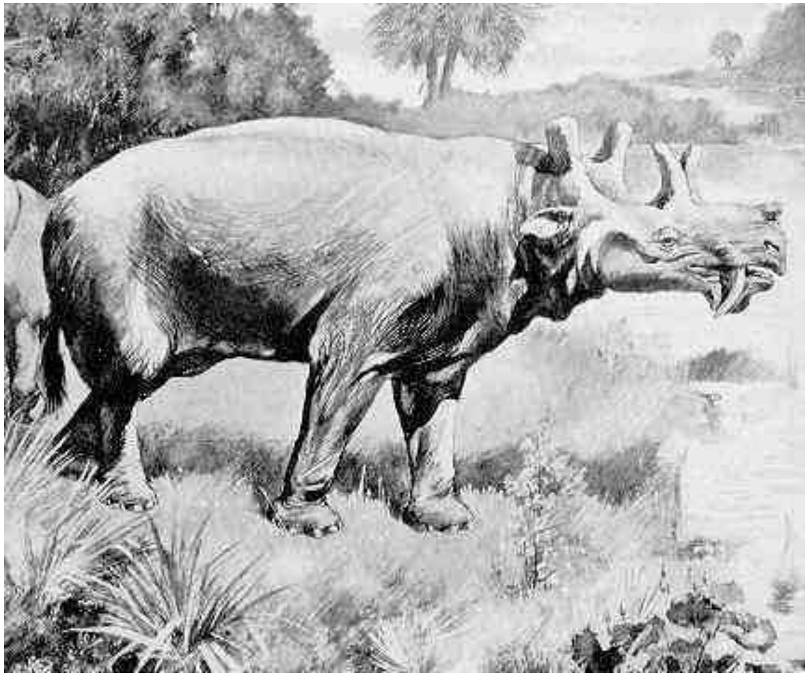

Artist: Charles R. Knight

Eocene Mammals

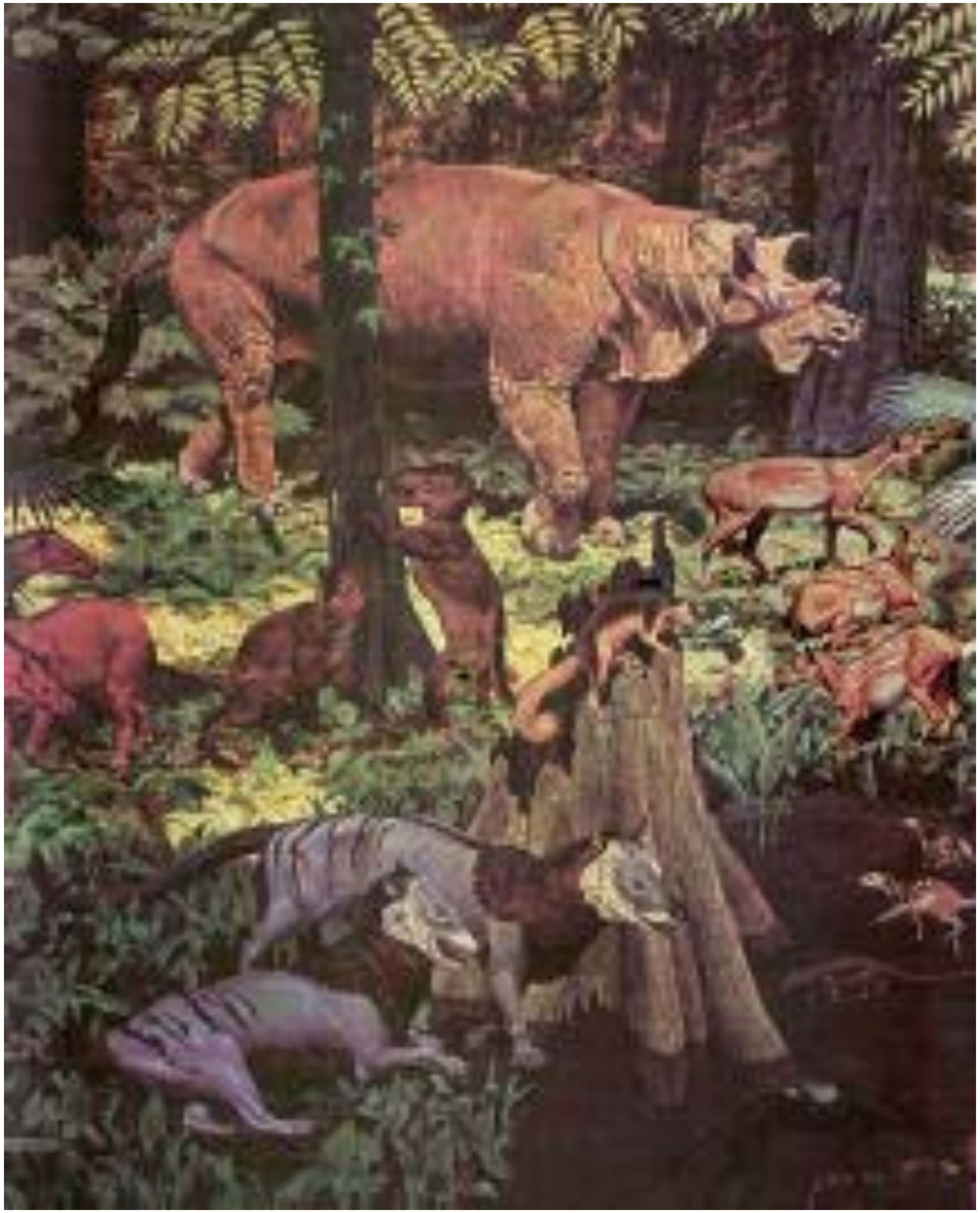

Artist: Jay Matternes

“Equable” climate

1. Surface temperatures at the poles were closer to surface temperatures at the equator.

2. The high latitude seasonal cycle was smaller: winter and surface temperature were closer.

“Hothouse/Equable” climates ~146–34 Ma

Cretaceous Paleocene Eocene

- Higher global mean temperature
- Lower equator-to-pole temperature diff.
- Less high latitude seasonality
- No significant ice
- Tropical SSTs >≈ modern
- Warm deep ocean
- CO_2=500–2,000 ppm?

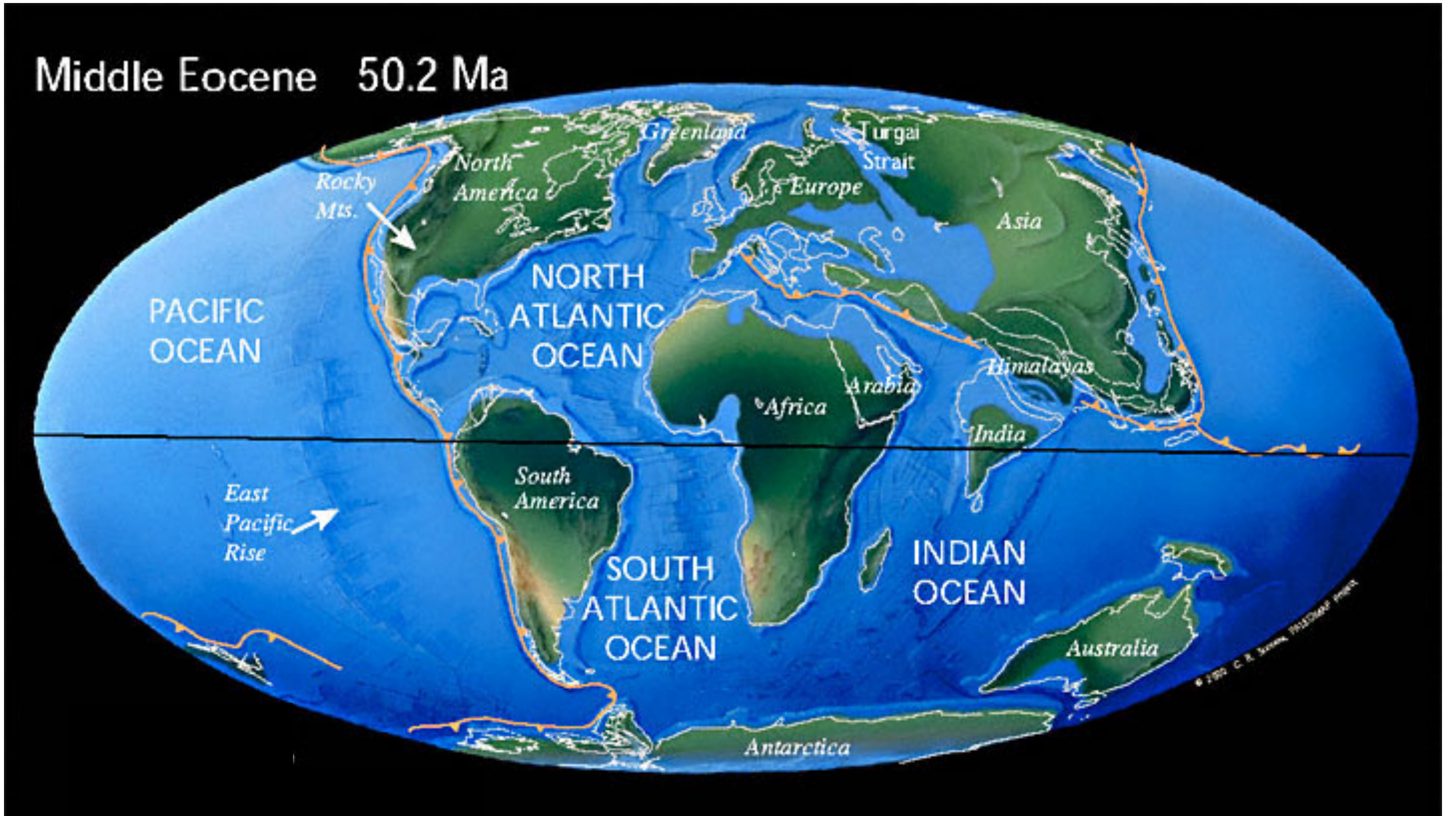

Plant and animal fossils

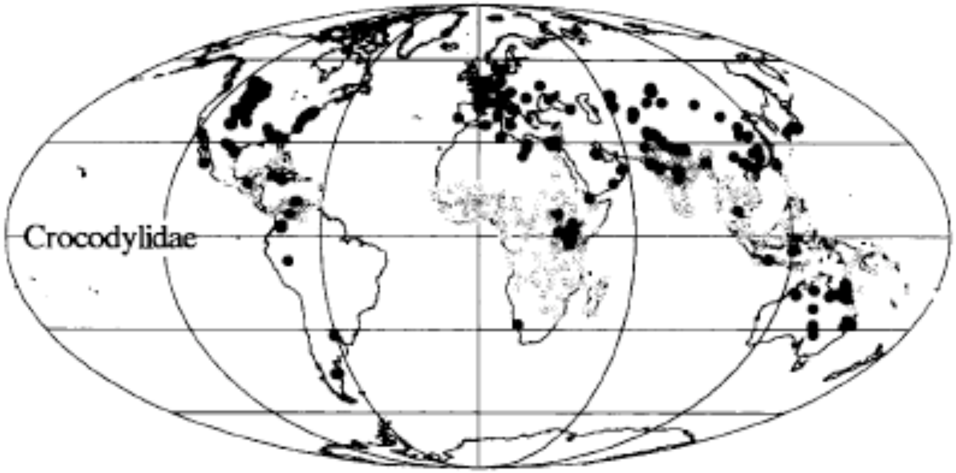

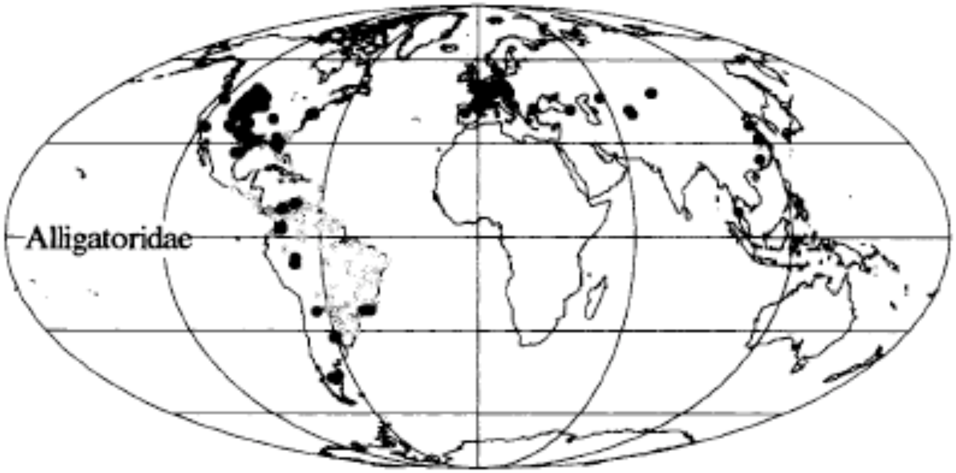

Crocodiles & Alligators today need:
MAT>14.2°C + CMM>5.5°C

MAT: mean annual temperature
CMM: cold month mean

[Markwick, 1998]

Eocene near living relative (NLR) Analysis

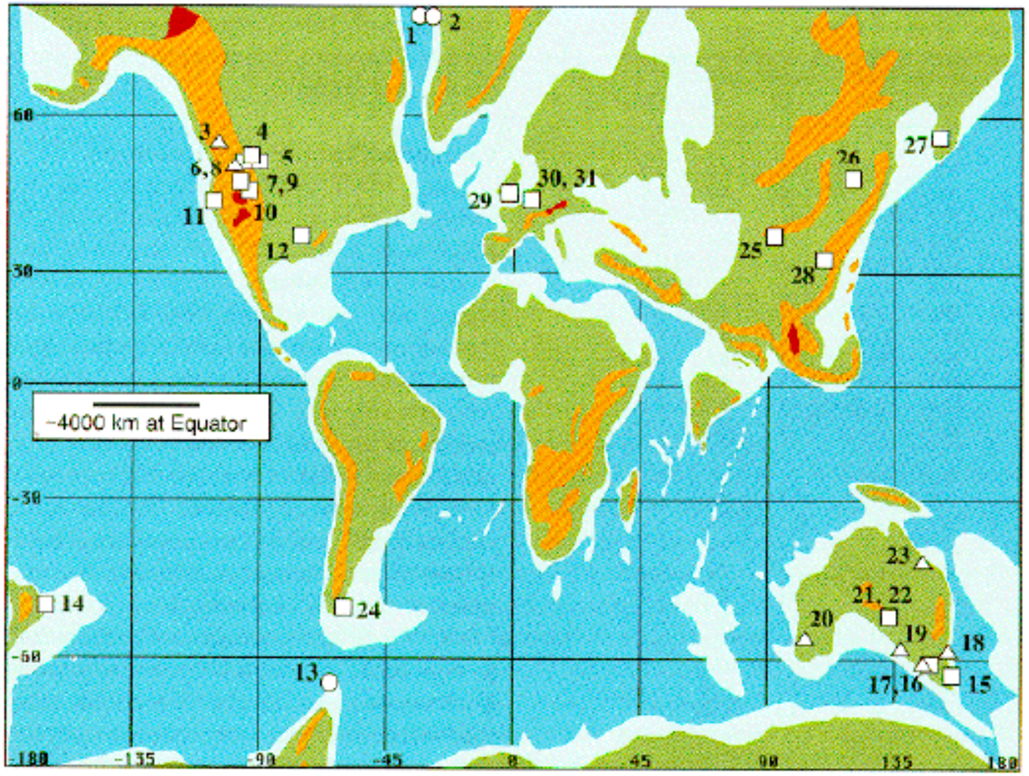

[Greenwood and Wing, 1995]

□ - palms

△ - cycads, gingers, tree ferns

○ - no frost intolerant plants

🟩 - lowlands

🟧 - uplands

🟥 - higher uplands

Leaf Margin Analysis (LMA)

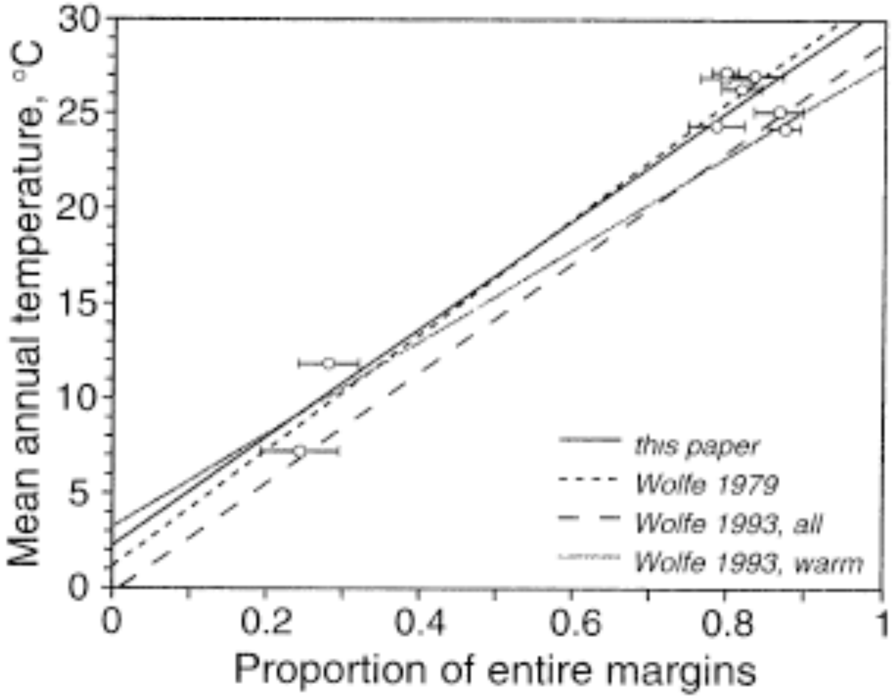

[Wilf, 1997]

Eastern Redbud - Untoothed (Entire Margin)

American Elm - Toothed

“The physiological basis for the MAT vs. leaf-margin correlation has never been adequately demonstrated.” [Wilf, 1997]

δ^{18}O Temperature reconstruction

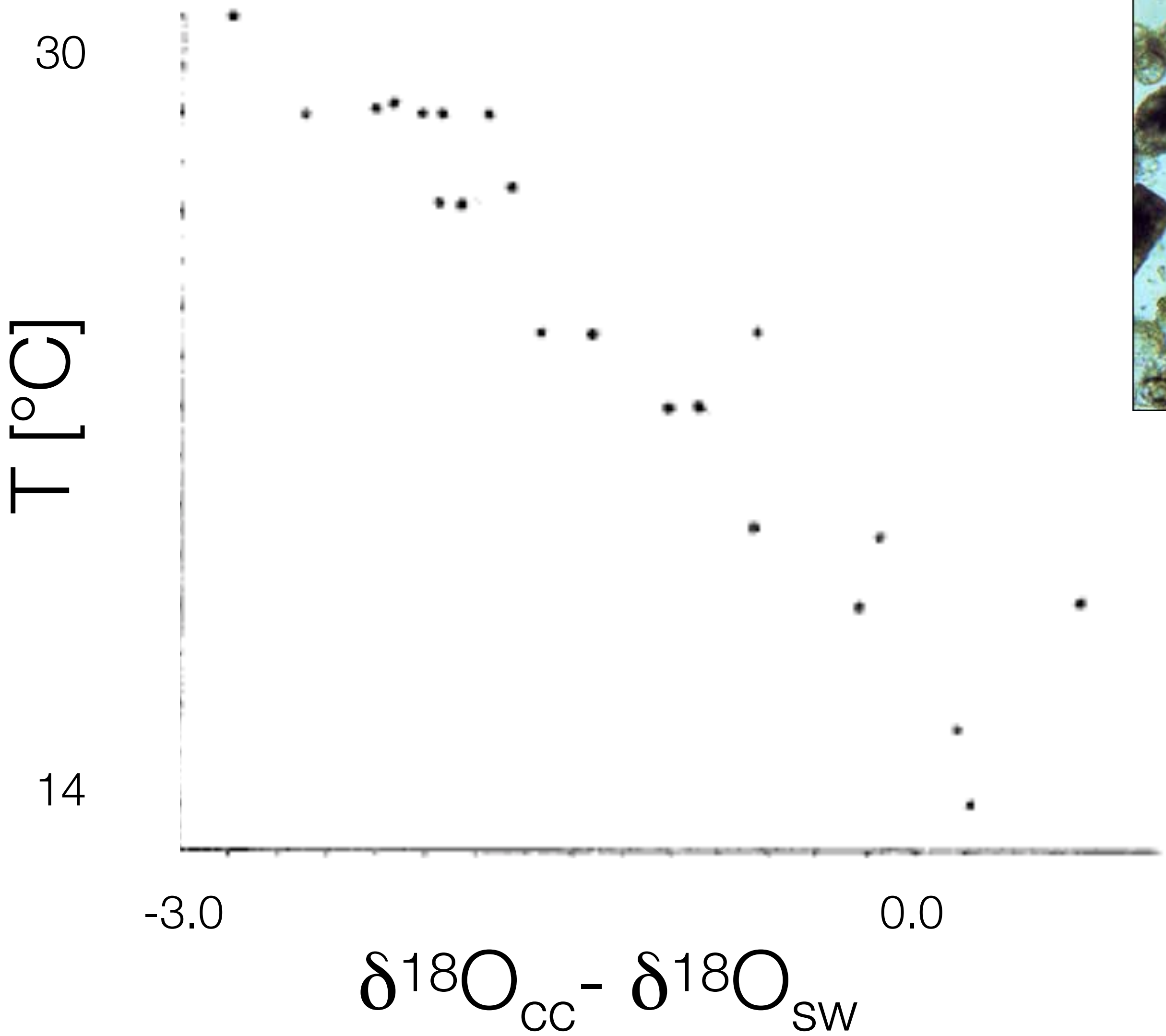

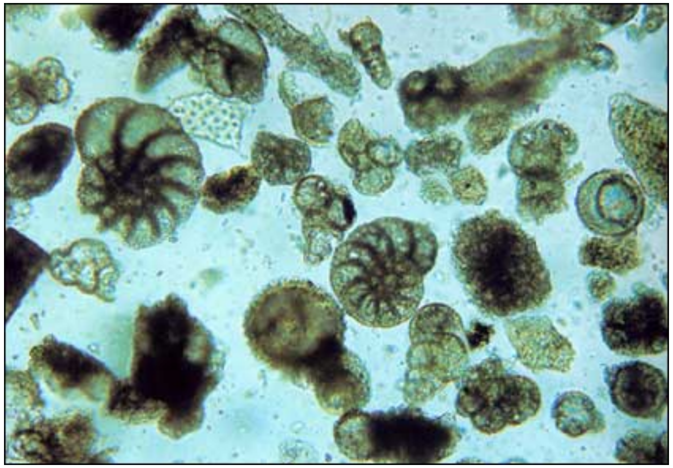

[Erez and Luz, 1983]

Latitudinal temperature distribution

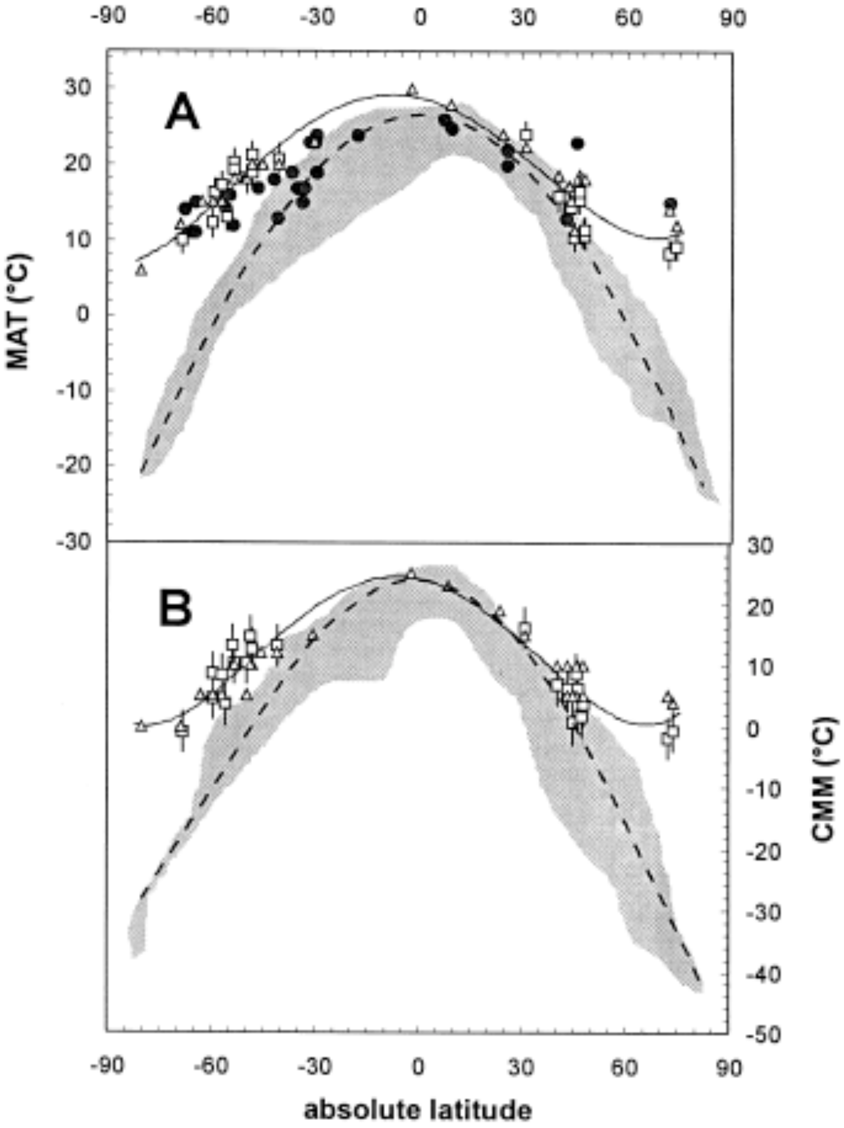

■ - Modern land temp.

● - Eocene SST

△ - Eocene NLR & LMA

□ - Eocene CLAMP

Much lower equator to pole temperature difference than at present

[Greenwood and Wing, 1995]

Re-evaluating planktonic δ^{18}O Data

Late Cretaceous

Middle Eocene

Late Eocene

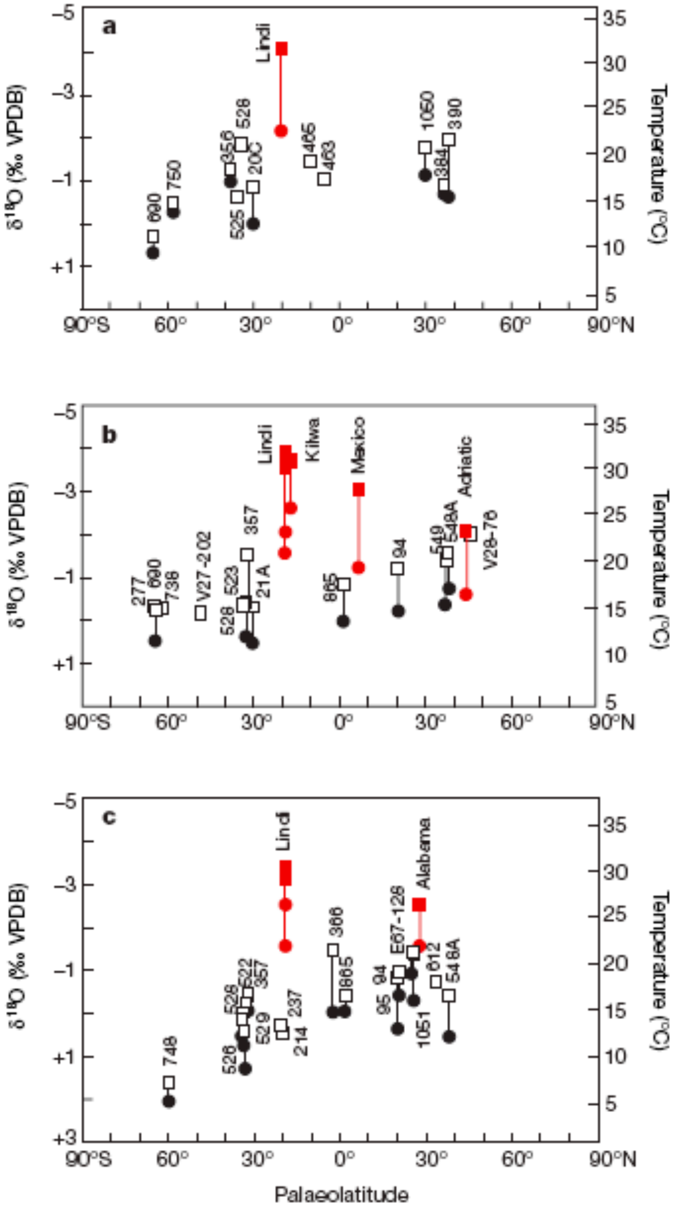

Equator during Eocene not as cool as thought initially

☐-Mixed Layer

○-Intermediate

🟥 -New

■ -Old

[Pearson et al., 2001]

In-class workshop

Consider an energy balance model for the Arctic:

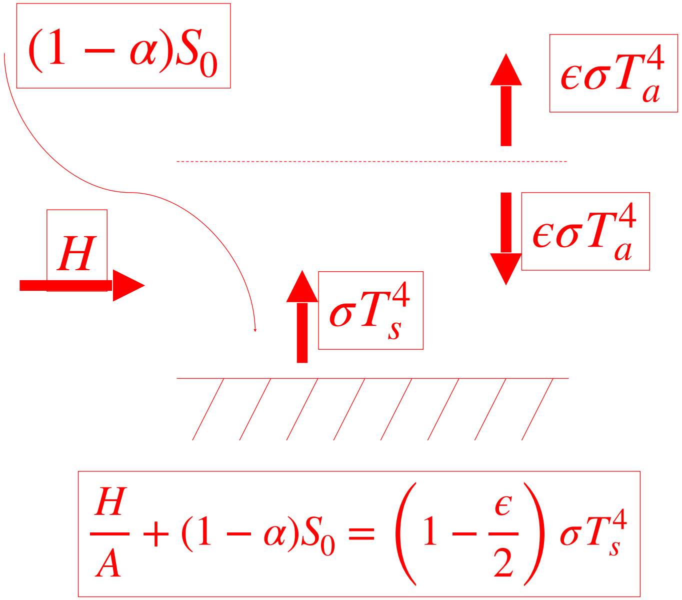

$$\frac{H}{A}+(1-\alpha)S_0=\left(1-\frac{\epsilon}{2}\right)\sigma T_s^4$$

Modern climate:

S_0 (W/m^2)	H [PW]	**ε**	**α**
200	3.5	0.60	0.55

A=area north of 60N

1) Calculate the present-day Arctic temperature from this energy balance.
2) Calculate the changes to the mid-latitude heat transport required to increase the high latitude temperature by 20 °C

Energy balance for the Arctic: Back of the envelope…

Changes required to reduce equator-to-pole temperature gradient by increasing CO_2 or meridional heat fluxes or albedo or long-wave emissivity (clouds!):

Energy-balance model

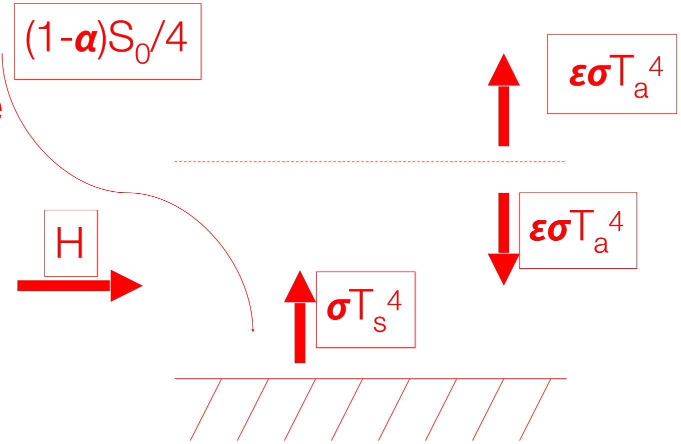

$$H/A+(1-\alpha)S_0/4=(1-\epsilon/2)\sigma T_s^4$$

Modern climate:

T [C]	H [PW]	ε	α
-8.0	3.5	0.60	0.55

Changes required to increase high latitude temperature:

ΔT [◦C]	ΔH [PW]	Δε	$[CO_2]_{dry}$ [ppm]	$[CO_2]_{wet}$ [ppm]	Δα
10.0	1.1	0.20	$X2^5 \approx 9x10^3$	$x2^{2.5} \approx 2x10^3$	-0.15
15.0	1.7	0.28	$x2^{7.5} \approx 5x10^4$	$x2^{3.75} \approx 4x10^3$	-0.23

Proposed mechanisms

Equator-to-pole Hadley cell:

(1)

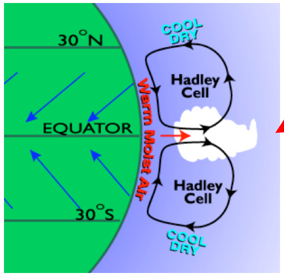

Today

Eocene?
(Like Venus…)

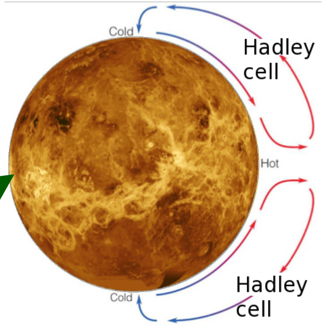

(B. Farrell, 1990)

Proposed mechanisms

Equator-to-pole Hadley cell:

(1)

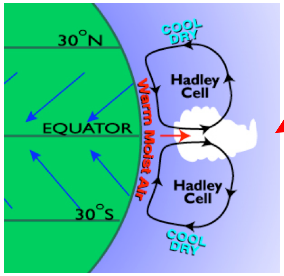

Today

Eocene?
(Like Venus…)

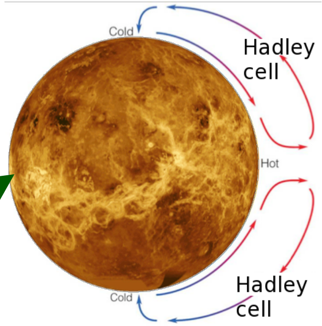

(B. Farrell, 1990)

Polar Stratospheric Clouds (PSCs,15-25 km)

PSCs at dusk over Arctic Sweden

(2)

due to methane: Sloan 1992;
weakening Brewer-Dobson circulation:
Kirk-Davidoff et al. 2002

Proposed mechanisms

Equator-to-pole Hadley cell:

(1)

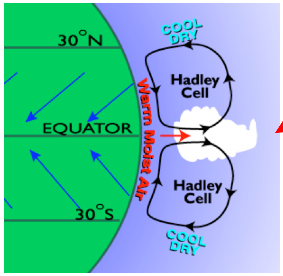

Today

Eocene?
(Like Venus…)

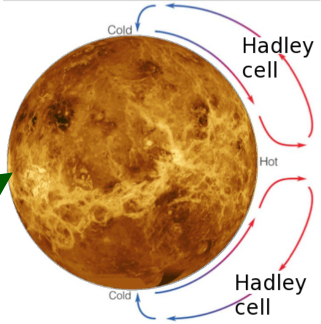

(B. Farrell, 1990)


www.nasa.gov/images/content/65932main_sageii_psc_640x480.jpg

Polar Stratospheric Clouds (PSCs,15-25 km)

PSCs at dusk over Arctic Sweden

(2)

due to methane: Sloan 1992;
weakening Brewer-Dobson circulation:
Kirk-Davidoff et al. 2002

Stronger hurricanes

(3)

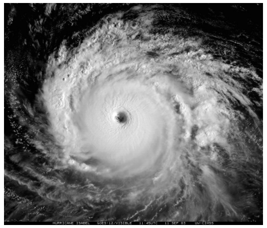

stronger AMOC

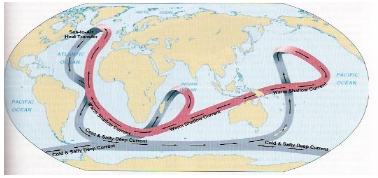

Warmer high latitudes

(K. Emanuel, 2002)

Proposed mechanisms

Breakup of subtropical stratocumulus cloud decks at high SST

Causing albedo decrease and warming of mid-latitudes

Schneider et al 2019, (Bretherton et al)

https://www.shutterstock.com/image-photo/aerial-view-layer-stratocumulus-clouds-369408491

(4)

Proposed mechanisms

Breakup of subtropical stratocumulus cloud decks at high SST

Causing albedo decrease and warming of mid-latitudes

Schneider et al 2019, (Bretherton et al)

https://www.shutterstock.com/image-photo/aerial-view-layer-stratocumulus-clouds-369408491

(4)

(5)

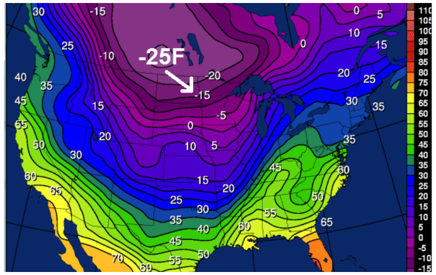

Arctic air suppression over high latitude land

By low cloud forming due to moisture arriving from over warmer ocean

Cronin & Tziperman 2015

Proposed mechanisms

Breakup of subtropical stratocumulus cloud decks at high SST

https://www.shutterstock.com/image-photo/aerial-view-layer-stratocumulus-clouds-369408491

(4)

Causing albedo decrease and warming of mid-latitudes

Schneider et al 2019, (Bretherton et al)

Arctic air suppression over high latitude land

(5)

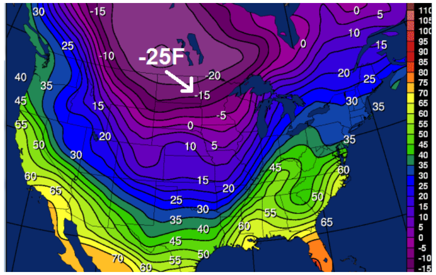

By low cloud forming due to moisture arriving from over warmer ocean

Cronin & Tziperman 2015

Arctic convective cloud feedback

wintertime deep Arctic convection

→ high cloud emissivity/ greenhouse effect → Warmer winter Arctic

(6)

Abbot & Tziperman 2008

Equator-to-pole Hadley cell:

(1)

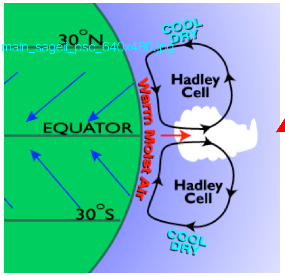

www.nasa.gov/images/content/65932main_sagei_psc_640x480.jpg

Today

Eocene?
(Like Venus…)

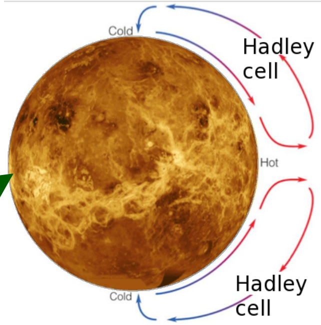

(B. Farrell, 1990)

notes:

- Hadley cell Held/Hou model from Vallis.
- Heuristic equator-to-pole Hadley cell idea based on Farrell (1990).

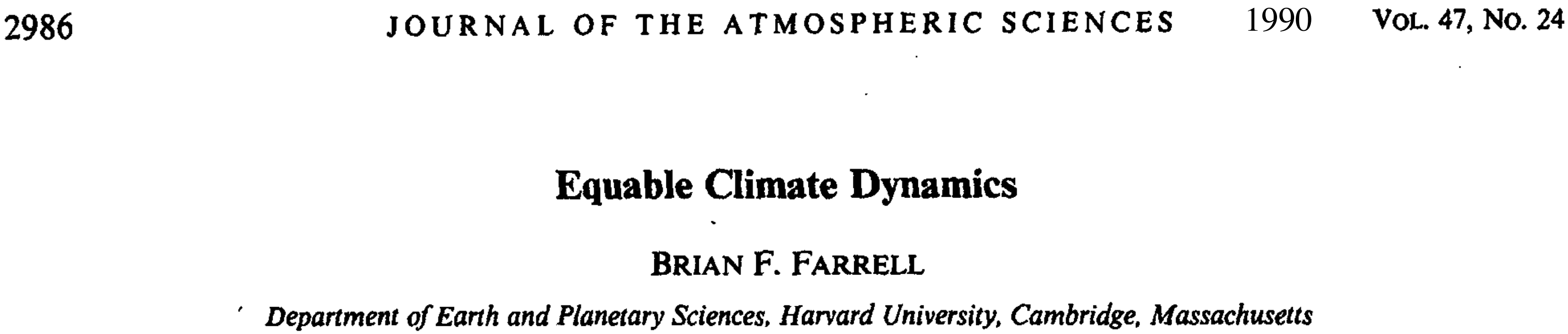

2986 JOURNAL OF THE ATMOSPHERIC SCIENCES 1990 VOL. 47, NO. 24

Equable Climate Dynamics

BRIAN F. FARRELL

Department of Earth and Planetary Sciences, Harvard University, Cambridge, Massachusetts

In-class workshop

Use angular momentum conservation to calculate the subtropical jet speed at 30N

Equator-to-pole Hadley cell in class workshop

Consider the radiative-convective equilibrium temperature profile:

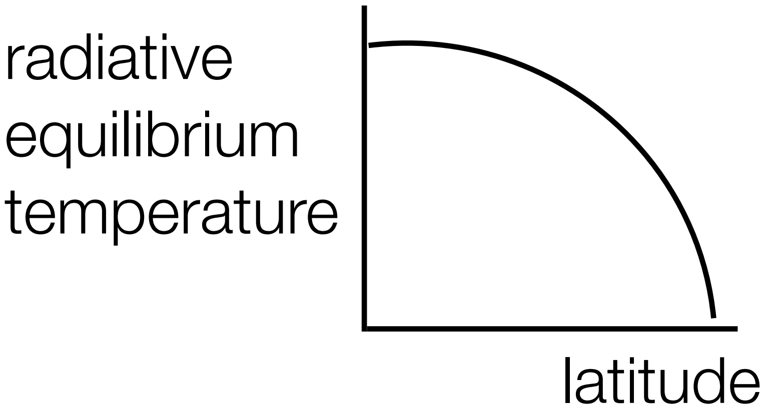

Draw the expected temperature profile including the effects of atmospheric heat transport

Polar Stratospheric Clouds (PSCs,15-25 km)

www.nasa.gov/images/content/
65932main_sageii_psc_640x480.jpg

PSCs at dusk over Arctic Sweden

(2)

due to methane: Sloan 1992;
weakening Brewer-Dobson circulation:
Kirk-Davidoff et al. 2002

Polar stratospheric clouds

PSCs form at very low temperatures, below –78 °C, at 15–30 km height, during winter, in polar areas, within polar stratospheric vortex

wikipedia

PSC, Elverum, Norway.

A type II (water) PSC showing iridescence

Due to their high altitude & Earth surface curvature, PSCs receive sunlight from below the horizon & reflect it to the ground, shining brightly well before dawn or after dusk

Composition: water ice, sulfuric acid H_2SO_4; nitric acid (HNO_3)

Polar stratospheric clouds in equable climate 1.0

Possible methane-induced polar warming in the early Eocene

L. Cirbus Sloan, James C. G. Walker, T. C. Moore Jr, David K. Rea & James C. Zachos **1992**

The proposed feedback:

warmer climate
➡ higher methane CH_4 emissions by anaerobic bacteria from swamps
➡ greenhouse effect in the troposphere & — unlike water — able to make it to the stratosphere (liquid only at –161.5 °C at 1 atm)
➡ oxidizes into CO_2 and H_2O ($CH_4 + 2O_2 = CO_2 + 2H_2O$)
➡ H_2O forms PSCs
➡ further warms the poles.

PSCs: stratospheric temperature & circulation

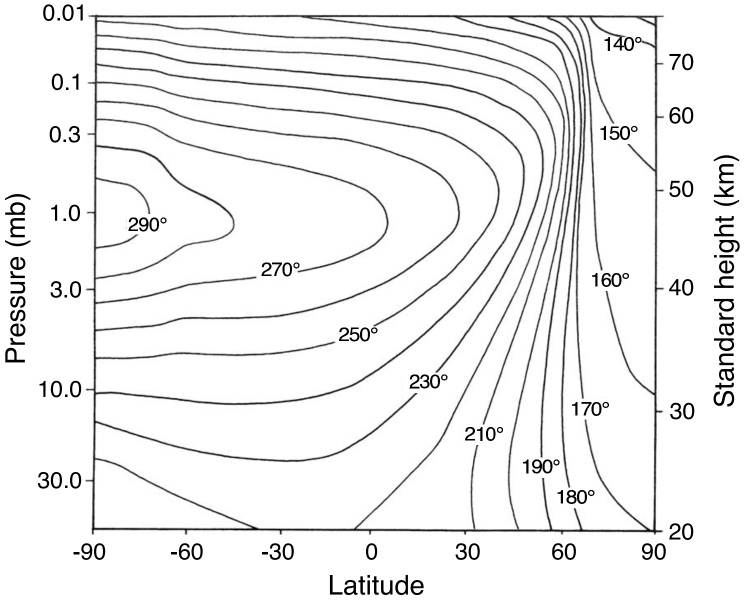

Fig. 13.11 The zonally-averaged radiative-equilibrium temperature in in January. The downwards solar radiation at the top of the atmosphere is given, and the upwards radiative flux into the stratosphere is based on observed properties, including temperature, of the troposphere.[18]

vallis AOFD

PSCs: stratospheric temperature & circulation

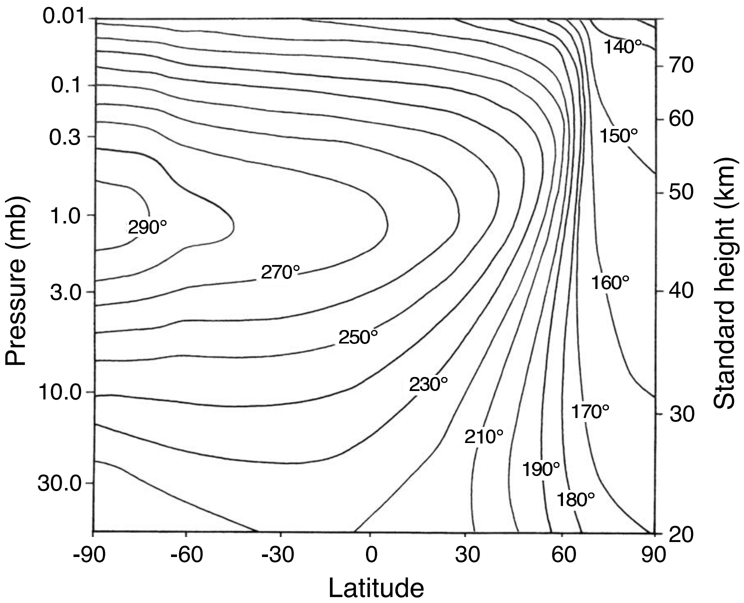

Fig. 13.11 The zonally-averaged radiative-equilibrium temperature in in January. The downwards solar radiation at the top of the atmosphere is given, and the upwards radiative flux into the stratosphere is based on observed properties, including temperature, of the troposphere.[18]

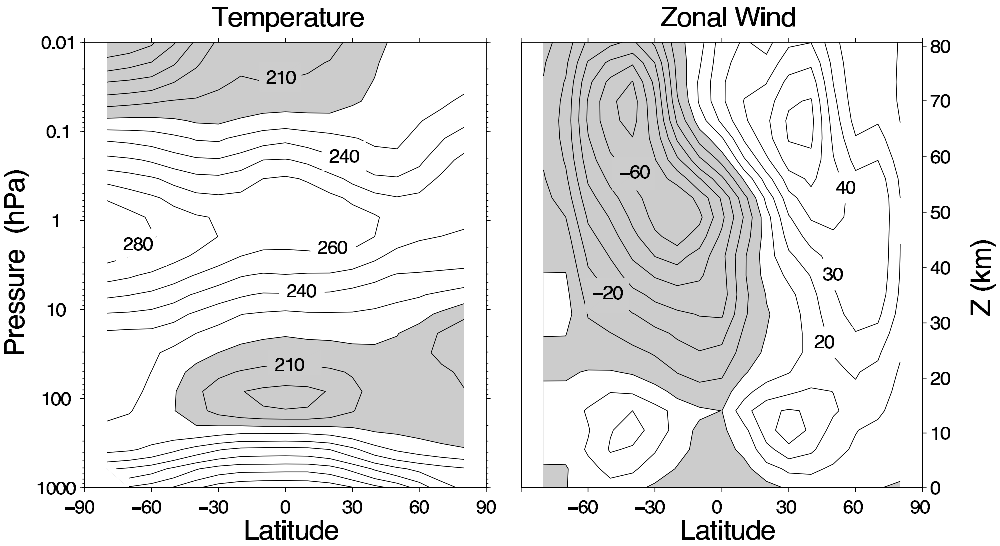

Fig. 13.12 The zonally averaged temperature and zonal wind in January. Temperature contour interval is 10 K, and values less than 220 K are shaded. Zonal wind contours are 10 m s^{1} and negative (westward) values are shaded.[19]

vallis AOFD

PSCs: stratospheric temperature & circulation

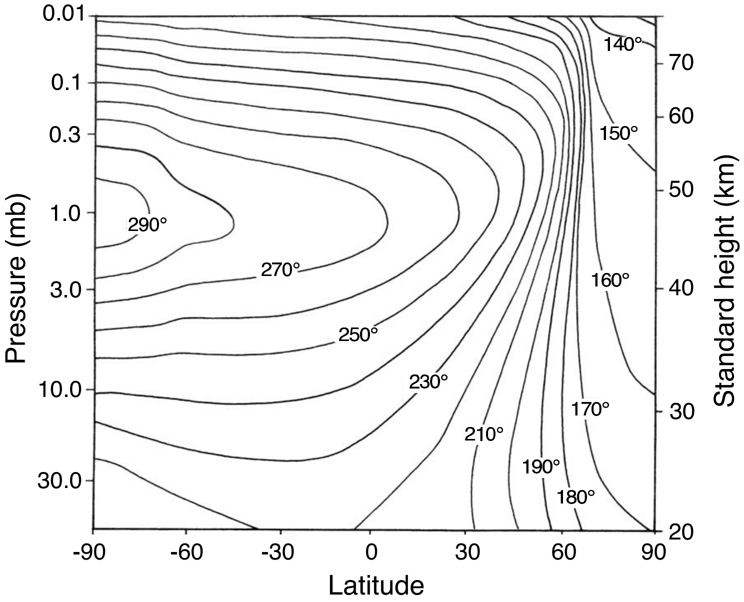

Fig. 13.11 The zonally-averaged radiative-equilibrium temperature in in January. The downwards solar radiation at the top of the atmosphere is given, and the upwards radiative flux into the stratosphere is based on observed properties, including temperature, of the troposphere.[18]

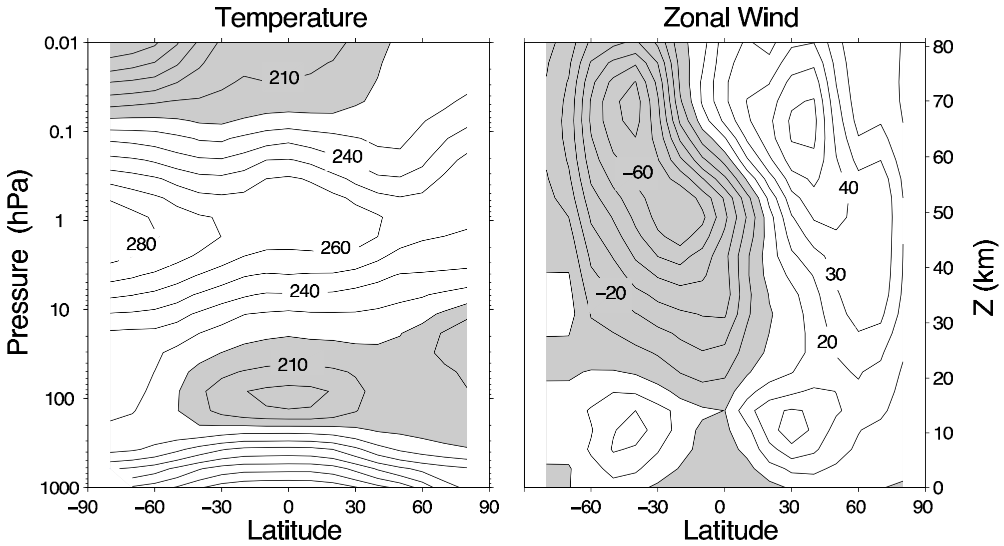

Fig. 13.12 The zonally averaged temperature and zonal wind in January. Temperature contour interval is 10 K, and values less than 220 K are shaded. Zonal wind contours are 10 m s^1 and negative (westward) values are shaded.[19]

Brewer Dobson circulation

Fig. 13.13 The observed mass-weighted streamfunction in the stratosphere, in Sverdrups (10^9 kg s^1). The circulation is clockwise where the contours are solid. Note the stronger circulation in the winter hemispheres, whereas the equinoctial circulation (September) is more inter-hemispherically symmetric.[21]

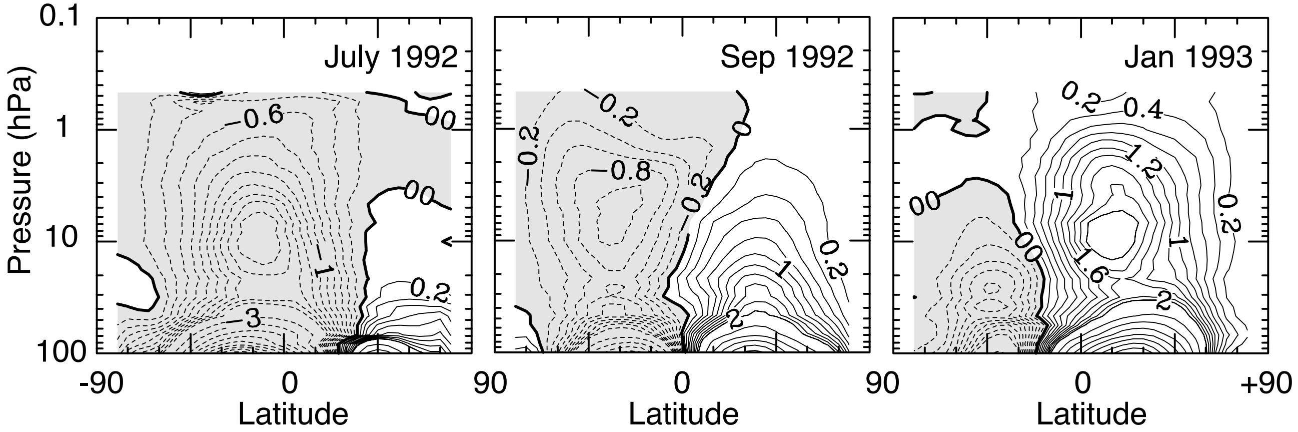

vallis AOFD

Polar stratospheric clouds in equable climate 2.0

On the feedback of stratospheric clouds on polar climate

Daniel B. Kirk-Davidoff, Daniel P. Schrag, and James G. Anderson **2002**

The propose feedback:

warmer climate,
➡ warmer troposphere in polar areas
➡ lower equator-to-pole temperature difference
➡ weaker mid-latitude weather systems
➡ weaker wave propagation into the stratosphere
➡ weaker Brewer-Dobson circulation
➡ colder poles in Stratosphere
➡ more PSC
➡ warmer troposphere in polar areas

Polar stratospheric clouds: TEM and B-D circulation

$$q = \beta y + \left[\nabla^2 + \frac{\partial}{\partial z} \left(\frac{f_0^2}{N^2} \frac{\partial}{\partial z} \right) \right] \psi.$$

$$\frac{\partial q}{\partial t} + J(\psi, q) = 0, \quad \zeta = \nabla^2 \psi, \quad b = f_0 \frac{\partial \psi}{\partial z},$$

Understanding the driving of the B-D circulation by wave flux

Vallis AOFD

Polar stratospheric clouds: TEM and B-D circulation

$$q = \beta y + \left[\nabla^2 + \frac{\partial}{\partial z} \left(\frac{f_0^2}{N^2} \frac{\partial}{\partial z} \right) \right] \psi.$$

$$\frac{\partial q}{\partial t} + J(\psi, q) = 0, \quad \zeta = \nabla^2 \psi, \quad b = f_0 \frac{\partial \psi}{\partial z},$$

$$\frac{\partial b}{\partial t} + J(\psi, b) + wN^2 = J,$$

Understanding the driving of the B-D circulation by wave flux

Vallis AOFD

Polar stratospheric clouds: TEM and B-D circulation

$$q = \beta y + \left[\nabla^2 + \frac{\partial}{\partial z}\left(\frac{f_0^2}{N^2}\frac{\partial}{\partial z}\right)\right]\psi.$$

$$\frac{\partial q}{\partial t} + J(\psi, q) = 0, \quad \zeta = \nabla^2\psi, \quad b = f_0\frac{\partial \psi}{\partial z},$$

$$\frac{\partial b}{\partial t} + J(\psi, b) + wN^2 = J,$$

$$\overline{v'q'} = -\frac{\partial}{\partial y}\overline{u'v'} + \frac{\partial}{\partial z}\left(\frac{f_0}{N^2}\overline{v'b'}\right)$$

Vallis AOFD

Understanding the driving of the B-D circulation by wave flux

Polar stratospheric clouds: TEM and B-D circulation

$$q = \beta y + \left[\nabla^2 + \frac{\partial}{\partial z}\left(\frac{f_0^2}{N^2}\frac{\partial}{\partial z}\right)\right]\psi.$$

$$\frac{\partial q}{\partial t} + J(\psi, q) = 0, \quad \zeta = \nabla^2\psi, \quad b = f_0\frac{\partial \psi}{\partial z},$$

$$\frac{\partial b}{\partial t} + J(\psi, b) + wN^2 = J,$$

$$\overline{v'q'} = -\frac{\partial}{\partial y}\overline{u'v'} + \frac{\partial}{\partial z}\left(\frac{f_0}{N^2}\overline{v'b'}\right)$$

$$\boldsymbol{\mathcal{F}} \equiv -\overline{u'v'}\,\mathbf{j} + \frac{f_0}{N^2}\overline{v'b'}\,\mathbf{k}$$

$$\overline{v'q'} = \nabla_x \cdot \boldsymbol{\mathcal{F}},$$

Eliassen-Palm flux

Understanding the driving of the B-D circulation by wave flux

Vallis AOFD

Polar stratospheric clouds: TEM and B-D circulation

$$q = \beta y + \left[\nabla^2 + \frac{\partial}{\partial z}\left(\frac{f_0^2}{N^2}\frac{\partial}{\partial z}\right)\right]\psi.$$

$$\frac{\partial q}{\partial t} + J(\psi, q) = 0, \quad \zeta = \nabla^2\psi, \quad b = f_0\frac{\partial \psi}{\partial z},$$

$$\frac{\partial b}{\partial t} + J(\psi, b) + wN^2 = J,$$

$$\overline{v'q'} = -\frac{\partial}{\partial y}\overline{u'v'} + \frac{\partial}{\partial z}\left(\frac{f_0}{N^2}\overline{v'b'}\right)$$

$$\boldsymbol{\mathcal{F}} \equiv -\overline{u'v'}\,\mathbf{j} + \frac{f_0}{N^2}\overline{v'b'}\,\mathbf{k}$$

$$\overline{v'q'} = \nabla_x \cdot \boldsymbol{\mathcal{F}},$$

Eliassen-Palm flux

$$\overline{v}^* = \overline{v} - \frac{\partial}{\partial z}\left(\frac{1}{N^2}\overline{v'b'}\right)$$

residual velocities

$$\overline{w}^* = \overline{w} + \frac{\partial}{\partial y}\left(\frac{1}{N^2}\overline{v'b'}\right)$$

Understanding the driving of the B-D circulation by wave flux

Vallis AOFD

Polar stratospheric clouds: TEM and B-D circulation

$$q = \beta y + \left[\nabla^2 + \frac{\partial}{\partial z}\left(\frac{f_0^2}{N^2}\frac{\partial}{\partial z}\right)\right]\psi.$$

$$\frac{\partial q}{\partial t} + J(\psi, q) = 0, \quad \zeta = \nabla^2\psi, \quad b = f_0\frac{\partial\psi}{\partial z},$$

$$\frac{\partial b}{\partial t} + J(\psi, b) + wN^2 = J,$$

$$\overline{v'q'} = -\frac{\partial}{\partial y}\overline{u'v'} + \frac{\partial}{\partial z}\left(\frac{f_0}{N^2}\overline{v'b'}\right)$$

$$\boldsymbol{\mathcal{F}} \equiv -\overline{u'v'}\,\mathbf{j} + \frac{f_0}{N^2}\overline{v'b'}\,\mathbf{k}$$

$$\overline{v'q'} = \nabla_x \cdot \boldsymbol{\mathcal{F}},$$

Eliassen-Palm flux

$$\overline{v}^* = \overline{v} - \frac{\partial}{\partial z}\left(\frac{1}{N^2}\overline{v'b'}\right)$$

residual velocities

$$\overline{w}^* = \overline{w} + \frac{\partial}{\partial y}\left(\frac{1}{N^2}\overline{v'b'}\right)$$

$$\frac{\partial\overline{v}^*}{\partial y} + \frac{\partial\overline{w}^*}{\partial z} = 0.$$

$$\frac{\partial\overline{u}}{\partial t} = f_0\overline{v}^* + \overline{v'q'} + \overline{F}$$

$$\frac{\partial\overline{b}}{\partial t} = -N^2\overline{w}^* + \overline{J}$$

Understanding the driving of the B-D circulation by wave flux

Vallis AOFD

Polar stratospheric clouds: TEM and B-D circulation

$$q = \beta y + \left[\nabla^2 + \frac{\partial}{\partial z}\left(\frac{f_0^2}{N^2}\frac{\partial}{\partial z}\right)\right]\psi.$$

$$\frac{\partial q}{\partial t} + J(\psi, q) = 0, \quad \zeta = \nabla^2\psi, \quad b = f_0\frac{\partial \psi}{\partial z},$$

$$\frac{\partial b}{\partial t} + J(\psi, b) + wN^2 = J,$$

$$\frac{\partial \overline{v}^*}{\partial y} + \frac{\partial \overline{w}^*}{\partial z} = 0.$$

$$\cancel{\frac{\partial \overline{u}}{\partial t}} = f_0\overline{v}^* + \overline{v'q'} + \cancel{\overline{F}}$$

$$\frac{\partial \overline{b}}{\partial t} = -N^2\overline{w}^* + \overline{J}$$

$$\overline{v'q'} = -\frac{\partial}{\partial y}\overline{u'v'} + \frac{\partial}{\partial z}\left(\frac{f_0}{N^2}\overline{v'b'}\right)$$

$$\boldsymbol{\mathcal{F}} \equiv -\overline{u'v'}\,\mathbf{j} + \frac{f_0}{N^2}\overline{v'b'}\,\mathbf{k}$$

$$\overline{v'q'} = \nabla_x \cdot \boldsymbol{\mathcal{F}},$$

← Eliassen-Palm flux

$$\overline{v}^* = \overline{v} - \frac{\partial}{\partial z}\left(\frac{1}{N^2}\overline{v'b'}\right)$$

residual velocities

$$\overline{w}^* = \overline{w} + \frac{\partial}{\partial y}\left(\frac{1}{N^2}\overline{v'b'}\right)$$

Vallis AOFD

Understanding the driving of the B-D circulation by wave flux

Polar stratospheric clouds: TEM and B-D circulation

$$q = \beta y + \left[\nabla^2 + \frac{\partial}{\partial z}\left(\frac{f_0^2}{N^2}\frac{\partial}{\partial z}\right)\right]\psi.$$

$$\frac{\partial q}{\partial t} + J(\psi, q) = 0, \quad \zeta = \nabla^2\psi, \quad b = f_0\frac{\partial \psi}{\partial z},$$

$$\frac{\partial b}{\partial t} + J(\psi, b) + wN^2 = J,$$

$$\frac{\partial \overline{v}^*}{\partial y} + \frac{\partial \overline{w}^*}{\partial z} = 0.$$

$$\cancel{\frac{\partial \overline{u}}{\partial t}} = f_0\overline{v}^* + \overline{v'q'} + \cancel{\overline{F}}$$

$$\frac{\partial \overline{b}}{\partial t} = -N^2\overline{w}^* + \overline{J}$$

wave forcing

$$-f_0\overline{v}^* \approx \overline{v'q'}, \quad > 0$$

$$\overline{v'q'} = -\frac{\partial}{\partial y}\overline{u'v'} + \frac{\partial}{\partial z}\left(\frac{f_0}{N^2}\overline{v'b'}\right)$$

$$\boldsymbol{\mathcal{F}} \equiv -\overline{u'v'}\,\mathbf{j} + \frac{f_0}{N^2}\overline{v'b'}\,\mathbf{k}$$

$$\overline{v'q'} = \nabla_x \cdot \boldsymbol{\mathcal{F}},$$

Eliassen-Palm flux

$$\overline{v}^* = \overline{v} - \frac{\partial}{\partial z}\left(\frac{1}{N^2}\overline{v'b'}\right)$$

residual velocities

$$\overline{w}^* = \overline{w} + \frac{\partial}{\partial y}\left(\frac{1}{N^2}\overline{v'b'}\right)$$

Vallis AOFD

Understanding the driving of the B-D circulation by wave flux

Polar stratospheric clouds: TEM and B-D circulation

$$q = \beta y + \left[\nabla^2 + \frac{\partial}{\partial z}\left(\frac{f_0^2}{N^2}\frac{\partial}{\partial z}\right)\right]\psi.$$

$$\frac{\partial q}{\partial t} + J(\psi, q) = 0, \quad \zeta = \nabla^2\psi, \quad b = f_0\frac{\partial \psi}{\partial z},$$

$$\frac{\partial b}{\partial t} + J(\psi, b) + wN^2 = J,$$

$$\overline{v'q'} = -\frac{\partial}{\partial y}\overline{u'v'} + \frac{\partial}{\partial z}\left(\frac{f_0}{N^2}\overline{v'b'}\right)$$

$$\boldsymbol{\mathcal{F}} \equiv -\overline{u'v'}\,\mathbf{j} + \frac{f_0}{N^2}\overline{v'b'}\,\mathbf{k}$$

$$\overline{v'q'} = \nabla_x \cdot \boldsymbol{\mathcal{F}},$$

Eliassen-Palm flux

$$\overline{v}^* = \overline{v} - \frac{\partial}{\partial z}\left(\frac{1}{N^2}\overline{v'b'}\right)$$

residual velocities

$$\overline{w}^* = \overline{w} + \frac{\partial}{\partial y}\left(\frac{1}{N^2}\overline{v'b'}\right)$$

$$\frac{\partial \overline{v}^*}{\partial y} + \frac{\partial \overline{w}^*}{\partial z} = 0.$$

$$\cancel{\frac{\partial \overline{u}}{\partial t}} = f_0\overline{v}^* + \overline{v'q'} + \cancel{\overline{F}}$$

$$\frac{\partial \overline{b}}{\partial t} = -N^2\overline{w}^* + \overline{J}$$

wave forcing

$$-f_0\overline{v}^* \approx \overline{v'q'}, \quad > 0$$

Eddy q' flux is down gradient, $d\bar{q}/dy \approx \beta > 0$, which means equatorward: $\overline{v'q'} < 0$

➡ $\bar{v}^* > 0$ in NH

➡ poleward B-D circulation

Understanding the driving of the B-D circulation by wave flux

Vallis AOFD

In-class workshop

$$q = \beta y + \left[\nabla^2 + \frac{\partial}{\partial z} \left(\frac{f_0^2}{N^2} \frac{\partial}{\partial z} \right) \right] \psi. \qquad \frac{\partial \overline{u}}{\partial t} = f_0 \overline{v}^* + \overline{v'q'} + \overline{F}$$

given the above, and the fact that the eddy flux of PV is from high to low values of $\bar{q}$ because it is a conserved quantity, what is the direction of the Brewer-Dobson circulation

In-class workshop

$$q = \beta y + \left[\nabla^2 + \frac{\partial}{\partial z}\left(\frac{f_0^2}{N^2}\frac{\partial}{\partial z} \right) \right] \psi.$$

$$\cancel{\frac{\partial \overline{u}}{\partial t}} = f_0 \overline{v}^* + \overline{v'q'} + \cancel{\overline{F}}$$

given the above, and the fact that the eddy flux of PV is from high to low values of $\bar{q}$ because it is a conserved quantity, what is the direction of the Brewer-Dobson circulation

Considering more carefully vertical wave propagation in equable climate (Korty and Emanuel)

Polar stratospheric clouds: vertical wave propagation

$$q = \nabla^2\psi + f + \frac{f_0^2}{\rho_R}\frac{\partial}{\partial z}\left(\frac{\rho_R}{N^2}\frac{\partial \psi}{\partial z}\right)$$

$$\frac{\partial q}{\partial t} + J(\psi, q) = 0, \;\; \zeta = \nabla^2\psi,$$

$$\rho_R \;=\; \rho_0 e^{-z/H}$$

$$\psi = -\overline{u}(z)y + \psi',$$

$$\frac{\partial q'}{\partial t} + \overline{u}\frac{\partial q'}{\partial x} + v'\frac{\partial \overline{q}}{\partial y} = 0,$$

$$\frac{\partial \overline{q}}{\partial y} = \beta - \frac{f_0^2}{\rho_R}\frac{\partial}{\partial z}\left(\cancel{\frac{\rho_R}{N^2}\frac{\partial \overline{u}}{\partial z}}\right)$$

$$\left(\frac{\partial}{\partial t} + \overline{u}\frac{\partial}{\partial x}\right)\left[\nabla^2\psi' + \frac{f_0^2}{\rho_R}\frac{\partial}{\partial z}\left(\frac{\rho_R}{N^2}\frac{\partial \psi'}{\partial z}\right)\right]$$

$$+\frac{\partial \psi'}{\partial x}\left[\beta - \cancel{\frac{f_0^2}{\rho_R}\frac{\partial}{\partial z}\left(\frac{\rho_R}{N^2}\frac{\partial \overline{u}}{\partial z}\right)}\right] = 0.$$

Vallis AOFD

Polar stratospheric clouds: vertical wave propagation

$$q = \nabla^2\psi + f + \frac{f_0^2}{\rho_R}\frac{\partial}{\partial z}\left(\frac{\rho_R}{N^2}\frac{\partial \psi}{\partial z}\right)$$

$$\frac{\partial q}{\partial t} + J(\psi, q) = 0, \;\; \zeta = \nabla^2\psi,$$

$$\rho_R = \rho_0 e^{-z/H}$$

$$\psi = -\overline{u}(z)y + \psi',$$

$$\frac{\partial q'}{\partial t} + \overline{u}\frac{\partial q'}{\partial x} + v'\frac{\partial \overline{q}}{\partial y} = 0,$$

$$\frac{\partial \overline{q}}{\partial y} = \beta - \frac{f_0^2}{\rho_R}\frac{\partial}{\partial z}\cancel{\left(\frac{\rho_R}{N^2}\frac{\partial \overline{u}}{\partial z}\right)}$$

surface b.c $\boldsymbol{w} = \boldsymbol{u}\cdot\nabla \boldsymbol{h_b}$

$$\psi' = \mathrm{Re}\,\widetilde{\psi}(z)\sin ly e^{ik(x-ct)},$$

$$\left[\frac{f_0^2}{\rho_R}\frac{\partial}{\partial z}\left(\frac{\rho_R}{N^2}\frac{\partial \widetilde{\psi}}{\partial z}\right)\right] = \widetilde{\psi}\left(K^2 - \frac{\partial\overline{q}/\partial y}{\overline{u}-c}\right)$$

Assume constant $\bar{u}$, N^2 and let,

$$\Phi(z) = \widetilde{\psi}(z)\left(\frac{\rho_R}{\rho_R(0)}\right)^{1/2} = \widetilde{\psi}(z)e^{-z/2H}$$

$$\left(\frac{\partial}{\partial t} + \overline{u}\frac{\partial}{\partial x}\right)\left[\nabla^2\psi' + \frac{f_0^2}{\rho_R}\frac{\partial}{\partial z}\left(\frac{\rho_R}{N^2}\frac{\partial \psi'}{\partial z}\right)\right]$$

$$+\frac{\partial \psi'}{\partial x}\left[\beta - \frac{f_0^2}{\rho_R}\cancel{\frac{\partial}{\partial z}\left(\frac{\rho_R}{N^2}\frac{\partial \overline{u}}{\partial z}\right)}\right] = 0.$$

Vallis AOFD

Polar stratospheric clouds: vertical wave propagation

$$\psi' = \mathrm{Re}\,\widetilde{\psi}(z)\sin ly\, e^{ik(x-ct)},$$

$$\Phi(z) = \widetilde{\psi}(z)\left(\frac{\rho_{\mathrm{R}}}{\rho_{\mathrm{R}}(0)}\right)^{1/2} = \widetilde{\psi}(z)e^{-z/2H}$$

➡ $$\frac{\mathrm{d}^2\Phi}{\mathrm{d}z^2} + m^2\Phi = 0,$$

$$m^2 = \frac{N^2}{f_0^2}\left(\frac{\beta}{\overline{u}-c} - K^2 - \gamma^2\right),$$

$$\gamma^2 = f_0^2/(4N^2H^2) = 1/(2L_d)^2$$

vertical propagation: if $m^2 > 0$

Vallis AOFD

Polar stratospheric clouds: vertical wave propagation

$$\psi' = \mathrm{Re}\,\tilde{\psi}(z)\sin ly\,e^{ik(x-ct)},$$

$$\Phi(z) = \tilde{\psi}(z)\left(\frac{\rho_{\mathrm{R}}}{\rho_{\mathrm{R}}(0)}\right)^{1/2} = \tilde{\psi}(z)e^{-z/2H}$$

➡ $$\frac{\mathrm{d}^2\Phi}{\mathrm{d}z^2} + m^2\Phi = 0,$$

$$m^2 = \frac{N^2}{f_0^2}\left(\frac{\beta}{\overline{u} - c} - K^2 - \gamma^2\right),$$

$$\gamma^2 = f_0^2/(4N^2H^2) = 1/(2L_d)^2$$

vertical propagation: if $m^2 > 0$

stationary waves: $c = 0$

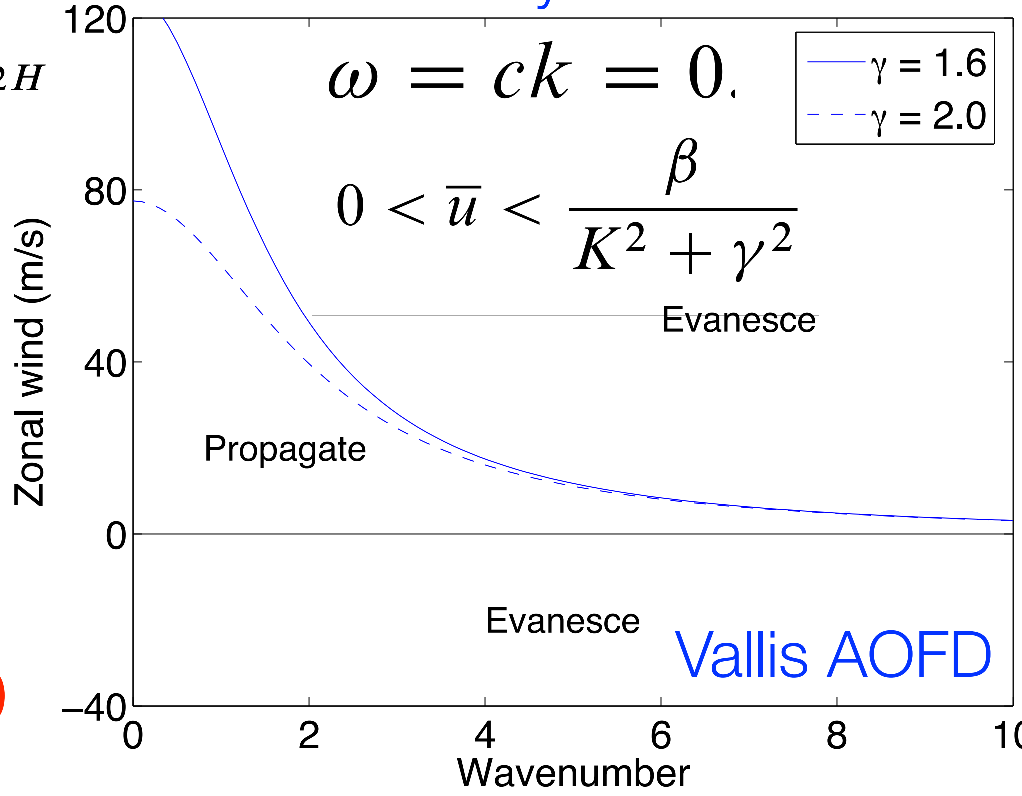

$$\omega = ck = 0.$$

$$0 < \overline{u} < \frac{\beta}{K^2 + \gamma^2}$$

Vallis AOFD

Figure 13.7 The boundary between propagating and evanescent waves as a function of zonal wind & wavenumber, using (13.61), for N=2x10^{-2}s^{-1}, $\gamma = 1.6$ ($\gamma = 2$) corresponding to a scale height of 7 km (5.5 km); deformation radius NH/f of 1,400 km (1,100 km).

vertical propagation in class workshop

Consider the equation

$$\frac{\mathrm{d}^2\Phi}{\mathrm{d}z^2} + m^2\Phi = 0,$$

$$m^2 = \frac{N^2}{f_0^2}\left(\frac{\beta}{\overline{u}-c} - K^2 - \gamma^2\right),$$

$$\gamma^2 = f_0^2/(4N^2H^2) = 1/(2L_d)^2$$

A. Analytically: for what values of $\bar{u}$ do we expect vertical propagation, assuming stationary waves ($\omega = 0$)

B. Suppose $N = 2 \times 10^{-2}\ s^{-1}$; $H = 7$ km, and $\bar{u} = 40$ m/s, f_0 at 60N. what values of k propagate? We want that in units of n, where $n = kL_x/2\pi$ and L_x is the length of the equator.

PSCs: surprising wave propagation into stratosphere in equable climate

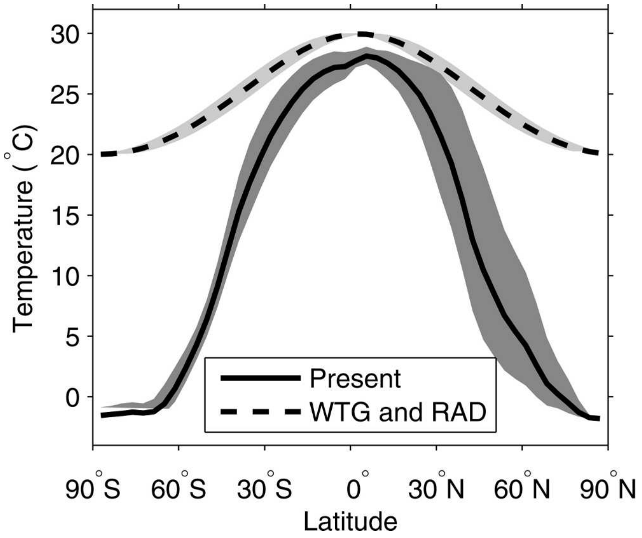

FIG. 1. Zonal- & annual-mean SSTs prescribed in the simulations. Gray bands show temporal range of zonal mean SST.

3 runs: present-day, WTG with present-day CO$_2$, WTG with high CO$_2$ (RAD)

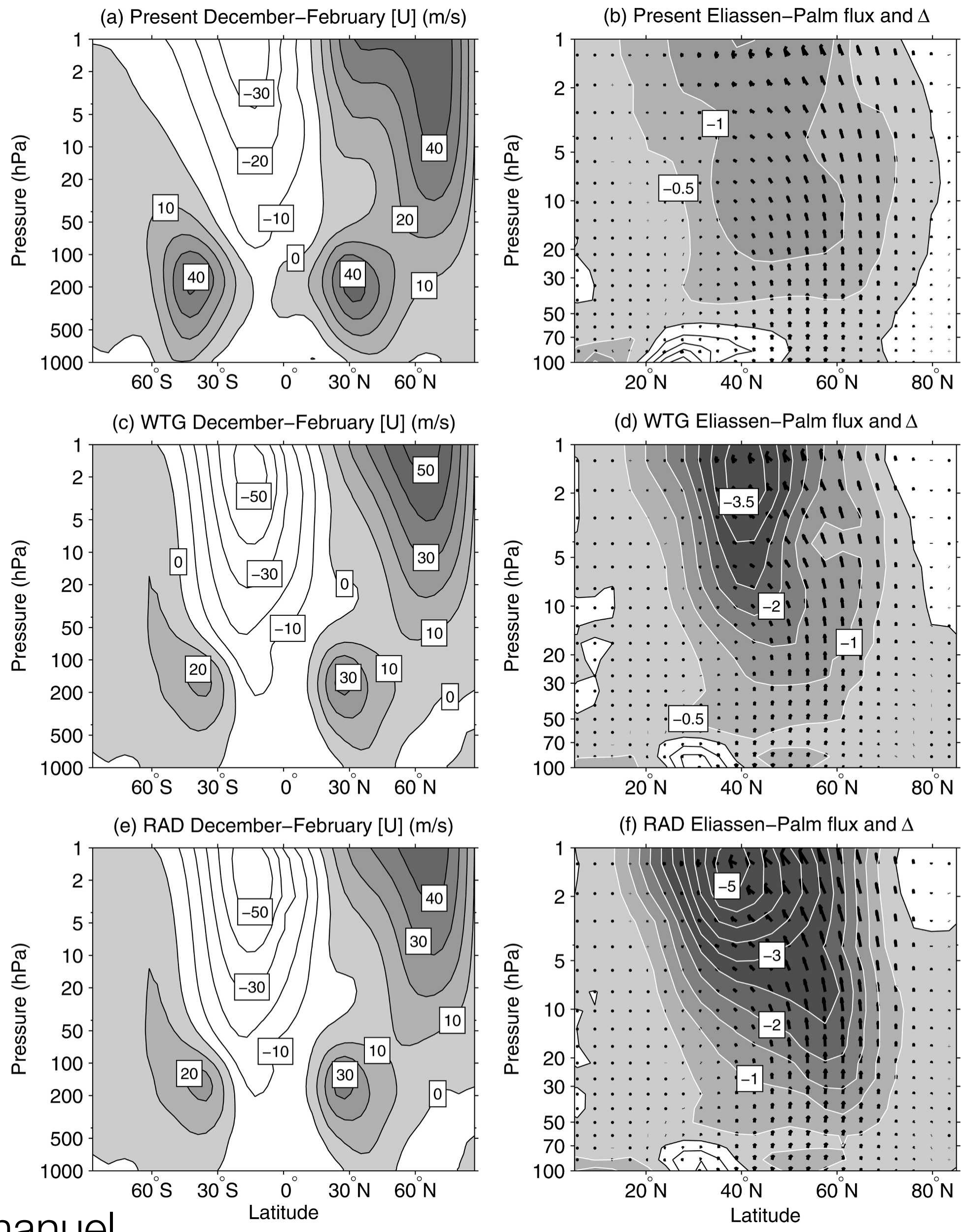
(a) Present December–February [U] (m/s)

(b) Present Eliassen–Palm flux and Δ

(c) WTG December–February [U] (m/s)

(d) WTG Eliassen–Palm flux and Δ

(e) RAD December–February [U] (m/s)

(f) RAD Eliassen–Palm flux and Δ

FIG. 3. (a) Zonal-mean zonal wind averaged over the last 5 DJF of Present; westerly winds are shaded. (b) EP (arrows) & its divergence Δ (contours) in Northern Hemisphere stratosphere @ Present; Δ units: 10^{15} m^3. As in (a), (b) but for (c), (d) WTG and (e), (f) RAD.

Korty and Emanuel

PSCs: surprising wave propagation into stratosphere in equable climate

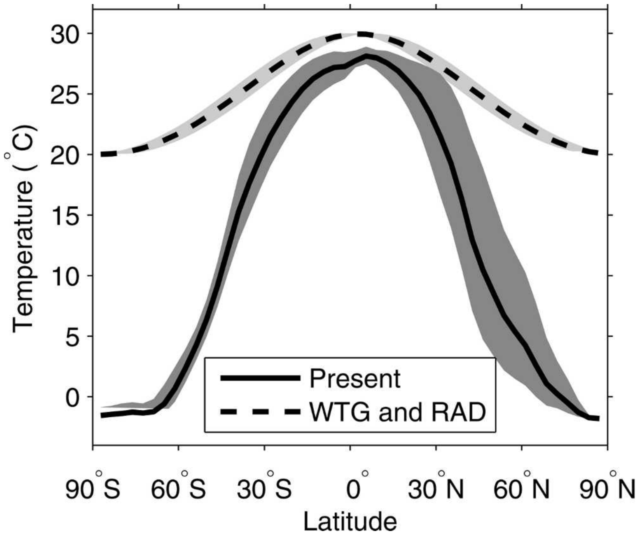

FIG. 1. Zonal- & annual-mean SSTs prescribed in the simulations. Gray bands show temporal range of zonal mean SST.

3 runs: present-day, WTG with present-day CO_2, WTG with high CO_2 (RAD)

FIG. 3. (a) Zonal-mean zonal wind averaged over the last 5 DJF of Present; westerly winds are shaded. (b) EP (arrows) & its divergence Δ (contours) in Northern Hemisphere stratosphere @ Present; Δ units: 10^{15} m^3. As in (a), (b) but for (c), (d) WTG and (e), (f) RAD.

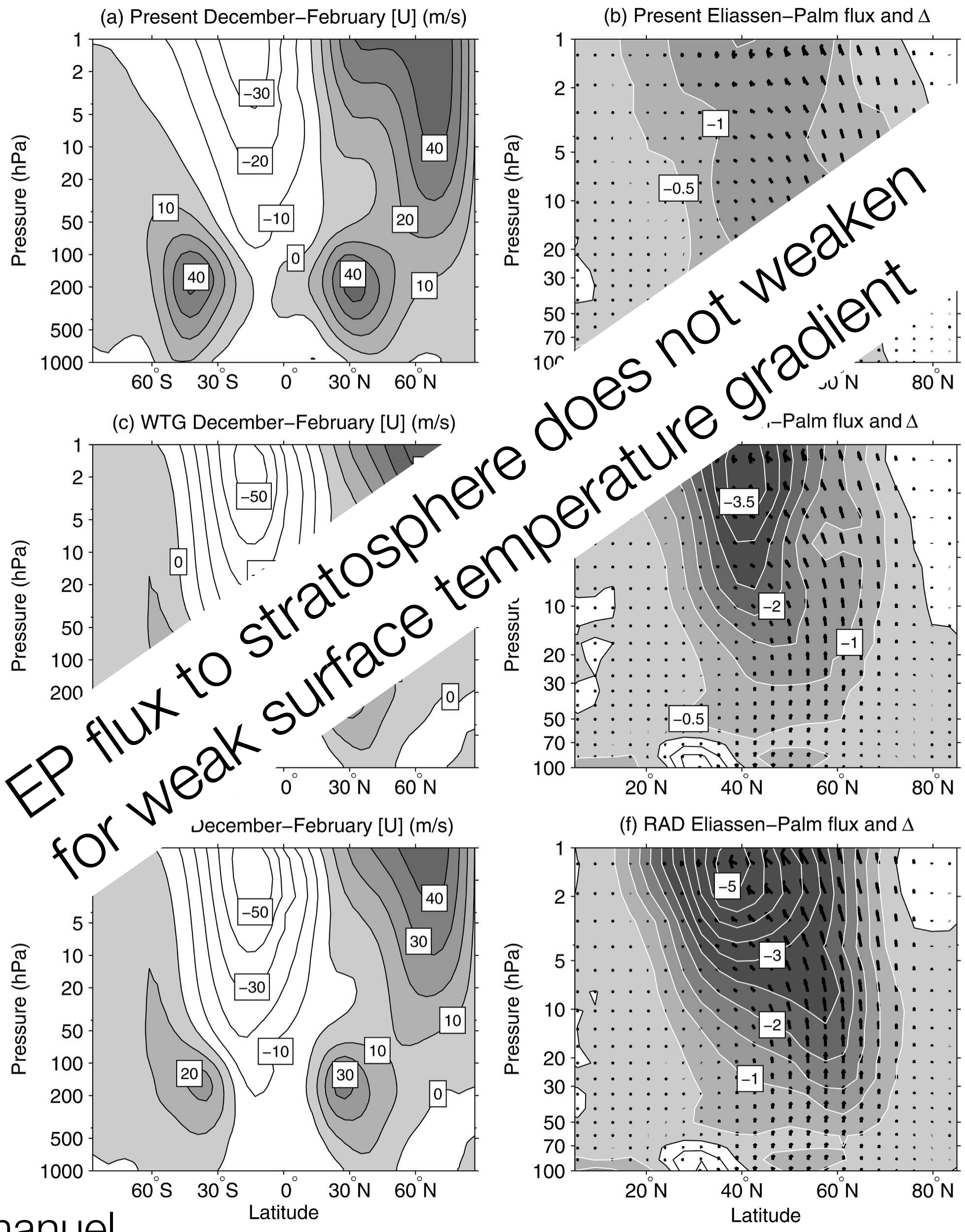

EP flux to stratosphere does not weaken for weak surface temperature gradient

Korty and Emanuel

PSCs: surprising wave propagation into stratosphere in equable climate

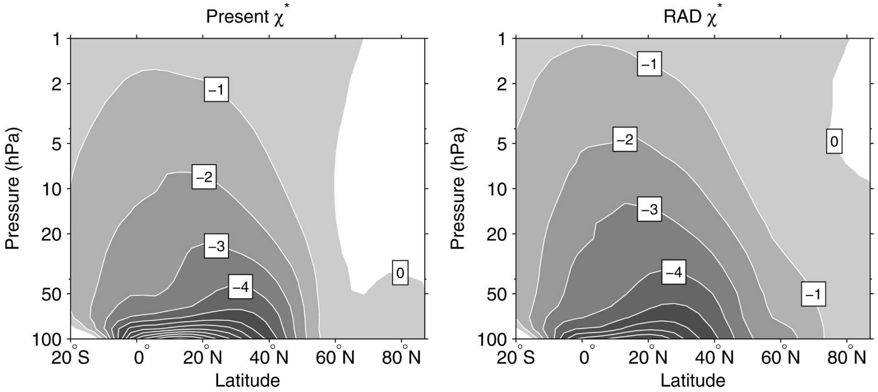

FIG. 5. The residual mean circulation in the stratosphere for (a) Present and (b) RAD. The flow circulates clockwise around negative contours. Contours are plotted and labeled every 10^9 kg s^{-1}.

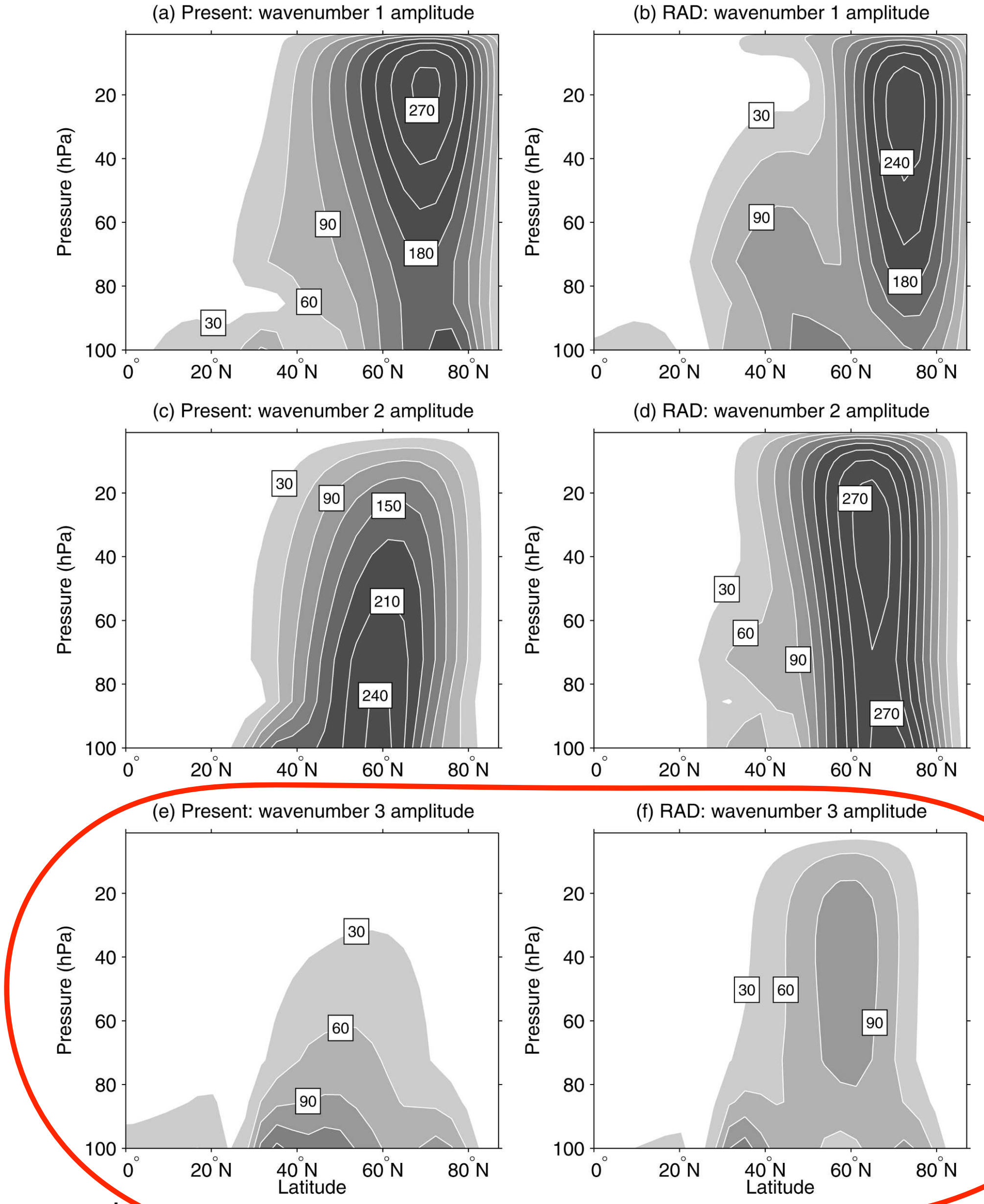

FIG. 4. Amplitude of wavenumber 1 (normalized by $\sqrt{p/p_o}$ to compensate for increasing amplitudes with decreasing density) in (a) Present; (b) RAD from data averaged over last five DJFs; units=m. As in (a), (b) but for (c), (d) wavenumber 2 and (e), (f) wavenumber 3.

Korty and Emanuel

PSCs: surprising wave propagation into stratosphere in equable climate

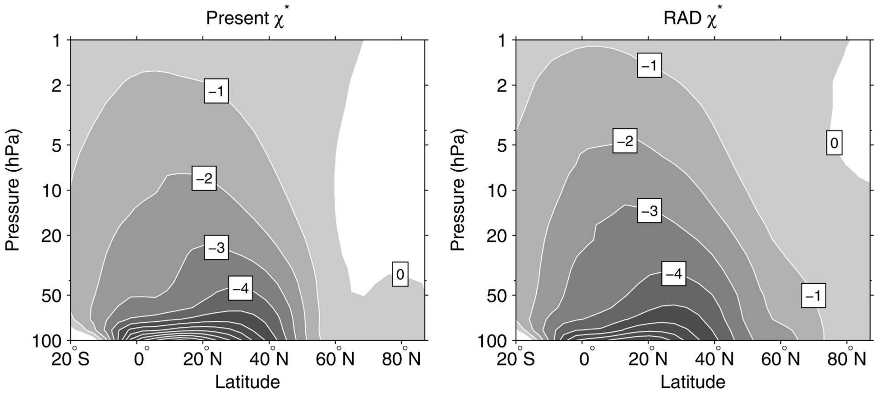

FIG. 5. The residual mean circulation in the stratosphere for (a) Present and (b) RAD. The flow circulates clockwise around negative contours. Contours are plotted and labeled every 10^9 kg s^{-1}.

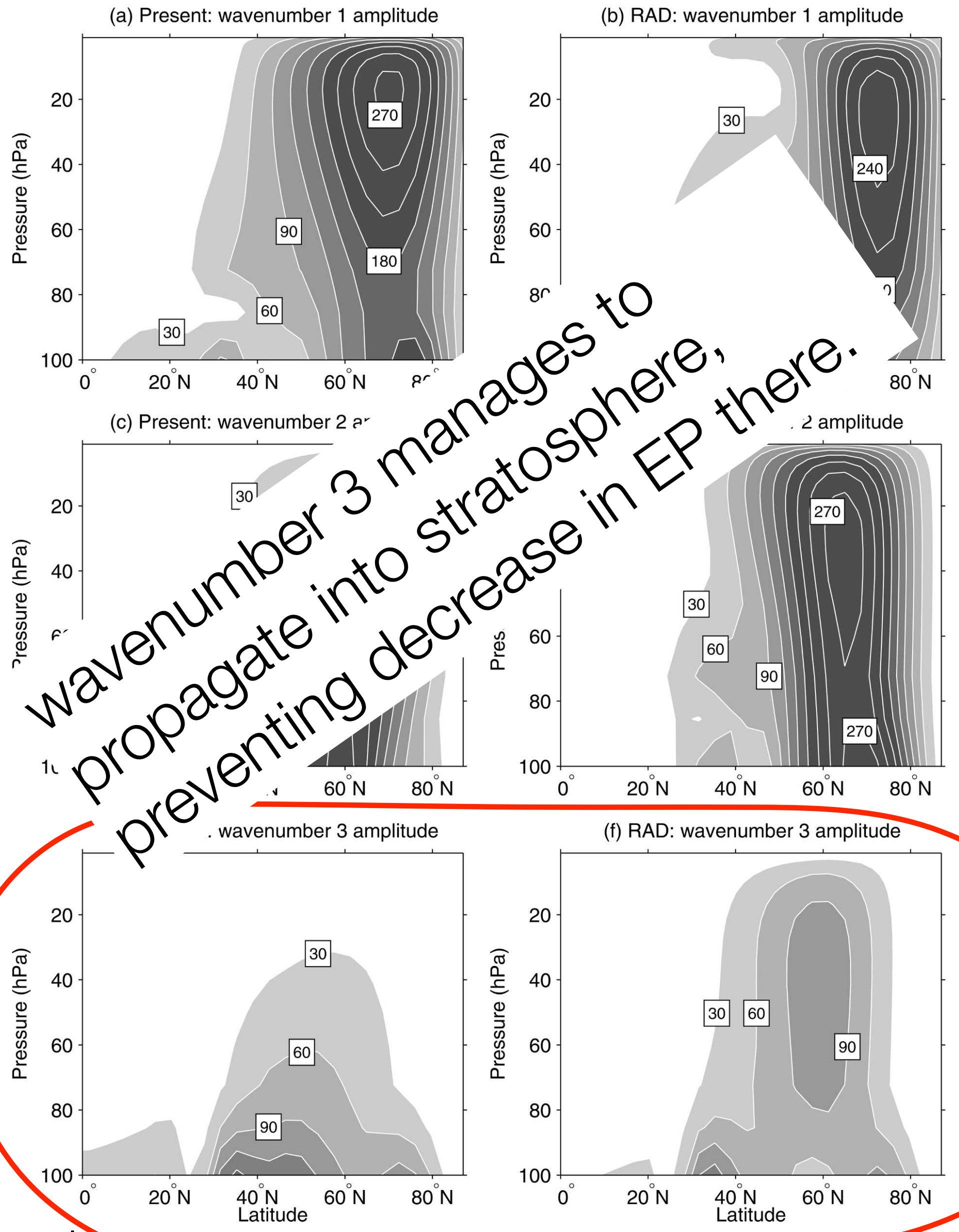

wavenumber 3 manages to propagate into stratosphere, preventing decrease in EP there.

FIG. 4. Amplitude of wavenumber 1 (normalized by $\sqrt{p/p_o}$ to compensate for increasing amplitudes with decreasing density) in (a) Present; (b) RAD from data averaged over last five DJFs; units=m. As in (a), (b) but for (c), (d) wavenumber 2 and (e), (f) wavenumber 3.

Korty and Emanuel

Brewer-Dobson circ. projected to **strengthen** in a future warmer climate

Figure 8. Projected trends in tropical upwelling in percent per decade based on a linear fit to the years 2006–2099 from RCP8.5 scenario simulations of eight stratosphere-resolving GCMs. The black line is the multi-model mean with the shading showing the inter-model standard error, scaled to represent a 95% confidence interval.

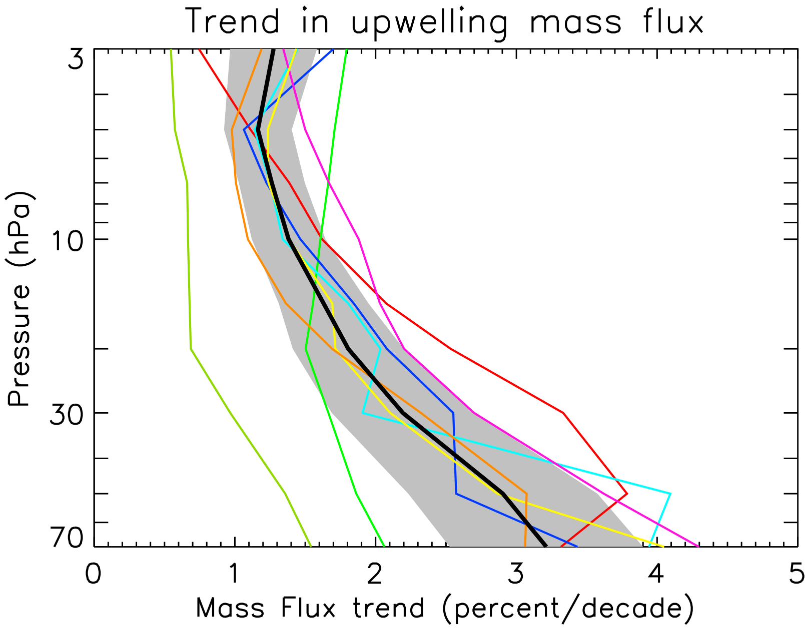

1. Changes in the Brewer-Dobson circulation are mainly a response to the tropospheric warming, including the accompanying SST changes, and not the direct radiative effect of increasing GHG amounts cooling the stratosphere.

Butchart 2014

Brewer-Dobson circ. projected to **strengthen** in a future warmer climate

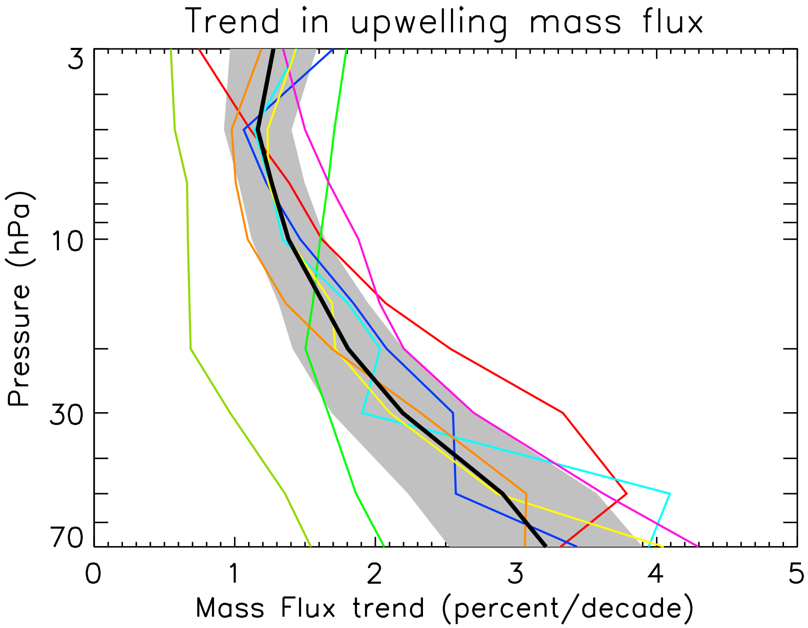

Figure 8. Projected trends in tropical upwelling in percent per decade based on a linear fit to the years 2006–2099 from RCP8.5 scenario simulations of eight stratosphere-resolving GCMs. The black line is the multi-model mean with the shading showing the inter-model standard error, scaled to represent a 95% confidence interval.

1. Changes in the Brewer-Dobson circulation are mainly a response to the tropospheric warming, including the accompanying SST changes, and not the direct radiative effect of increasing GHG amounts cooling the stratosphere.
2. Both resolved & parameterized unresolved gravity waves drive a stronger BD circulation in RCP-type model projections.

Butchart 2014

Brewer-Dobson circ. projected to **strengthen** in a future warmer climate

Figure 8. Projected trends in tropical upwelling in percent per decade based on a linear fit to the years 2006–2099 from RCP8.5 scenario simulations of eight stratosphere-resolving GCMs. The black line is the multi-model mean with the shading showing the inter-model standard error, scaled to represent a 95% confidence interval.

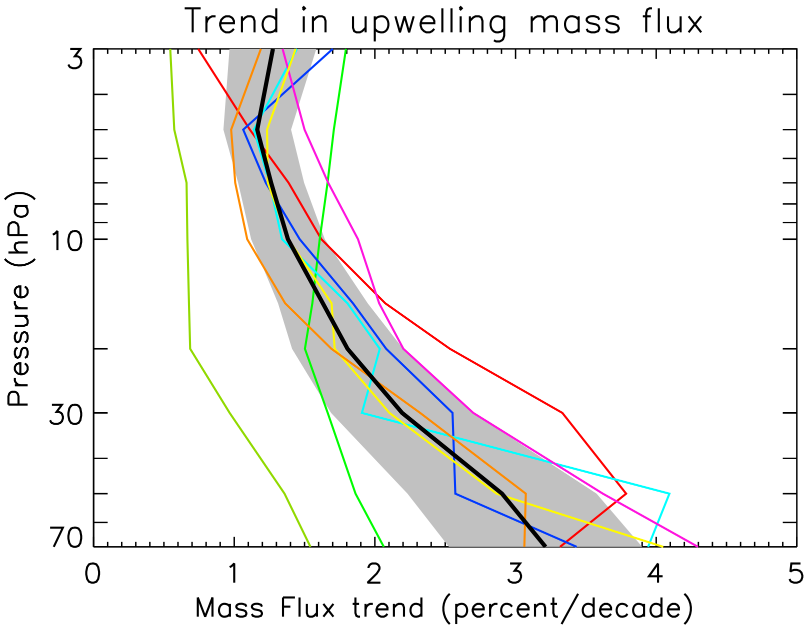

1. Changes in the Brewer-Dobson circulation are mainly a response to the tropospheric warming, including the accompanying SST changes, and not the direct radiative effect of increasing GHG amounts cooling the stratosphere.
2. Both resolved & parameterized unresolved gravity waves drive a stronger BD circulation in RCP-type model projections.
3. Currently, there is no consensus on the mechanism of the increase in stratospheric wave drag from resolved planetary & synoptic-scale Rossby waves.

Butchart 2014

Brewer-Dobson circ. projected to **strengthen** in a future warmer climate

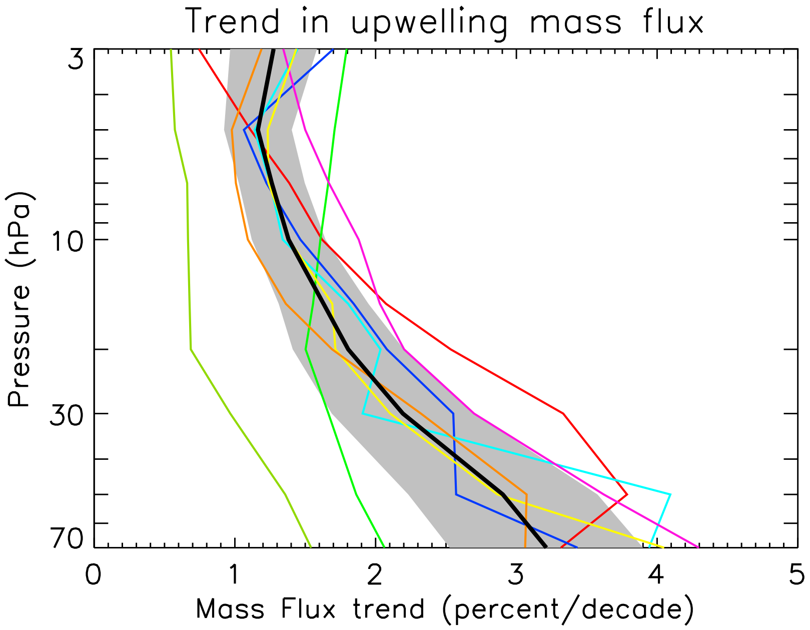

Figure 8. Projected trends in tropical upwelling in percent per decade based on a linear fit to the years 2006–2099 from RCP8.5 scenario simulations of eight stratosphere-resolving GCMs. The black line is the multi-model mean with the shading showing the inter-model standard error, scaled to represent a 95% confidence interval.

1. Changes in the Brewer-Dobson circulation are mainly a response to the tropospheric warming, including the accompanying SST changes, and not the direct radiative effect of increasing GHG amounts cooling the stratosphere.
2. Both resolved & parameterized unresolved gravity waves drive a stronger BD circulation in RCP-type model projections.
3. Currently, there is no consensus on the mechanism of the increase in stratospheric wave drag from resolved planetary & synoptic-scale Rossby waves.
4. The mechanism may be related to a shift in critical layer where wave breaking occurs, due to eastward acceleration & upward movement of the subtropical jets

Butchart 2014

Summary of obstacles for Polar Stratospheric Clouds dynamical feedback idea

Summary of obstacles for Polar Stratospheric Clouds dynamical feedback idea

- EP flux into the stratosphere may not decrease even for very weak meridional surface temperature gradient, although synoptic-scale wave forcing is weaker

Summary of obstacles for Polar Stratospheric Clouds dynamical feedback idea

- EP flux into the stratosphere may not decrease even for very weak meridional surface temperature gradient, although synoptic-scale wave forcing is weaker
- The reason is that wavenumber #3 may be able to propagate vertically

Summary of obstacles for Polar Stratospheric Clouds dynamical feedback idea

- EP flux into the stratosphere may not decrease even for very weak meridional surface temperature gradient, although synoptic-scale wave forcing is weaker
- The reason is that wavenumber #3 may be able to propagate vertically

➨ B-D circulation would then not weaken.

Summary of obstacles for Polar Stratospheric Clouds dynamical feedback idea

- EP flux into the stratosphere may not decrease even for very weak meridional surface temperature gradient, although synoptic-scale wave forcing is weaker
- The reason is that wavenumber #3 may be able to propagate vertically

➨ B-D circulation would then not weaken.

- Also: future warm climate projections show a strengthening of the Brewer-Dobson circulation.

Summary of obstacles for Polar Stratospheric Clouds dynamical feedback idea

- EP flux into the stratosphere may not decrease even for very weak meridional surface temperature gradient, although synoptic-scale wave forcing is weaker
- The reason is that wavenumber #3 may be able to propagate vertically

➡ B-D circulation would then not weaken.

- Also: future warm climate projections show a strengthening of the Brewer-Dobson circulation.

➡ Dynamical feedback that was proposed to cool the Arctic polar stratosphere and allow PSCs to develop is running into difficulties.

Stronger hurricanes

(3)

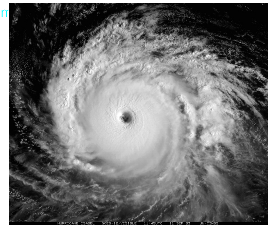

www.nasa.gov/images/content/65932m

→

stronger AMOC

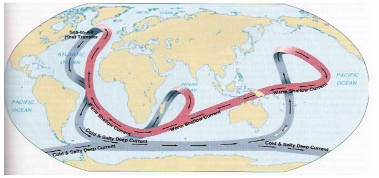

→

Warmer high latitudes

(K. Emanuel, 2002)

Hurricanes and ocean mixing

The proposed feedback:

warmer climate, stronger Hurricanes
➡ stronger internal waves forced at the ocean surface
➡ propagate into deep ocean interior and break
➡ stronger deep ocean diapycnal mixing
➡ Stronger meridional overturning circulation
➡ Higher meridional heat flux into arctic
➡ Warmer Arctic, tropics warm less due to high CO_2

K. Emanuel 2002

notes
Potential intensity: Estimating hurricane strength from SST

Hurricanes and ocean mixing

Entropy reminder

Consider a container with fluid, divided into two equal parts with temperatures $T_H > T_C$. Removing the divider, the temperature will eventually be homogenized to $(T_C + T_H)/2$. During the process, the infinitesimal change in entropy due to the transfer of an infinitesimal amount of heat dQ > 0 between the two systems leads to a gain dQ for the cold system and a loss of dQ for the hot system (gain of –dQ); thus the entropy change is

$$dS = \frac{dQ}{T_C} + \frac{-dQ}{T_H} = dQ\frac{T_H - T_C}{T_H T_C} > 0,$$

so the increase in entropy is because heat flows from the hot reservoir to the cold one.

Hurricanes and ocean mixing

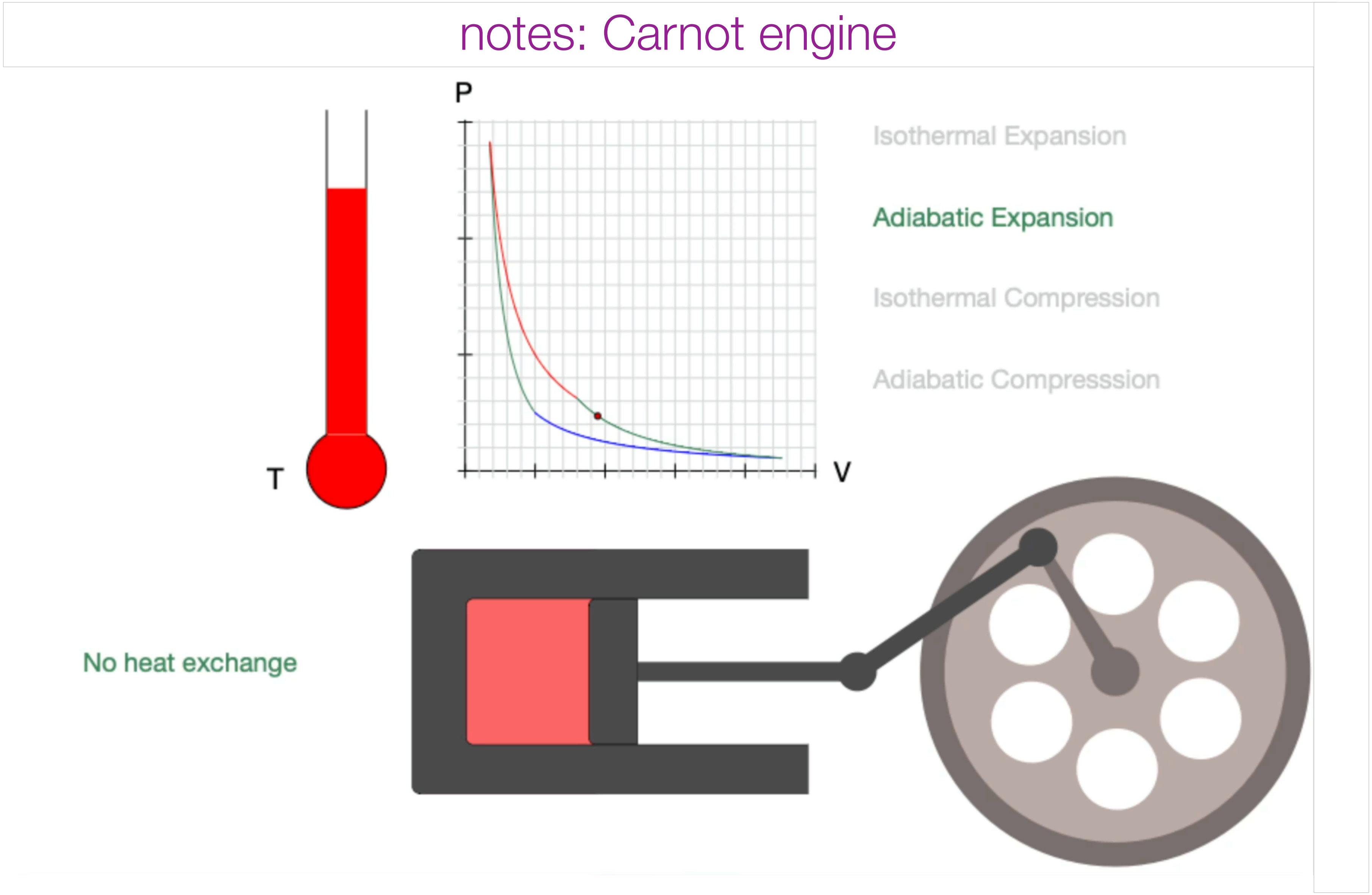

http://galileoandeinstein.phys.virginia.edu/more_stuff/Applets/carnot_cycle/carnot_cycle.html

Hurricanes and ocean mixing

notes: Carnot engine

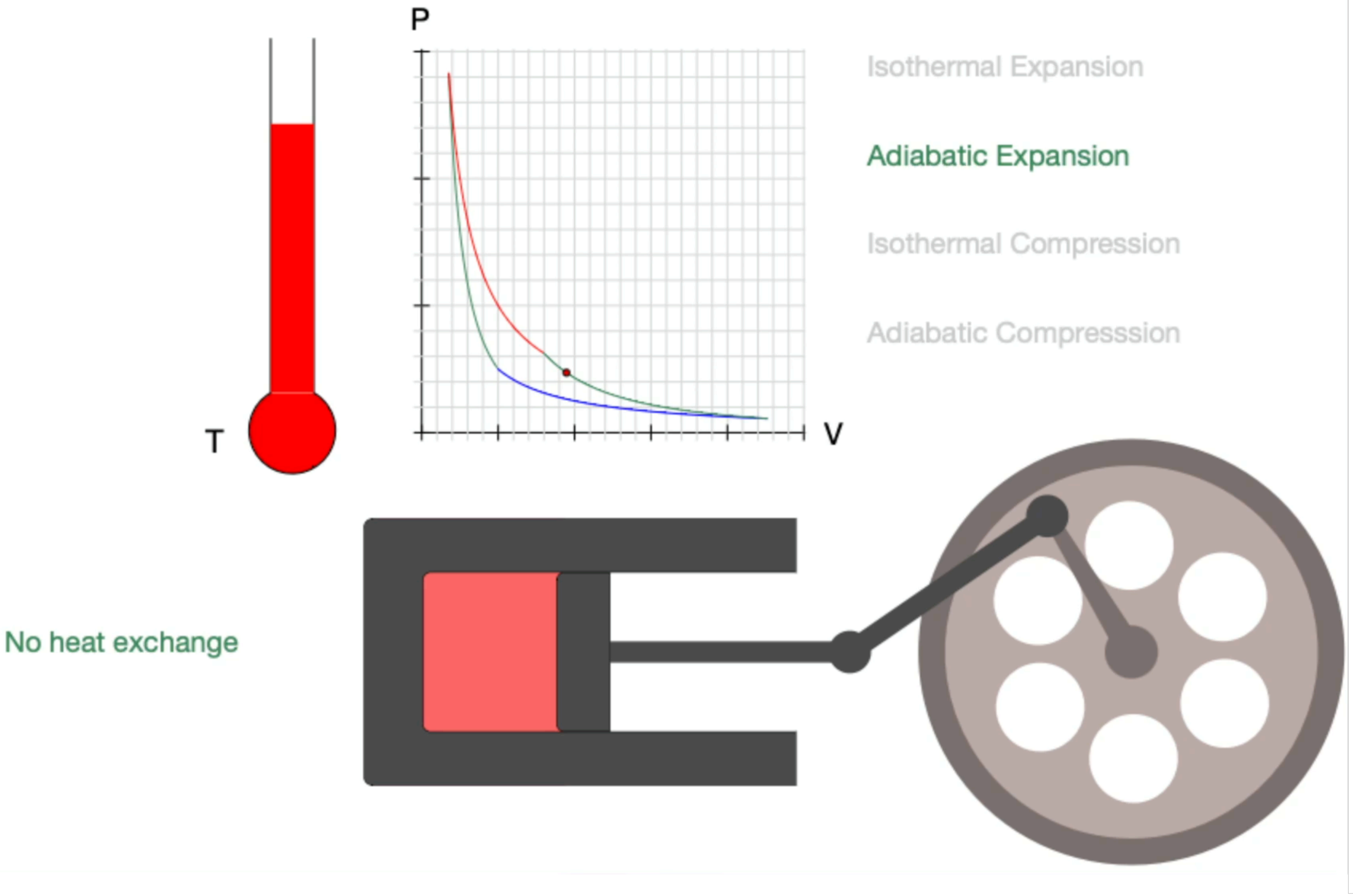

http://galileoandeinstein.phys.virginia.edu/more_stuff/Applets/carnot_cycle/carnot_cycle.html

Hurricanes and ocean mixing

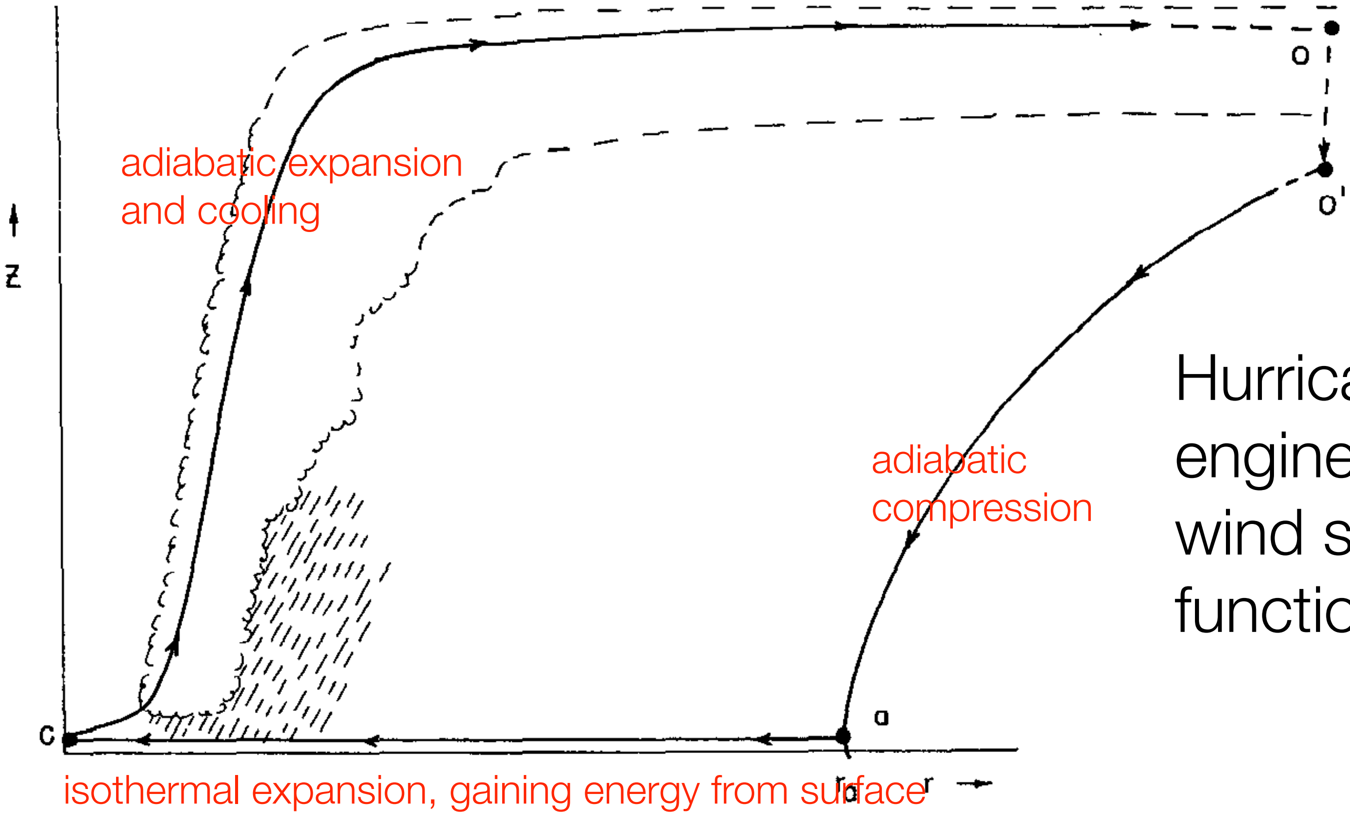

isothermal compression and radiative cooling

adiabatic expansion and cooling

adiabatic compression

isothermal expansion, gaining energy from surface

Hurricane as a heat engine, used to estimate wind strength as a function of SST

Figure 1 The hurricane Carnot cycle. Air begins spiraling in toward the storm center at point a, acquiring entropy from the ocean surface at fixed temperature T. It then ascends adiabatically from point c, flowing out near the storm top to some large radius, denoted symbolically by point o. The excess entropy is lost by export or by electromagnetic to space between o and o' at a much lower temperature To. The cycle is closed by integrating along an absolute vortex line between o' and a. The curves *c-o* and *o'-a* also represent surfaces of constant absolute angular momentum about the storm's axis.

Emanuel 1991

Efficiency of a Carnot cycle

The first law of thermodynamics, energy conservation $dU = dQ - dW$

dU: change in the internal energy

dQ: heat gain due to exchange of heat with an outside reservoir;

dW: is the work done by the system

Therefore:

for a Carnot engine

$$W = \oint dW = \oint PdV = \oint (dQ - dU) = \oint TdS - \cancel{\oint dU} = (T_H - T_c)(S_B - S_A)$$

Now, integrate $dQ = TdS$ to find that the total amount of thermal energy transferred between the hot reservoir and the engine is $Q_H = T_H(S_A - S_B)$, and with the cold reservoir $Q_C = T_C(S_A - S_B)$.

and the efficiency is $\eta = \dfrac{W}{Q_H} = \dfrac{T_H - T_C}{T_H}$.

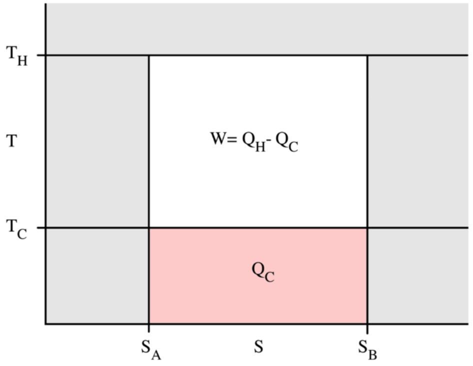

Hurricanes and ocean mixing

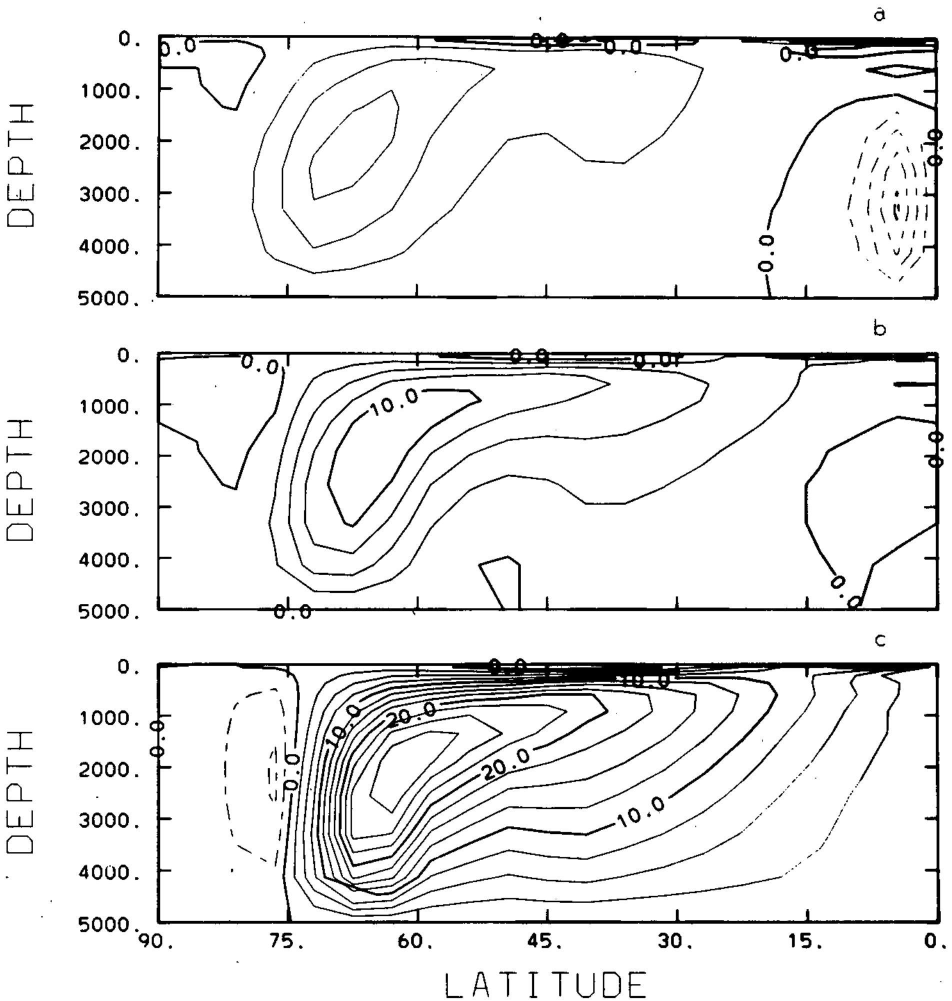

FIG. 7. Meridional overturning streamfunction for (a) $A_{HV} = 0.1$, (b) $A_{HV} = 0.5$, (c) $A_{HV} = 2.5$ (c.i. = 2.5×10^6 m^3 s^{-1}, solid contours indicate counterclockwise circulation).

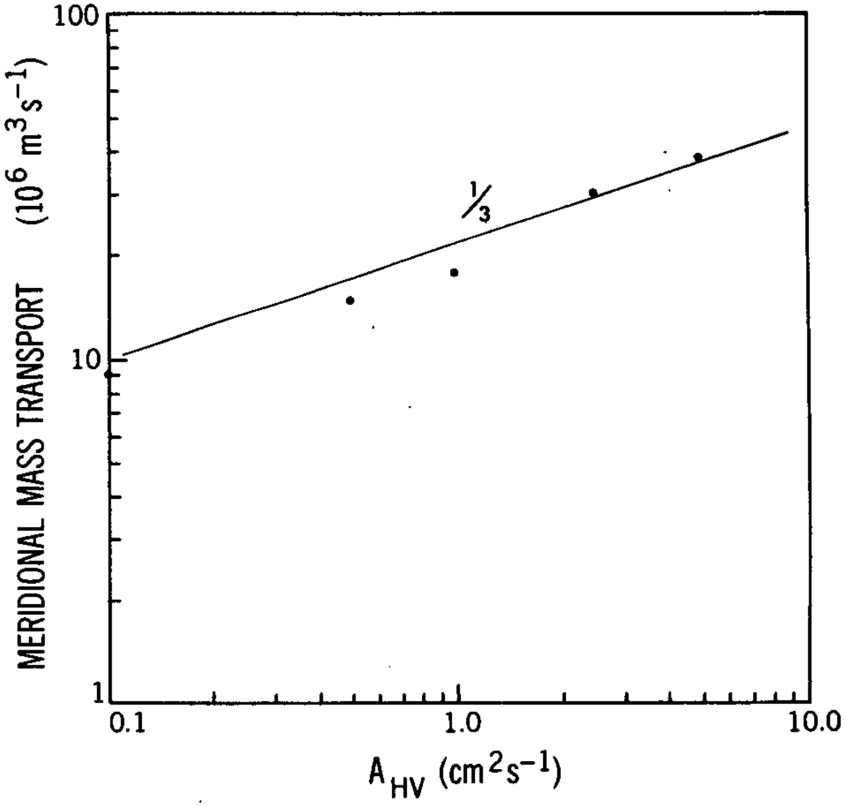

FIG. 8. Dependence of meridional overturning streamfunction on vertical diffusivity.

Frank Brian 1987

AMOC depends on vertical diapycnal mixing to the third power

Hurricanes and ocean mixing

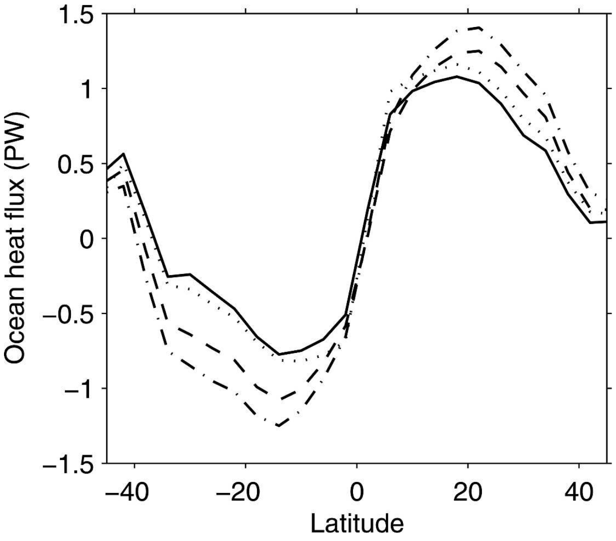

FIG. 2. Total ocean heat fluxes f
simulations with uniformly weak mixing and 338 ppm CO_2 (dotted), uniformly weak mixing and 3380 ppm CO_2 (solid), elevated tropical mixing to 220 m and 3380 ppm CO_2 (dashed), and elevated tropical mixing to 360 m and 3380 ppm CO_2 (dashed–dotted).

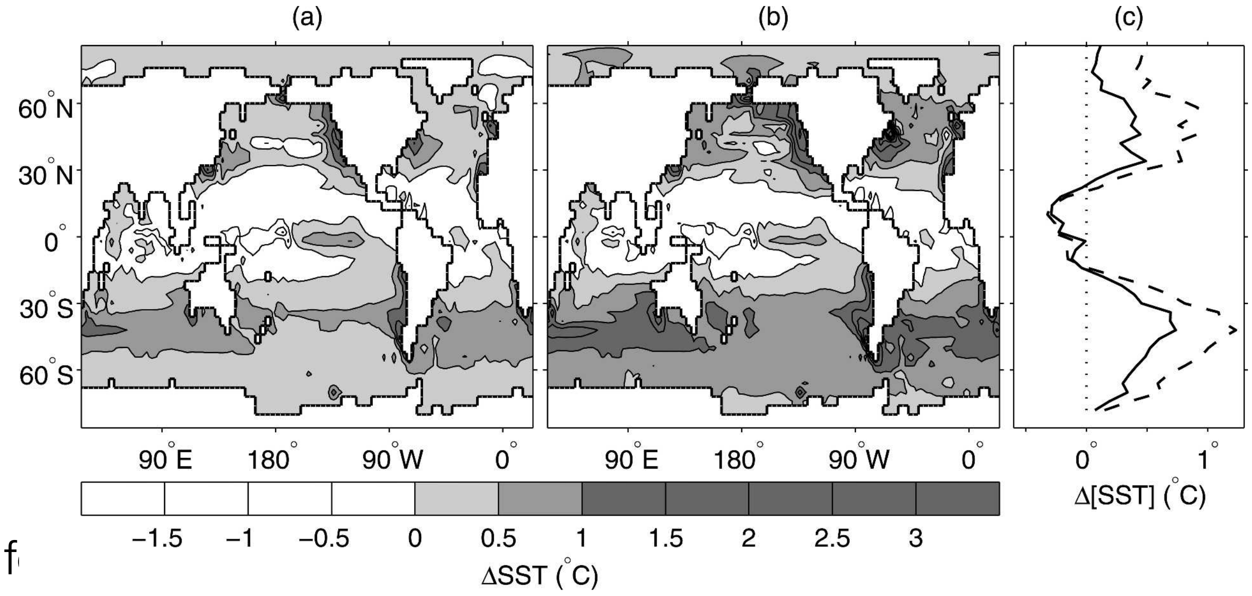

FIG. 4. Change in SSTs for runs with 3380 ppm CO_2 between (a) a simulation with elevated tropical mixing to 220 m and the control (uniformly weak mixing) and (b) a simulation with elevated tropical mixing to 360 m and the control. (c) Change in zonally averaged SST for the simulations shown in panels (a) (solid) and (b) (dashed).

Korty and Emanuel 2008

BUT: Enhanced vertical diapycnal mixing has a negligible effect on SST

Breakup of subtropical stratocumulus cloud decks at high SST

Causing albedo decrease and warming of mid-latitudes

Schneider et al 2019, (Bretherton et al)

https://www.shutterstock.com/image-photo/aerial-view-layer-stratocumulus-clouds-369408491

(4)

Breakdown of subtropical stratocumulus decks

Stratocumulus clouds at present:

- Cover broad regions (6.5% of Earth area) over the subtropical oceans.
- Characterized by lines, waves, and cellular structures.
- Radiative cooling from the cloud tops drives convection to surface, that replenishes liquid water in these clouds.
- Can often be seen out of an airplane window while flying.
- **Large SW albedo, strong cooling effects on climate.**

Stratocumulus clouds from a plane

http://www.pilotfriend.com/training/flight_training/met/clouds.htm

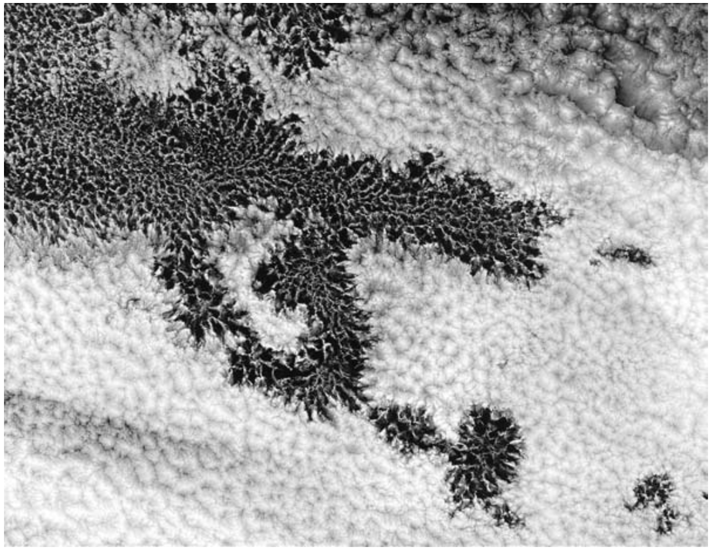

Cellular convective structures

https://visibleearth.nasa.gov/images/98570/clouds-in-eastern-south-pacific-ocean?size=small

Stratocumulus cloud model bias leads to significant SST errors

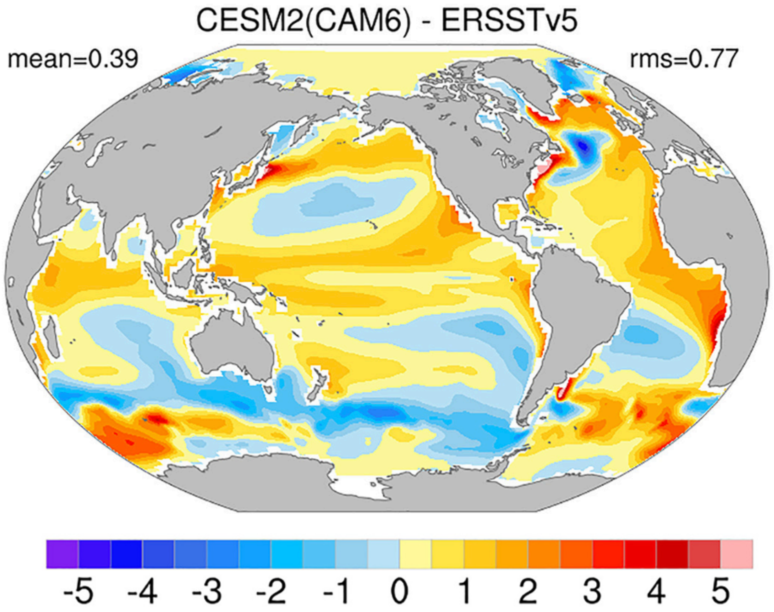

Model SST minus observations (°C)

G. Danabasoglu et al 2020, https://agupubs.onlinelibrary.wiley.com/doi/10.1029/2019MS001916

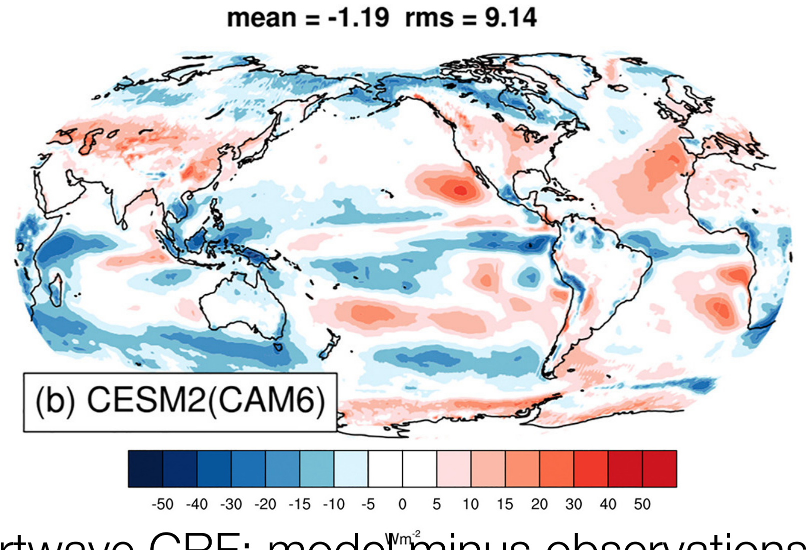

shortwave CRF: model minus observations

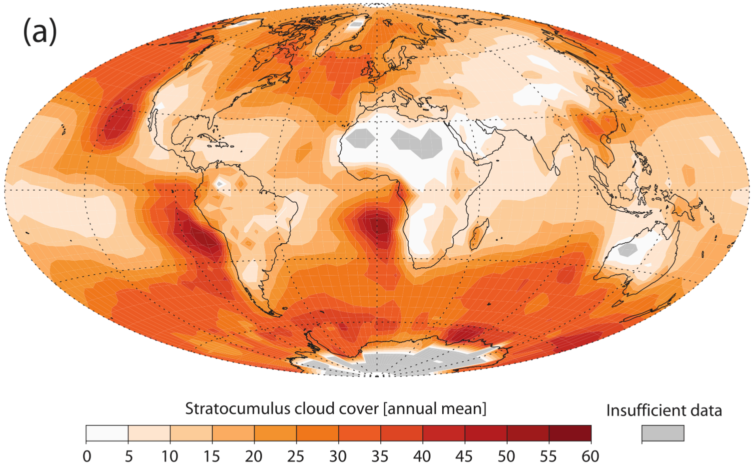

observed stratocumulus cloud fraction (%)

SST error (difference between model and observations) is large, ~2.5C in regions with underestimated stratocumulus cloud cover

Stratocumulus clouds: mechanism

Driving mechanism:

- Upward LW cooling at top of cloud layer because cloud layer is optically thick
- Cooling drives convective motions from surface to cloud layer
- Convection transports moisture to cloud layer and sustains it
- Convective motions also lead to uniform vertical distribution of moisture, forming a mix-layer

Opposing processes:

- Entrainment with dry air from cap-inversion layer
- Warming by downward LW radiation from the free troposphere toward top of cloud layer

Stratocumulus Topped Boundary Layer (STBL)

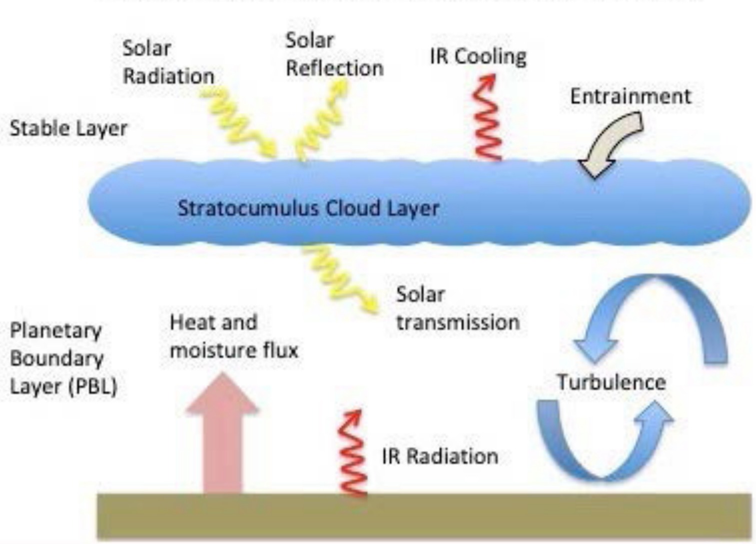

Fig. 3 Schematic diagram showing important dynamic and radiative features of the stratocumulus-topped boundary layer (STBL.) Adapted from Wood 2012

https://www.amsweatherband.org/weatherband/articles/a-day-in-the-life-of-stratocumulus/

Breakdown of subtropical stratocumulus decks

Cloud resolving simulation: stratocumulus decks break at high CO_2

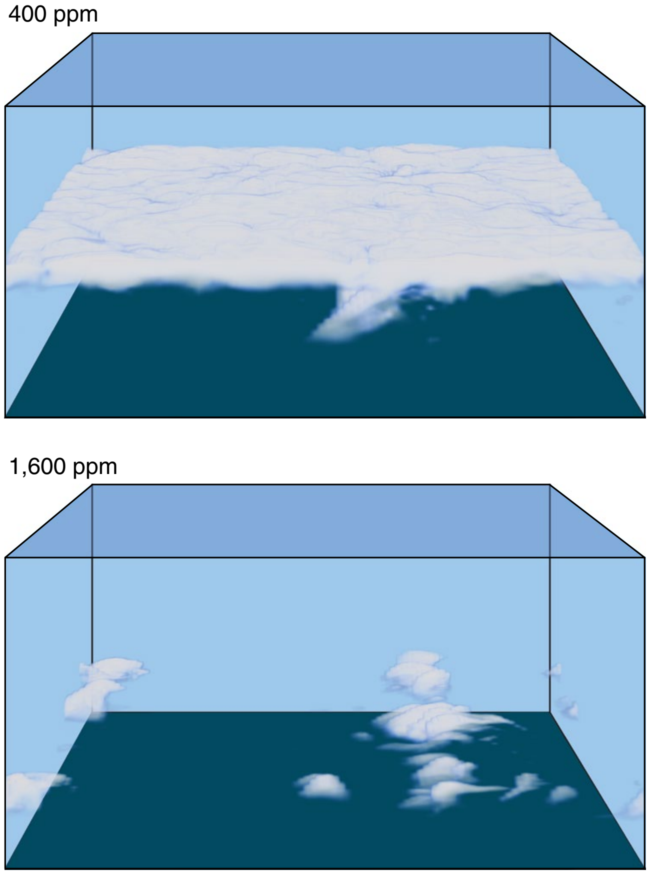

Possible climate transitions from breakup of stratocumulus decks under greenhouse warming

Tapio Schneider [1,2]*, Colleen M. Kaul[1] and Kyle G. Pressel[1] 2020

Schneider et al 2020

Breakdown of subtropical stratocumulus decks

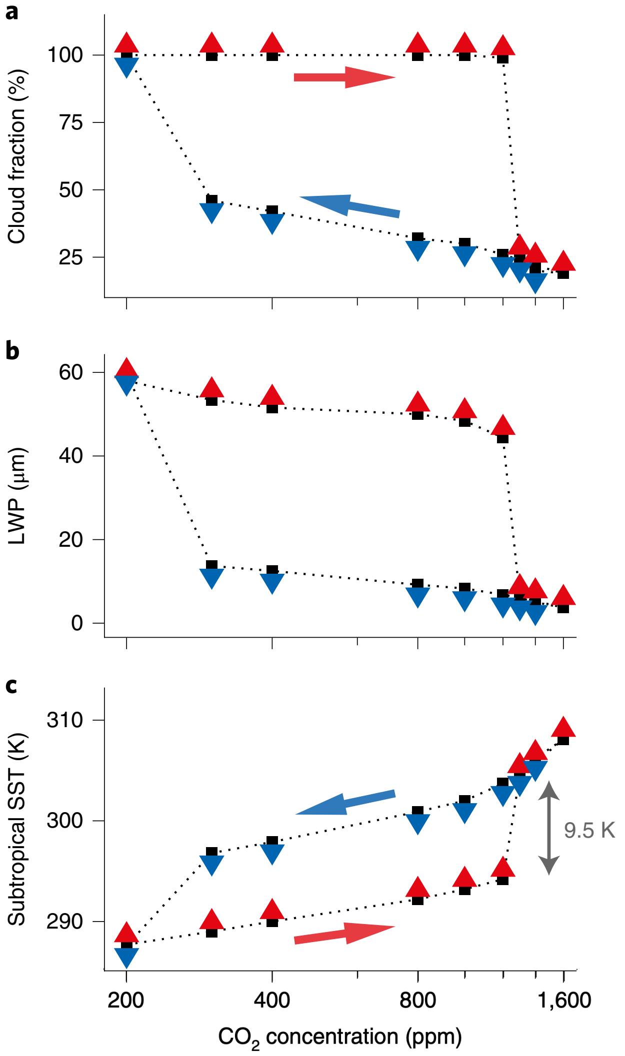

Cloud resolving simulation: stratocumulus decks break at high CO_2

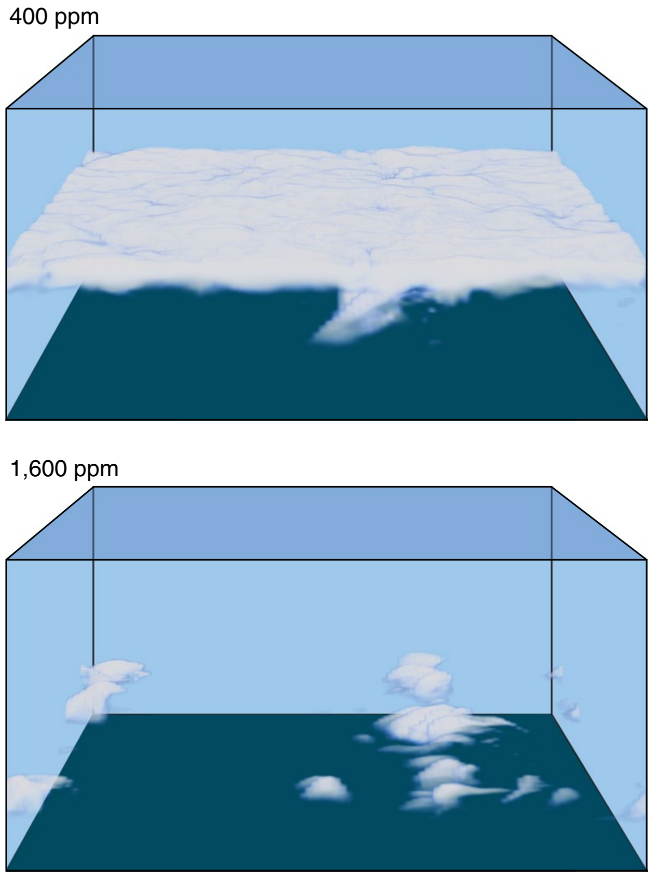

Hysteresis as a function of CO_2

Possible climate transitions from breakup of stratocumulus decks under greenhouse warming

Tapio Schneider [1,2]*, Colleen M. Kaul[1] and Kyle G. Pressel[1] **2020**

Schneider et al 2020

Breakdown of subtropical stratocumulus decks

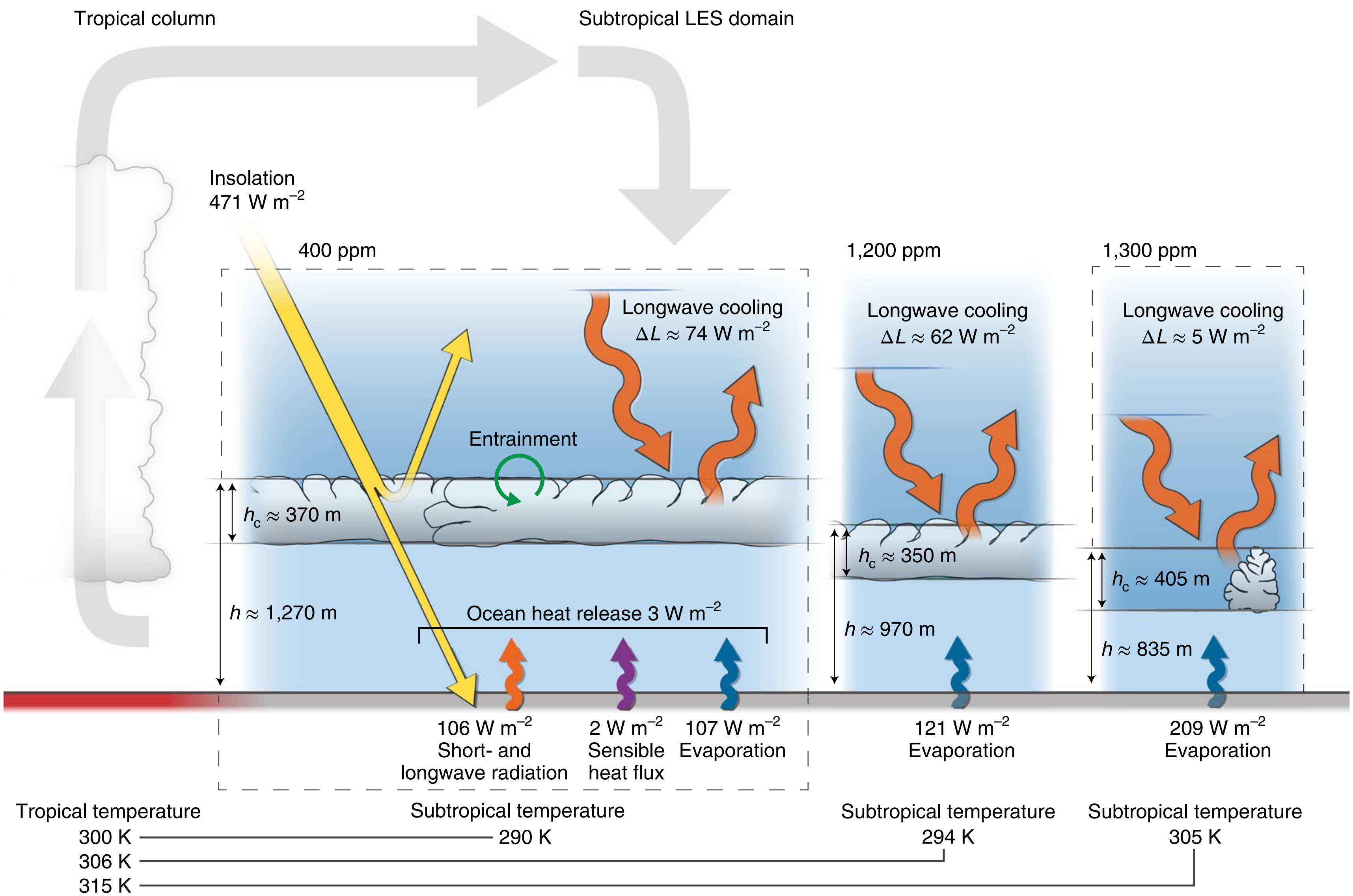

Schneider et al 2020

Breakdown of subtropical stratocumulus decks

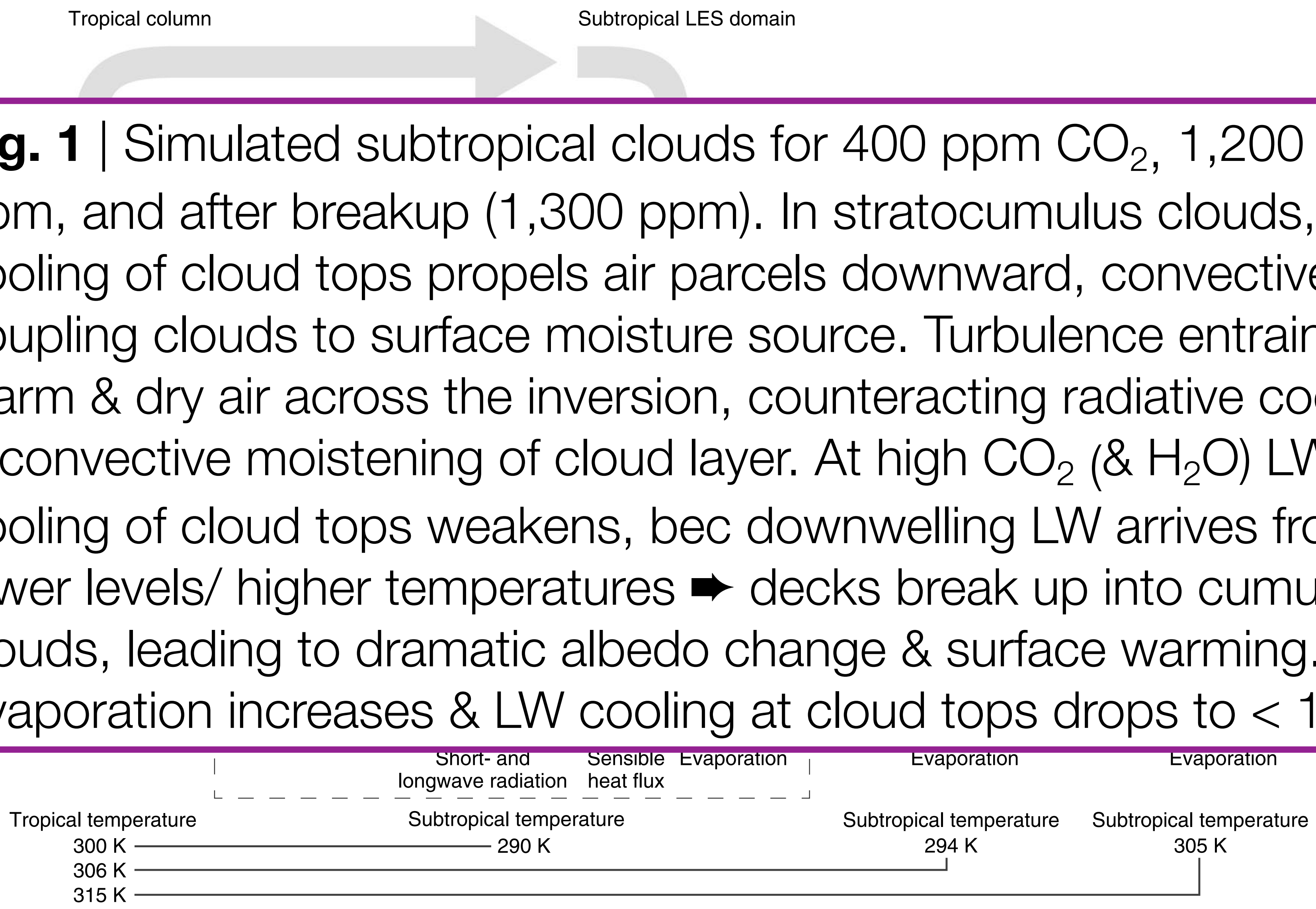

Fig. 1 | Simulated subtropical clouds for 400 ppm CO_2, 1,200 ppm, and after breakup (1,300 ppm). In stratocumulus clouds, LW cooling of cloud tops propels air parcels downward, convectively coupling clouds to surface moisture source. Turbulence entrains warm & dry air across the inversion, counteracting radiative cooling & convective moistening of cloud layer. At high CO_2 (& H_2O) LW cooling of cloud tops weakens, bec downwelling LW arrives from lower levels/ higher temperatures ➡ decks break up into cumulus clouds, leading to dramatic albedo change & surface warming. Evaporation increases & LW cooling at cloud tops drops to < 10%.

Schneider et al 2020

Breakdown of subtropical stratocumulus decks

Mechanism of breakup at high CO_2:

Higher CO_2: ➨ downwelling LW toward cloud tops ⬆ (increased atmc emissivity ➨ ⬆ LW coming from lower/warmer altitudes)

➨ decreased cloud top cooling ➨ decoupling from surface
➨ clouds dissipate

Schneider et al 2020

Breakdown of subtropical stratocumulus decks

Mechanism of breakup at high CO_2:

Higher CO_2: ➡ downwelling LW toward cloud tops ⬆ (increased atmc emissivity ➡ ⬆ LW coming from lower/warmer altitudes)

➡ decreased cloud top cooling ➡ decoupling from surface ➡ clouds dissipate

[paper mentions a 2nd mechanism: high T ➡ enhanced evaporation ➡ more turbulence at cloud level due to latent heat release ➡ more entrainment ➡ warming/drying & decoupling;
But: with clouds gone, is there still latent heat release?]

Schneider et al 2020

Breakdown of subtropical stratocumulus decks

Mechanism of breakup at high CO$_2$:

Higher CO$_2$: ➡ downwelling LW toward cloud tops ⬆ (increased atmc emissivity ➡ ⬆ LW coming from lower/warmer altitudes)

➡ decreased cloud top cooling ➡ decoupling from surface ➡ clouds dissipate

[paper mentions a 2nd mechanism: high T ➡ enhanced evaporation ➡ more turbulence at cloud level due to latent heat release ➡ more entrainment ➡ warming/drying & decoupling;
But: with clouds gone, is there still latent heat release?]

Consequences of stratocumulus breakup:

Subtropical SST jumps by 10K. Subtropical marine stratocumulus clouds cover ~6.5% of Earth's surface & reduce absorbed SW by ~110 W m^{-2}, compared to ~10 Wm^{-2} by scattered cumulus. With climate sensitivity of 1.2 K (Wm^{-2})$^{-1}$ (4.8 K/CO$_2$ doubling; high for current GCMs) implies (110–10) Wm^{-2} × 6.5% × 1.2 K (Wm^{-2})$^{-1}$ ≈ 8 K global-mean surface warming (stratocumulus clouds cover ~6.5% of Earth area). This seems to assume an infinitely efficient heat transport to the rest of the globe.

Schneider et al 2020

Two-box model for stratocumulus break-up

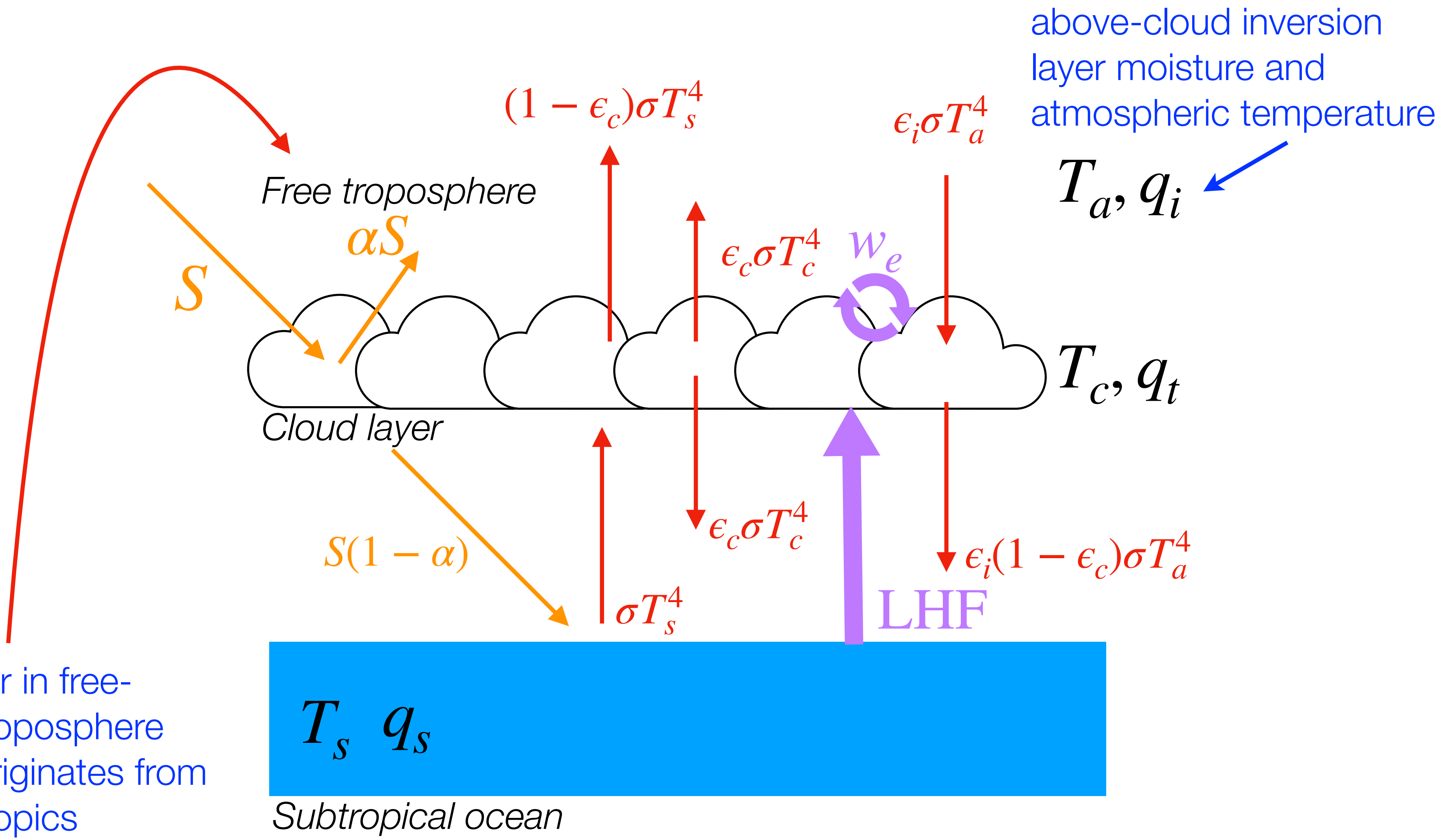

(Andrea Salazar, model adapted from Salazar & Tziperman, 2023)

Two-box model for stratocumulus break-up

Temperature:

$$C_s \frac{dT_s}{dt} = S(1-\alpha) - \sigma T_s^4 + \epsilon_c \sigma T_c^4 + \epsilon_i (1-\epsilon_c) \sigma T_i^4 - \mathrm{LHF}$$

surface energy balance

$$C_c \frac{dT_c}{dt} = \overbrace{-2\epsilon_c \sigma T_c^4 + \epsilon_c \sigma T_s^4 + \epsilon_i \epsilon_c \sigma T_a^4}^{\text{net longwave cooling} = LWC} + LQ + C_c w_e (T_a - T_c)$$

cloud layer energy balance

$$T_a = T_{a,0} + \Delta T \log_2(\mathrm{CO}_2/280)$$ free troposphere temperature

(Andrea Salazar, model adapted from Salazar & Tziperman, 2023)

Two-box model for stratocumulus break-up

Temperature:

$$C_s \frac{dT_s}{dt} = S(1-\alpha) - \sigma T_s^4 + \epsilon_c \sigma T_c^4 + \epsilon_i (1-\epsilon_c)\sigma T_i^4 - \mathrm{LHF}$$

surface energy balance

$$C_c \frac{dT_c}{dt} = \overbrace{-2\epsilon_c \sigma T_c^4 + \epsilon_c \sigma T_s^4 + \epsilon_i \epsilon_c \sigma T_a^4}^{\text{net longwave cooling} = LWC} + LQ + C_c w_e (T_a - T_c)$$

cloud layer energy balance

$$T_a = T_{a,0} + \Delta T \log_2(\mathrm{CO}_2/280)$$

free troposphere temperature

Moisture:

$$E = C_E V(q_s - q_t),\ LHF = L\,E$$

Evaporation, surface latent heat flux

$$q_t = q_l + q_c$$

total moisture in cloud layer

$$\frac{dq_t}{dt} = Q - w_e(q_t - q_i)$$

cloud moisture budget

$$q_c = \min[q_t, q^*(T_c)],\ q_l = q_t - q_c$$

$$Q = \begin{cases} E & \text{coupled} \\ 0 & \text{decoupled} \end{cases}$$

moisture flux into cloud layer

(Andrea Salazar, model adapted from Salazar & Tziperman, 2023)

Two-box model for stratocumulus break-up

Temperature:

$$C_s\frac{dT_s}{dt} = S(1-\alpha) - \sigma T_s^4 + \epsilon_c \sigma T_c^4 + \epsilon_i (1-\epsilon_c)\sigma T_i^4 - \mathrm{LHF}$$

surface energy balance

$$C_c\frac{dT_c}{dt} = \overbrace{-2\epsilon_c \sigma T_c^4 + \epsilon_c \sigma T_s^4 + \epsilon_i \epsilon_c \sigma T_a^4}^{\text{net longwave cooling} \,=\, LWC} + LQ + C_c w_e (T_a - T_c)$$

cloud layer energy balance

$$T_a = T_{a,0} + \Delta T \log_2(\mathrm{CO_2}/280)$$

free troposphere temperature

Moisture:

$$E = C_E V(q_s - q_t),\ LHF = L\,E$$

Evaporation, surface latent heat flux

$$q_t = q_l + q_c$$

total moisture in cloud layer

$$\frac{dq_t}{dt} = Q - w_e(q_t - q_i)$$

cloud moisture budget

$$q_c = \min[q_t, q^*(T_c)],\ q_l = q_t - q_c$$

$$Q = \begin{cases} E & \text{coupled} \\ 0 & \text{decoupled} \end{cases}$$

moisture flux into cloud layer

Decoupling criteria: $LHF/LWC > 1$

(Andrea Salazar, model adapted from Salazar & Tziperman, 2023)

Two-box model for stratocumulus break-up

Temperature:

$$C_s\frac{dT_s}{dt} = S(1-\alpha) - \sigma T_s^4 + \epsilon_c\sigma T_c^4 + \epsilon_i(1-\epsilon_c)\sigma T_i^4 - \mathrm{LHF}$$

surface energy balance

$$C_c\frac{dT_c}{dt} = \overbrace{-2\epsilon_c\sigma T_c^4 + \epsilon_c\sigma T_s^4 + \epsilon_i\epsilon_c\sigma T_a^4}^{\text{net longwave cooling} = LWC} + LQ + C_c w_e(T_a - T_c)$$

cloud layer energy balance

$$T_a = T_{a,0} + \Delta T \log_2(\mathrm{CO_2}/280)$$

free troposphere temperature

Moisture:

$$E = C_E V(q_s - q_t),\ LHF = L\,E$$

Evaporation, surface latent heat flux

$$q_t = q_l + q_c$$

total moisture in cloud layer

$$\frac{dq_t}{dt} = Q - w_e(q_t - q_i)$$

cloud moisture budget

$$q_c = \min[q_t, q^*(T_c)],\ q_l = q_t - q_c$$

$$Q = \begin{cases} E & \text{coupled} \\ 0 & \text{decoupled} \end{cases}$$

moisture flux into cloud layer

Coefficients:

$$\alpha = \alpha_c - (\alpha_c - \alpha_w)\ \exp(-D\kappa q_l)$$

$$\epsilon_c = 1 - (1 - \epsilon_{c,o})\ \exp(-D\kappa q_l)$$

$$\epsilon_i = \epsilon_{i,0} + A\log_2\left(\mathrm{CO_2}/280\right)$$

$$+B\log_2\left(q_i/q_{i,o}\right)$$

$$C_s = H_s c_p^w \rho_w,\ C_c = H_c c_p^a \rho_a$$

Decoupling criteria: $LHF/LWC > 1$

(Andrea Salazar, model adapted from Salazar & Tziperman, 2023)

Two-box model for stratocumulus break-up

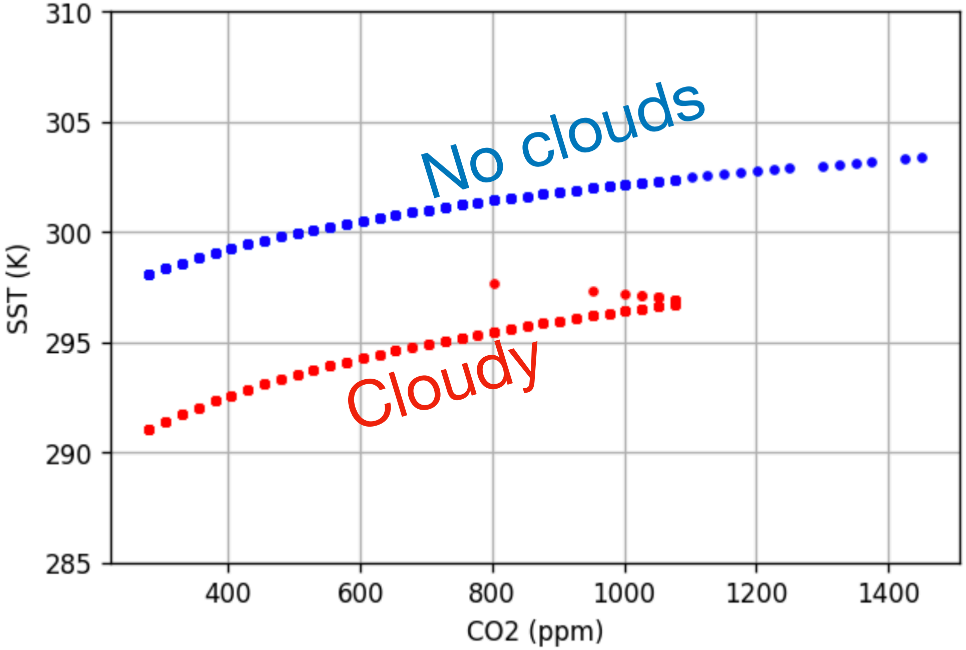

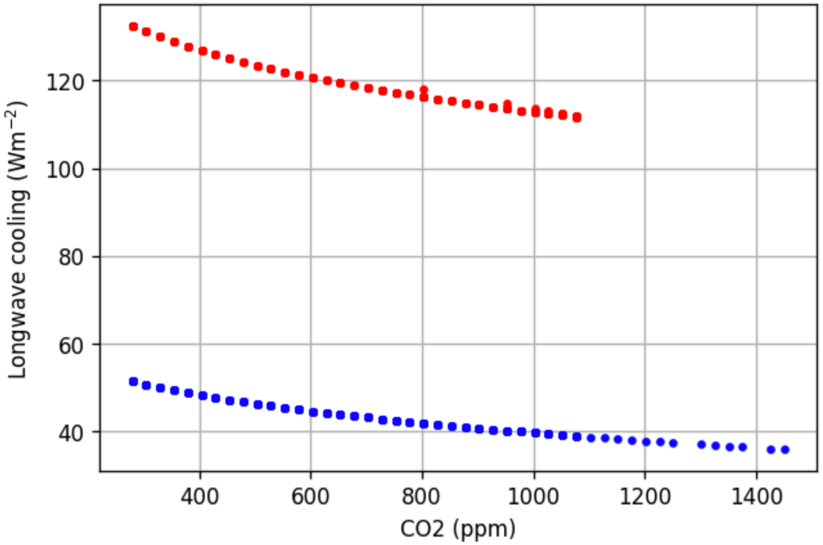

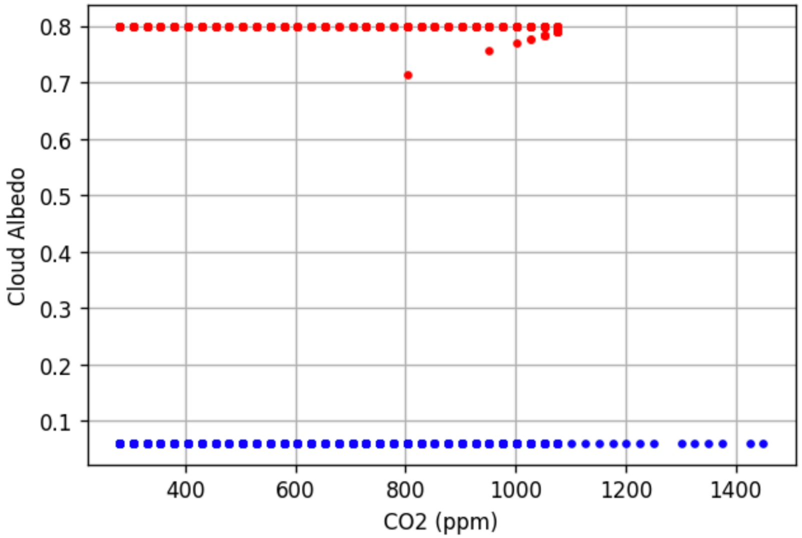

➨ Hysteresis in CO_2, as in the cloud resolving model study of Schneider et al 2020.

(Andrea Salazar, model adapted from Salazar & Tziperman, 2023)

(5)

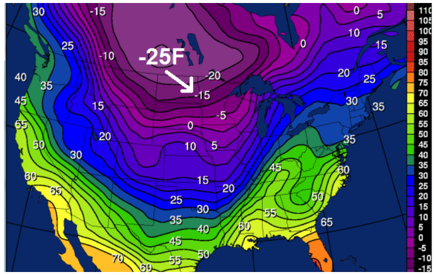

Arctic air suppression over high latitude land

By low cloud forming due to moisture arriving from over warmer ocean

Cronin & Tziperman 2015

Arctic air suppression

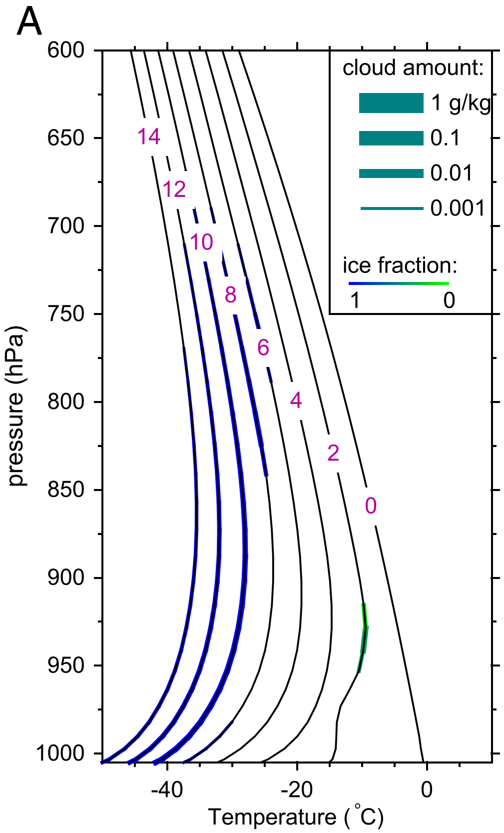

Arctic air formation

Single-column model (WRF) simulation of polar air formation with initial 2-m air temperature $T_2(t=0) = 0° C$. Simulating an air column going from ocean to over high-latitude land during winter, no solar forcing.

Results: surface temperature cools by about 60C in two weeks, strong inversion develops.

(following Judith Curry 1983)

Cronin and Tziperman 2015

Arctic air formation - mechanism

Arctic air formation for present-day initial conditions - mechanism

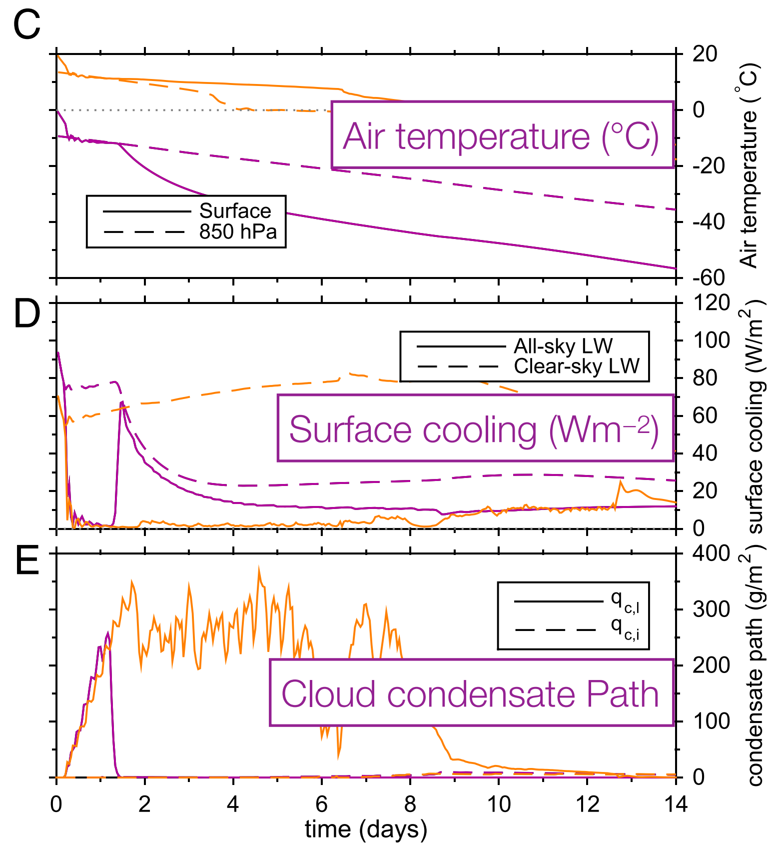

Single-column simulation of polar air formation with initial 2-m air temperature $T_2(t=0) = 0° C$

Consider purple curves only:

(following Curry 1983)

Cronin and Tziperman 2015

Arctic air formation - mechanism

Arctic air formation for present-day initial conditions - mechanism

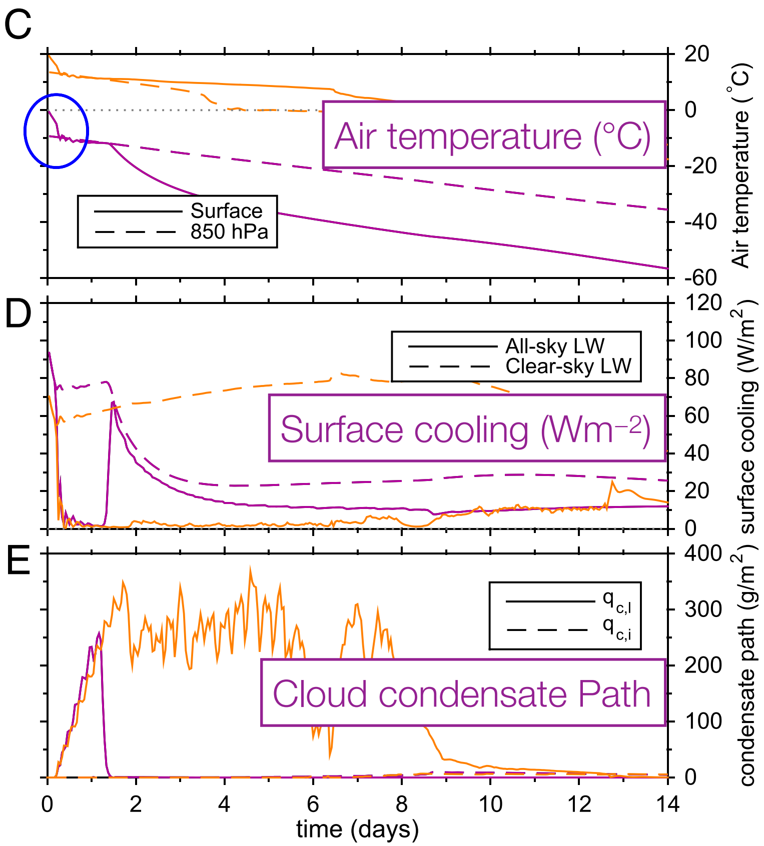

(following Curry 1983)

Single-column simulation of polar air formation with initial 2-m air temperature $T_2(t=0) = 0°$ C

Consider purple curves only:

- Rapid initial cooling to t=½ day

Cronin and Tziperman 2015

Arctic air formation - mechanism

Arctic air formation for present-day initial conditions - mechanism

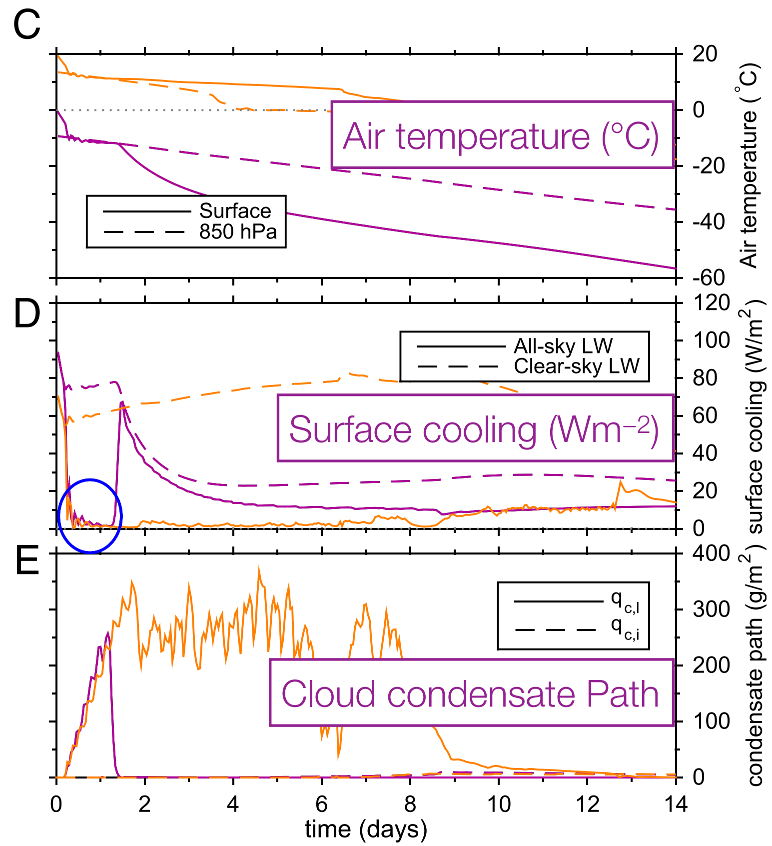

Single-column simulation of polar air formation with initial 2-m air temperature $T_2(t=0) = 0°$ C

Consider purple curves only:

- Rapid initial cooling to t=½ day
- Low clouds form during day 1, slow surface cooling, allowing the mid-atmosphere to cool very rapidly

(following Curry 1983)

Cronin and Tziperman 2015

Arctic air formation - mechanism

Arctic air formation for present-day initial conditions - mechanism

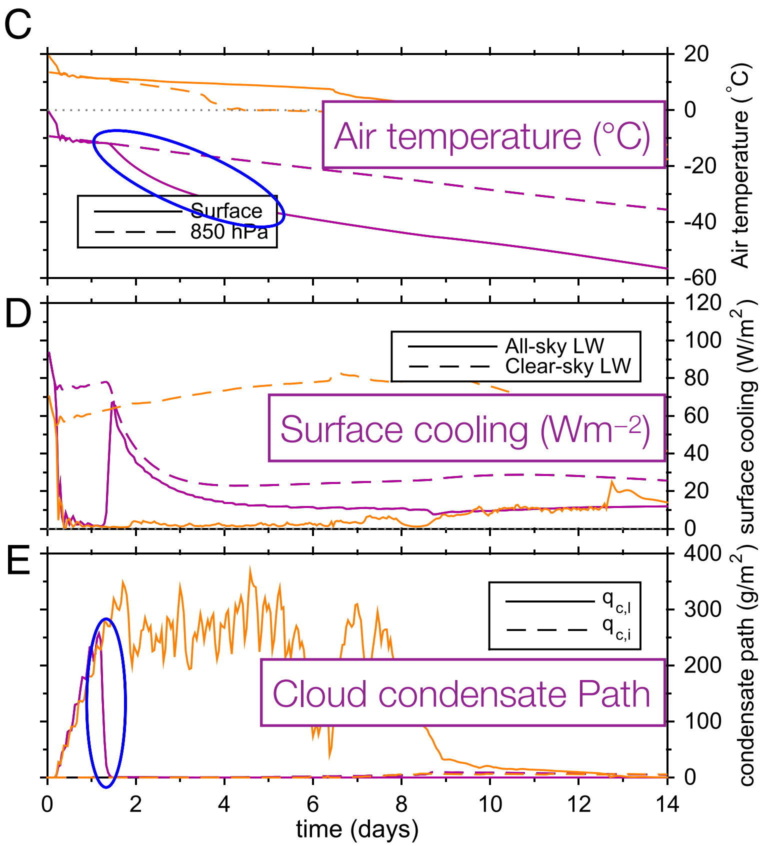

(following Curry 1983)

Single-column simulation of polar air formation with initial 2-m air temperature $T_2(t=0) = 0°\ C$

Consider purple curves only:

- Rapid initial cooling to t=½ day
- Low clouds form during day 1, slow surface cooling, allowing the mid-atmosphere to cool very rapidly
- Clouds dissipate within 1.5 days, surface cooling accelerates in the absence of LW from the mid-atmosphere.

Cronin and Tziperman 2015

Arctic air suppression

Suppression of Arctic air formation for warmer initial conditions (warmer ocean)

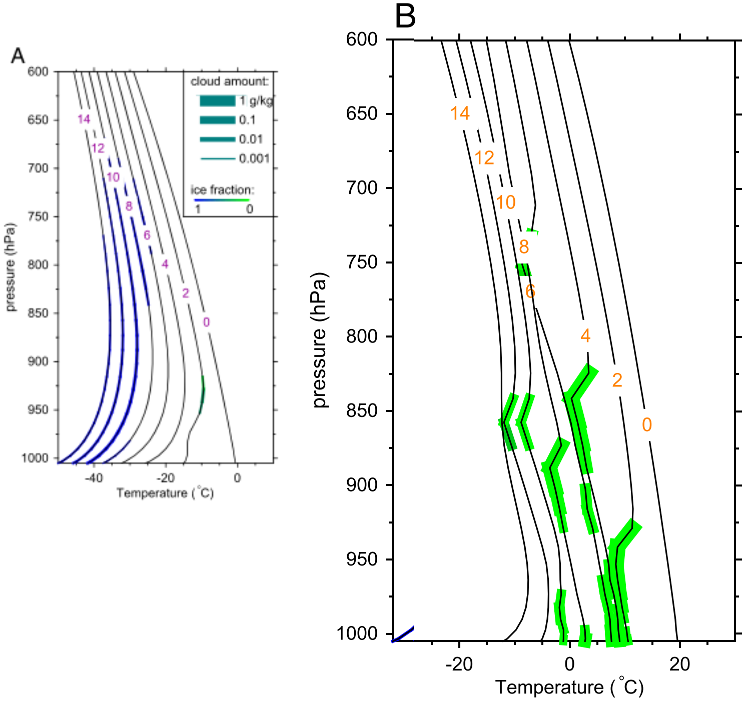

Single-column simulation of polar air formation with initial 2m air temperature $T_2(t=0) = 20^\circ$ C instead of 0° C

Day-1 cooling similar to cold initial conditions, but further surface cooling suppressed by LW effects of a liquid low cloud cloud layer!

Cronin and Tziperman 2015

Arctic air suppression

Suppression of Arctic air formation for warmer initial conditions - mechanism

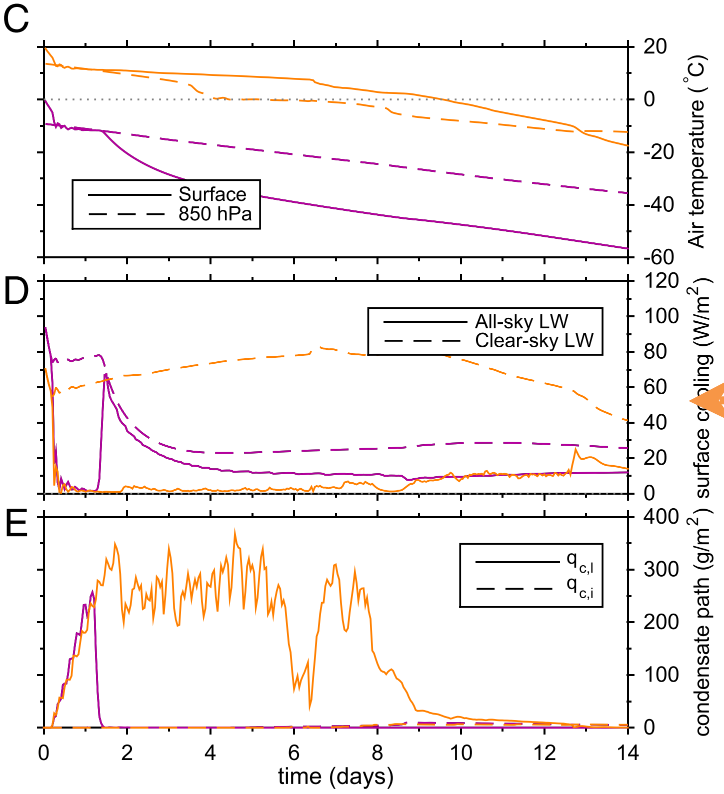

Single-column simulation of polar air formation w/initial 2-m air temperature $T_2(t=0) = 20°$ C

Consider orange curves

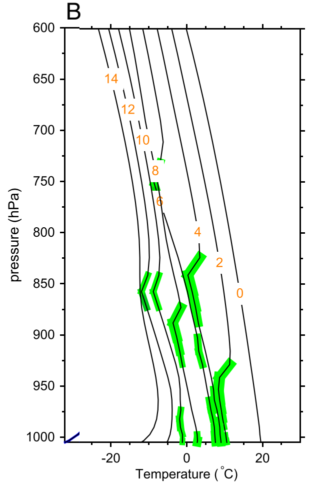

Day-1cooling similar to cold initial conditions, but further surface cooling suppressed by LW effects of a liquid low cloud cloud layer!

Cronin and Tziperman 2015

Arctic air suppression

Suppression of Arctic air formation for warmer initial conditions - mechanism

Temperature plateau, cooling surpassed

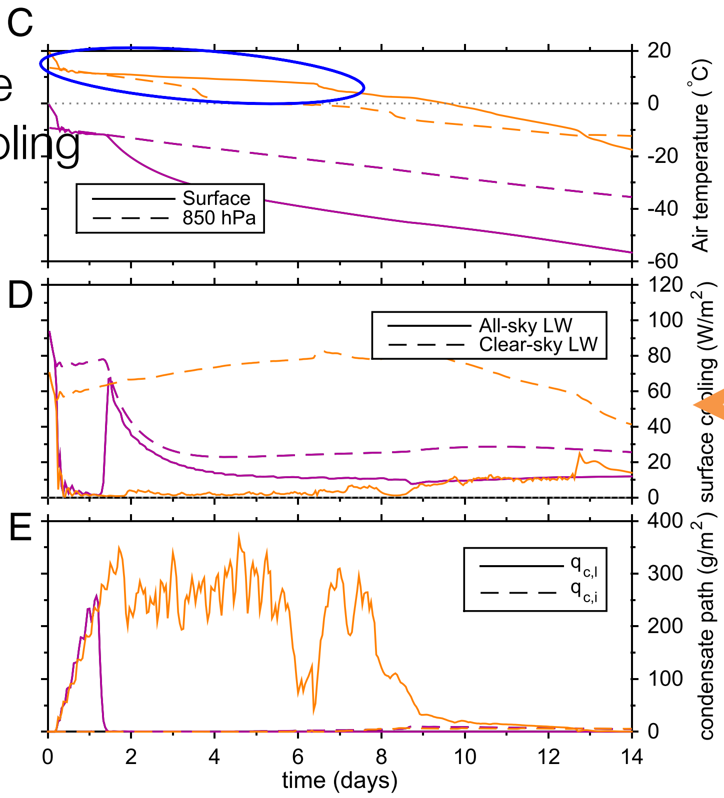

Single-column simulation of polar air formation w/initial 2-m air temperature $T_2(t=0) = 20°$ C

Consider orange curves

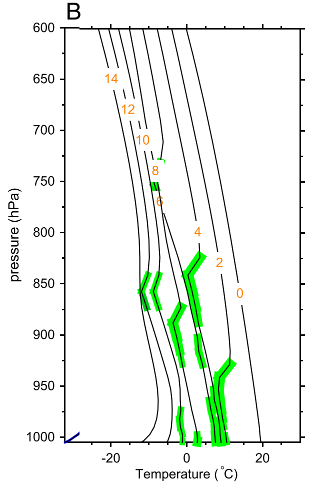

Day-1cooling similar to cold initial conditions, but further surface cooling suppressed by LW effects of a liquid low cloud cloud layer!

Cronin and Tziperman 2015

Arctic air suppression

Suppression of Arctic air formation for warmer initial conditions - mechanism

Temperature plateau, cooling surpassed

net LW cooling paused

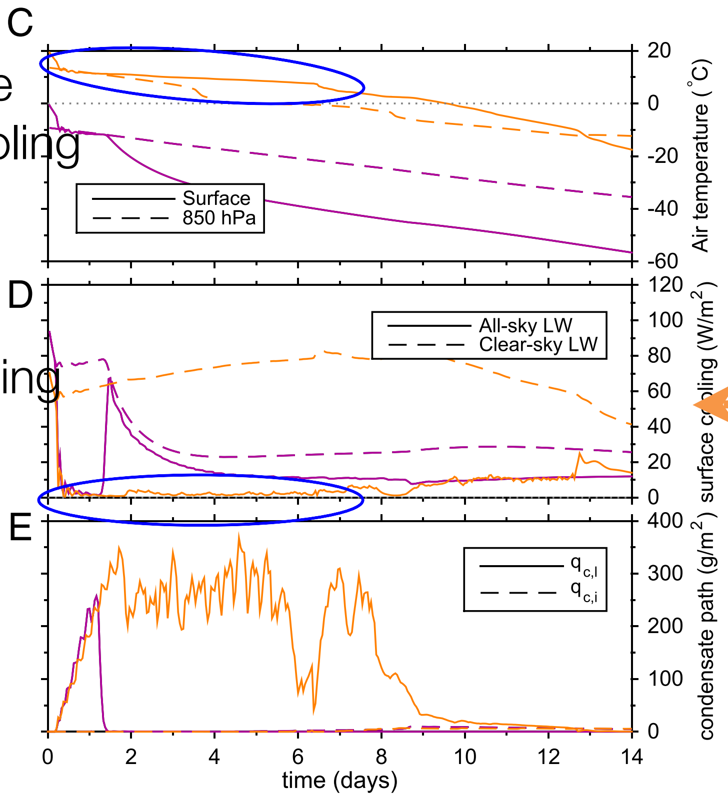

Single-column simulation of polar air formation w/initial 2-m air temperature $T_2(t=0) = 20°$ C

Consider orange curves

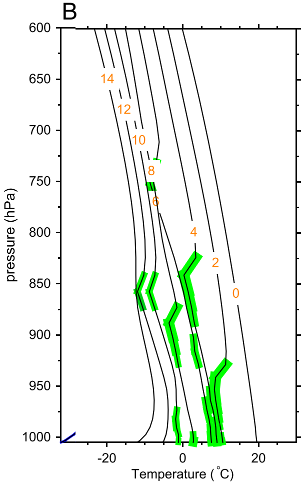

Day-1cooling similar to cold initial conditions, but further surface cooling suppressed by LW effects of a liquid low cloud cloud layer!

Cronin and Tziperman 2015

Arctic air suppression

Suppression of Arctic air formation for warmer initial conditions - mechanism

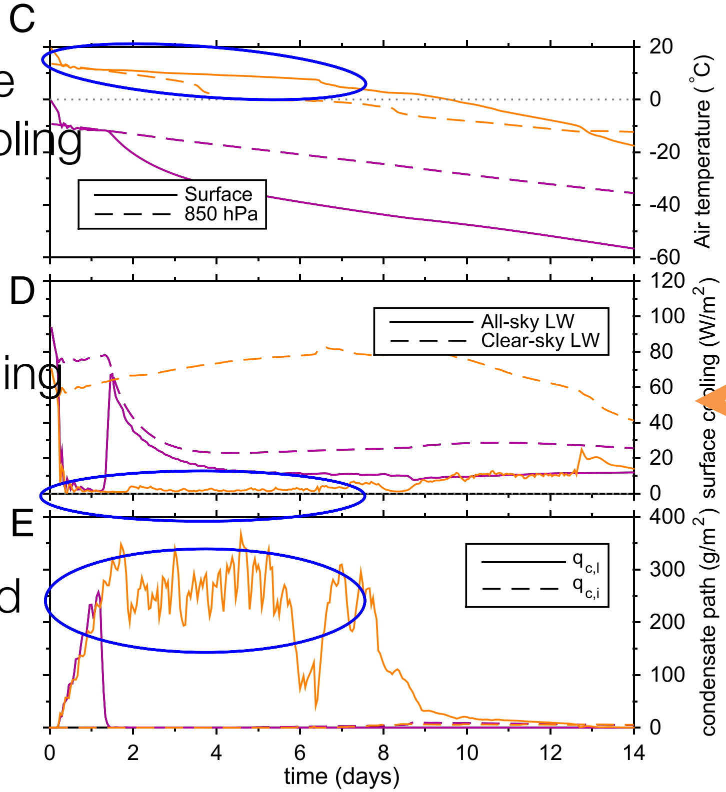

Temperature plateau, cooling surpassed

net LW cooling paused

Strong cloud liquid signal

Single-column simulation of polar air formation w/initial 2-m air temperature $T_2(t=0) = 20°$ C

Consider orange curves

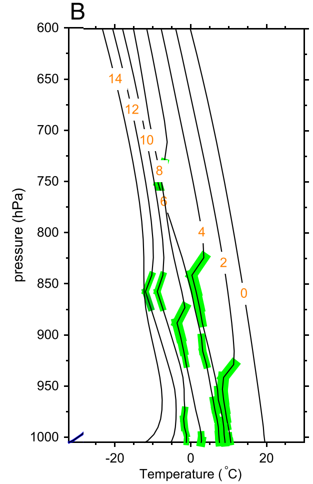

Day-1cooling similar to cold initial conditions, but further surface cooling suppressed by LW effects of a liquid low cloud cloud layer!

Cronin and Tziperman 2015

Arctic air suppression

Time-to-freezing increases nonlinearly w/initial (ocean) temperature

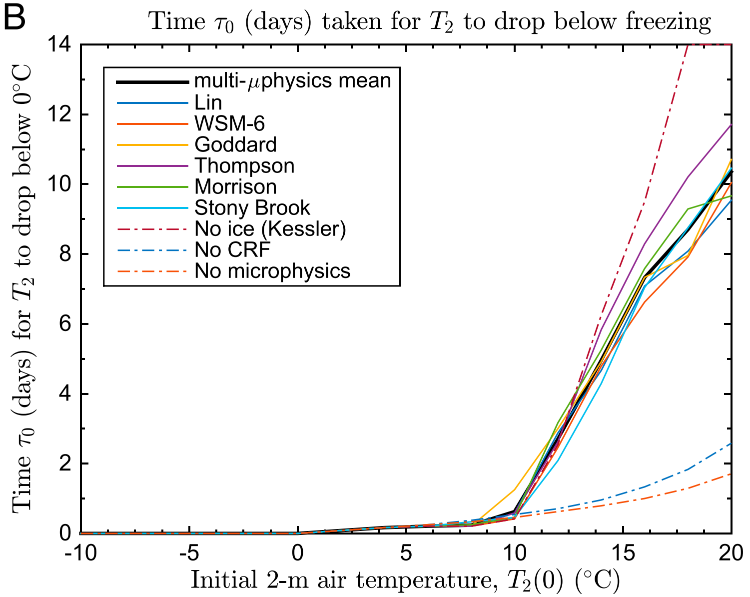

Cronin and Tziperman 2015

Arctic air suppression

Time-to-freezing increases nonlinearly w/initial (ocean) temperature

Cold initial conditions

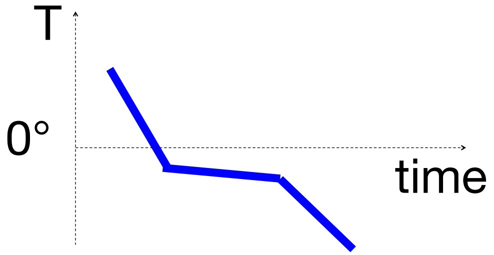

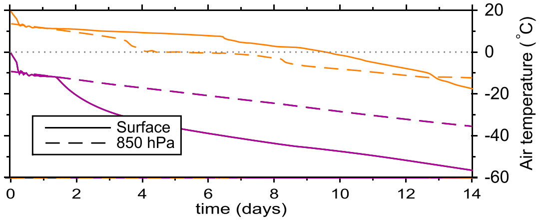

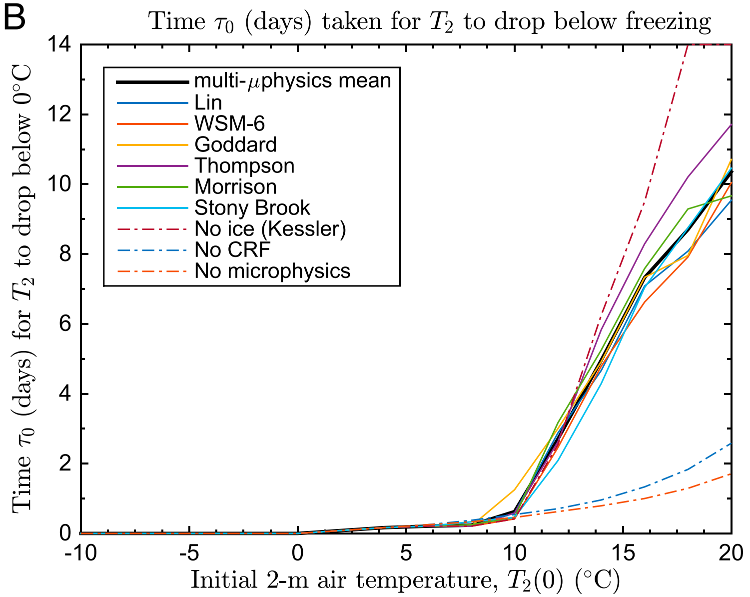

Cronin and Tziperman 2015

Arctic air suppression

Time-to-freezing increases nonlinearly w/initial (ocean) temperature

Cold initial conditions

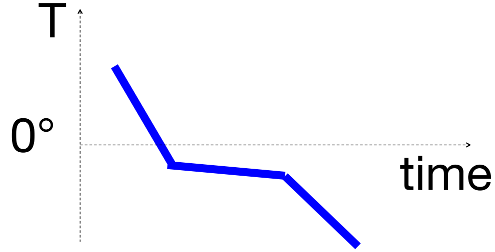

Warm initial conditions

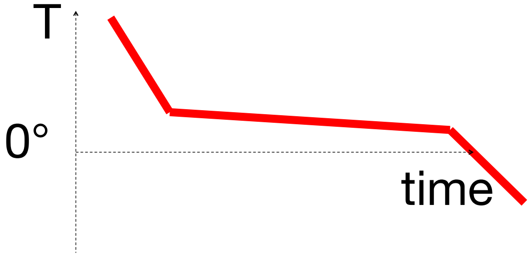

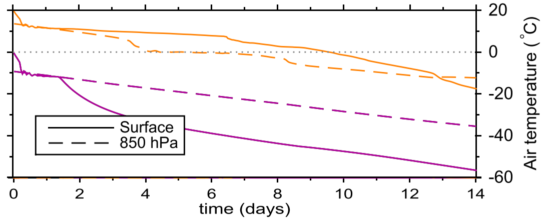

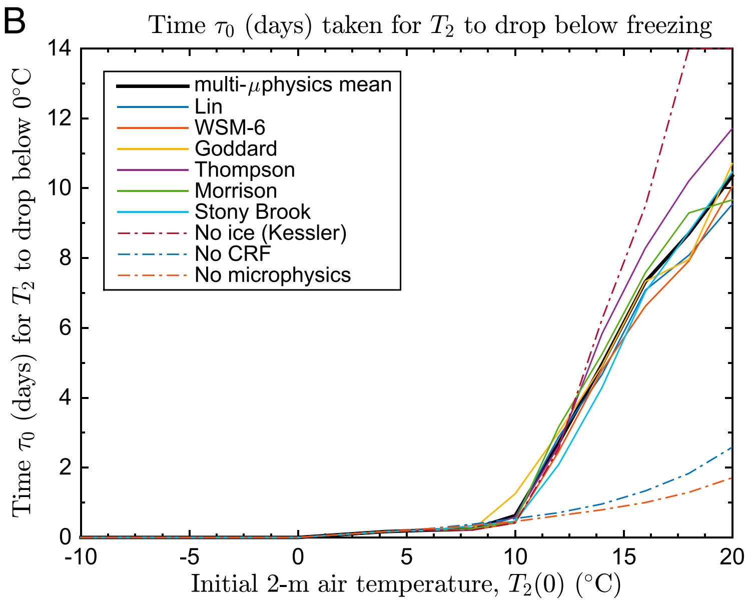

Cronin and Tziperman 2015

Arctic air suppression

Time-to-freezing increases nonlinearly w/initial (ocean) temperature

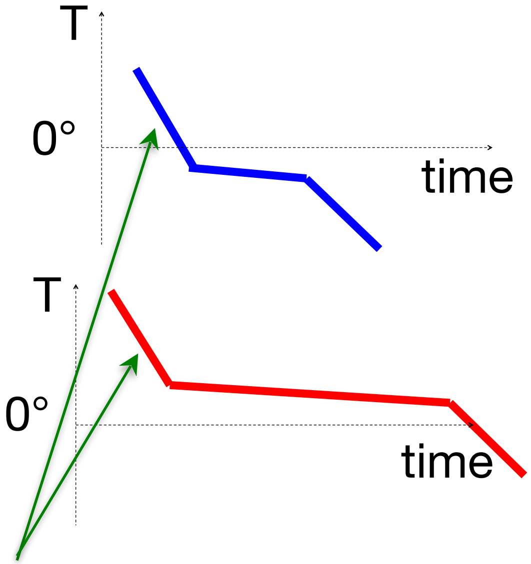

Cold initial conditions

Warm initial conditions

Initial cooling before low clouds

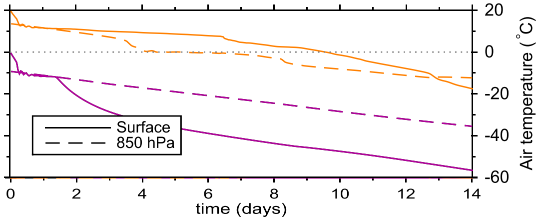

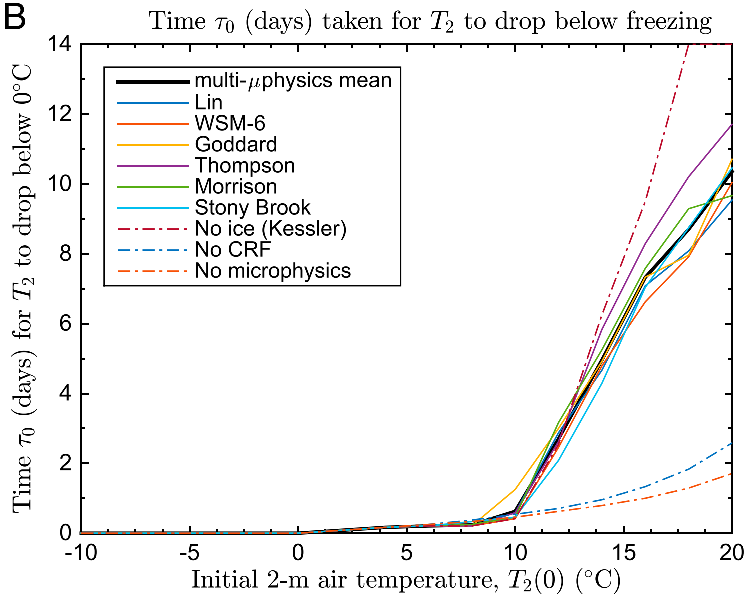

Cronin and Tziperman 2015

Arctic air suppression

Time-to-freezing increases nonlinearly w/initial (ocean) temperature

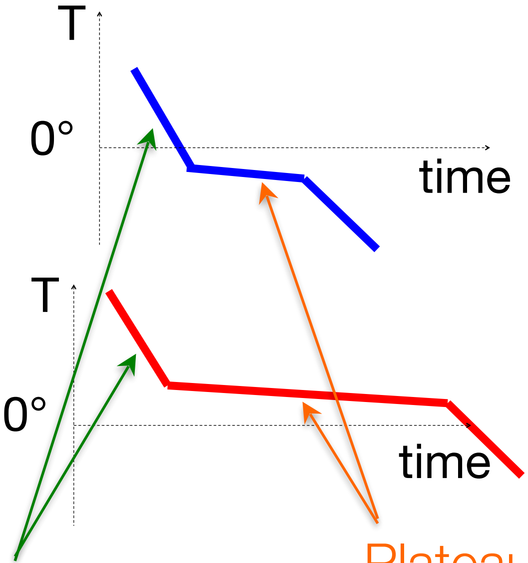

Cold initial conditions

Warm initial conditions

Initial cooling before low clouds

Plateau of suspended cooling due to low clouds

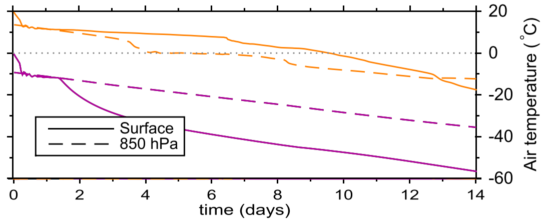

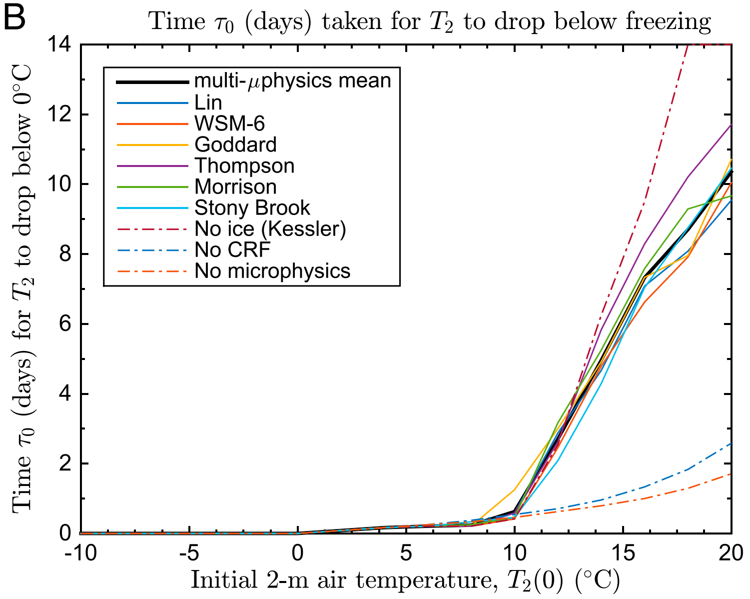

Cronin and Tziperman 2015

Arctic air suppression

Time-to-freezing increases nonlinearly w/initial (ocean) temperature

Cold initial conditions

Warm initial conditions

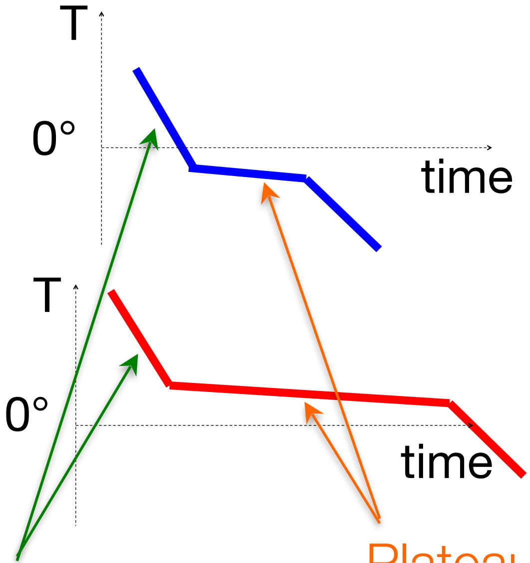

Initial cooling before low clouds

Plateau of suspended cooling due to low clouds

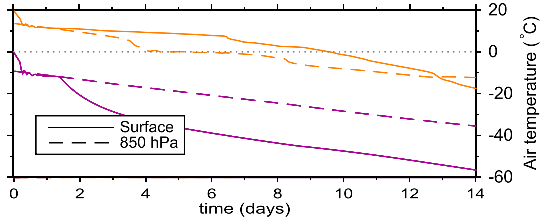

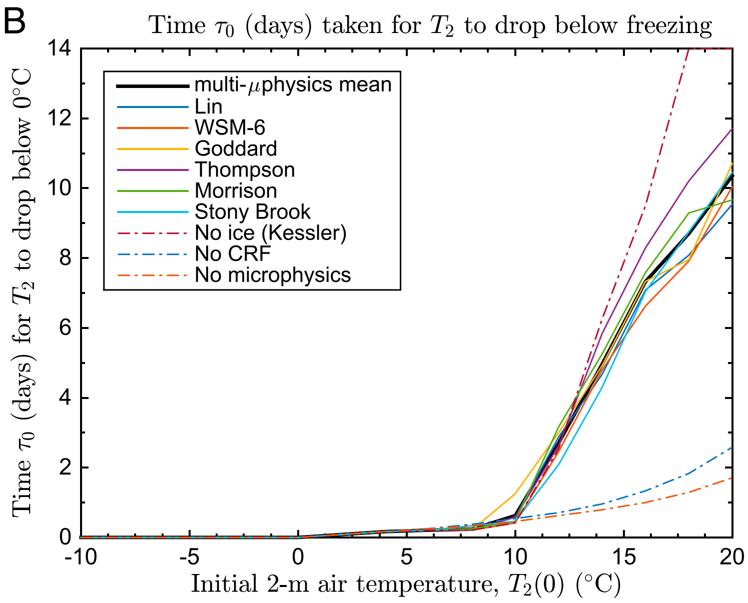

Time-to-freezing increases rapidly for $T_2(t=0)>10C$ because plateau occurs above freezing point then and keeps $T_2>0$ for a few days.

Cronin and Tziperman 2015

Arctic air suppression in a 3-dimensional atmospheric GCM

Preindustrial SST

Warmer SST

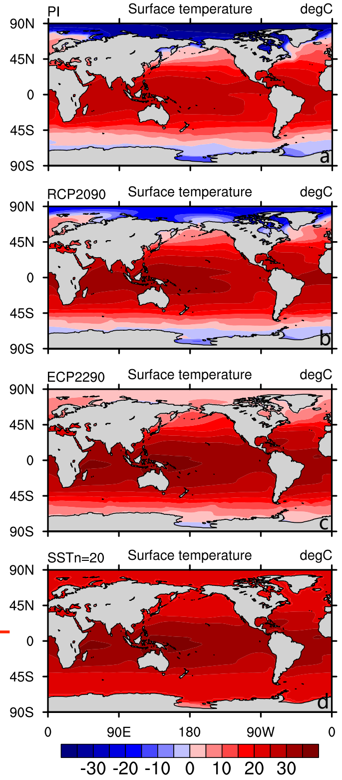

Hu, Cronin, Tziperman, 2018

Arctic air suppression in a 3-dimensional atmospheric GCM

Preindustrial SST

Warmer SST

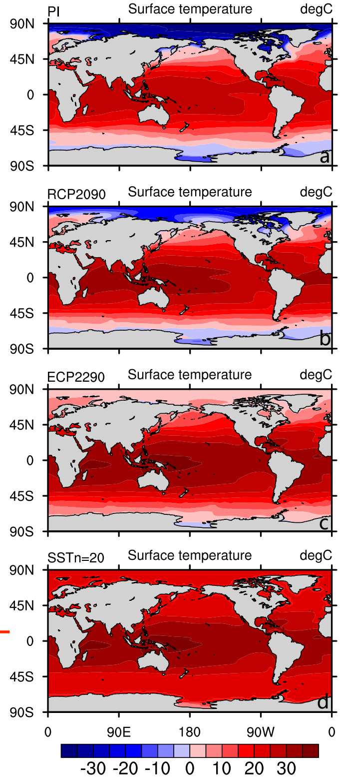

coldest 2m T for PI

coldest 2m T for warm SST

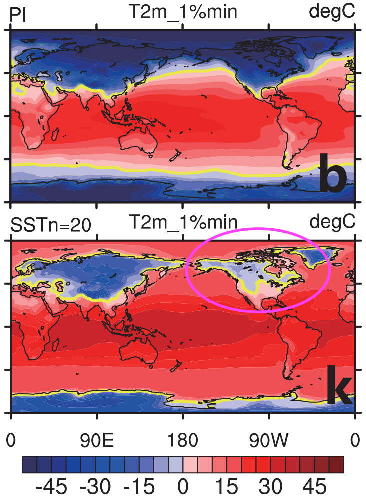

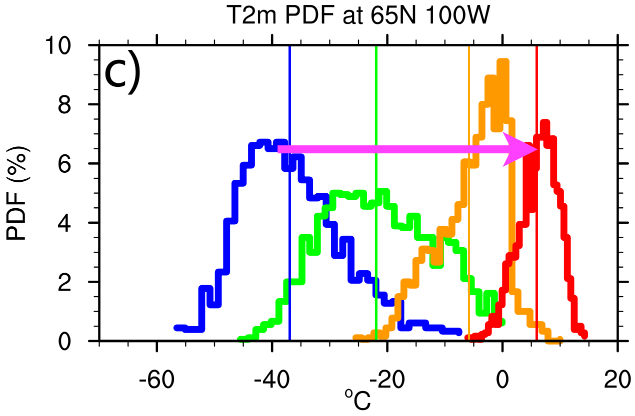

Coldest temperatures warm (mean&pdf),

Hu, Cronin, Tziperman, 2018

Arctic air suppression in a 3-dimensional atmospheric GCM

Preindustrial SST

Warmer SST

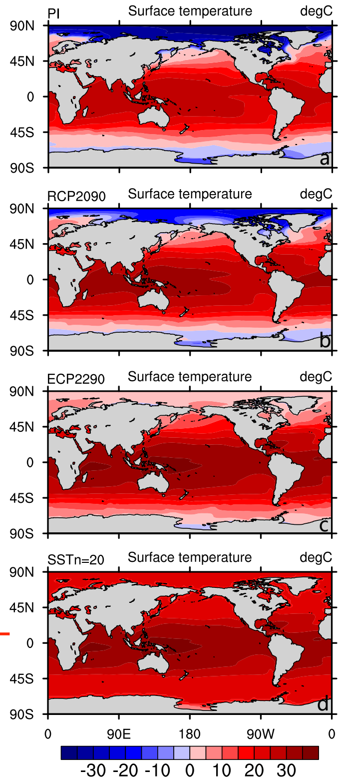

coldest 2m T for PI

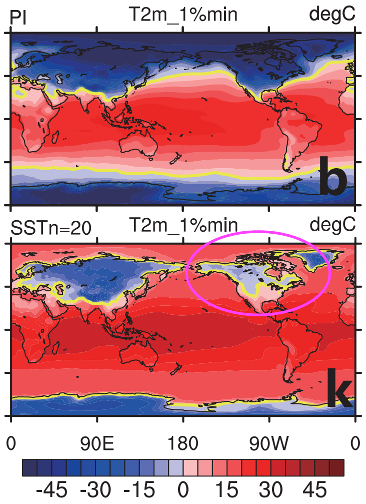

coldest 2m T for warm SST

low clouds increase over land

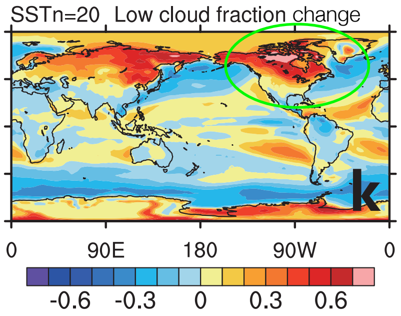

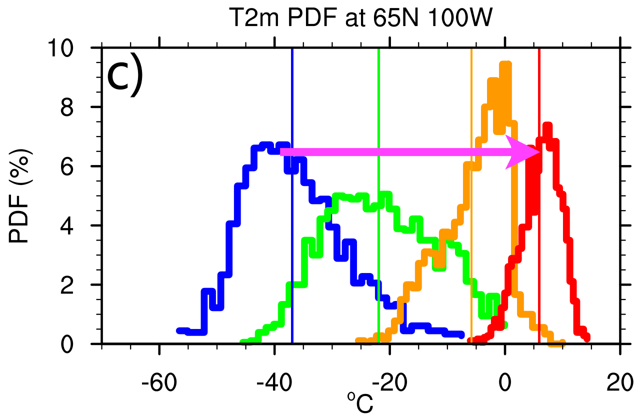

Coldest temperatures warm (mean&pdf), more low clouds over land,

Hu, Cronin, Tziperman, 2018

Arctic air suppression in a 3-dimensional atmospheric GCM

Preindustrial SST

Warmer SST

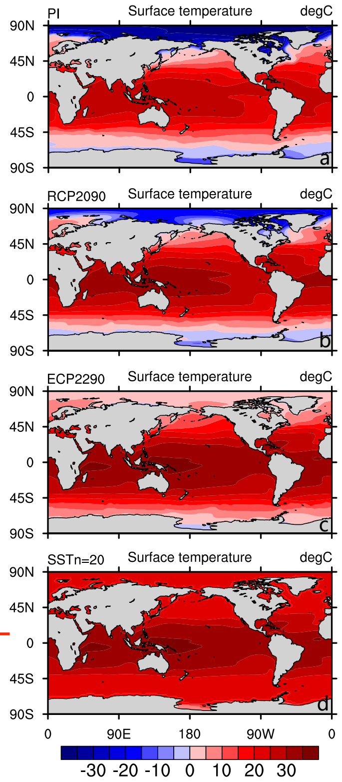

coldest 2m T for PI

coldest 2m T for warm SST

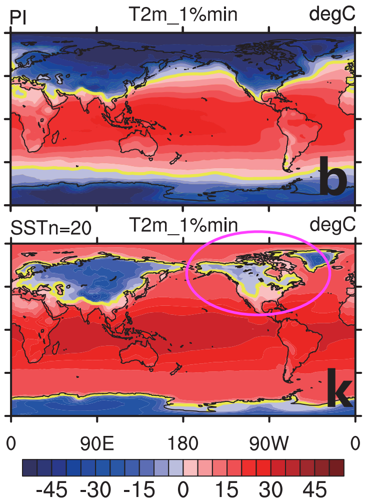

low clouds increase over land

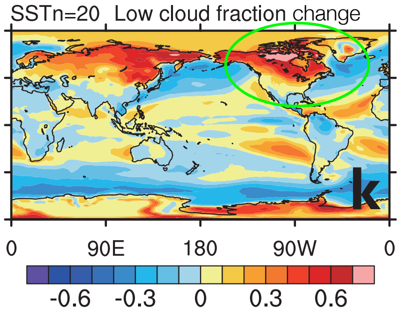

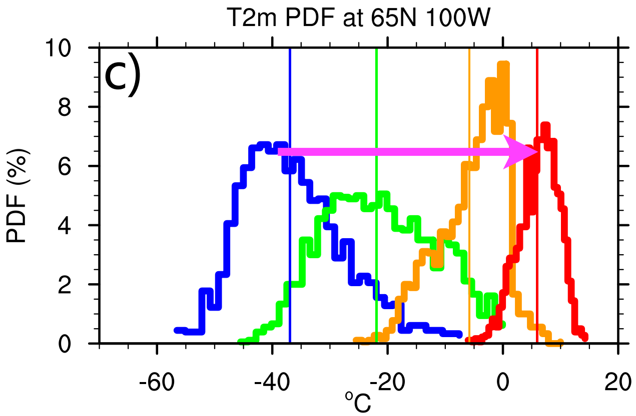

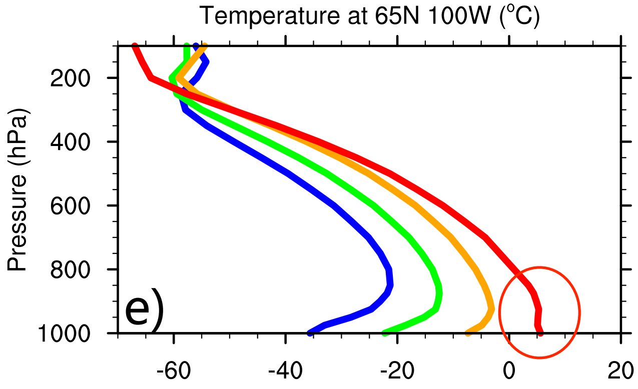

Coldest temperatures warm (mean&pdf),

more low clouds over land,

T profile without inversion

Hu, Cronin, Tziperman, 2018

Arctic air suppression in a 3-dimensional atmospheric GCM

Preindustrial SST

Warmer SST

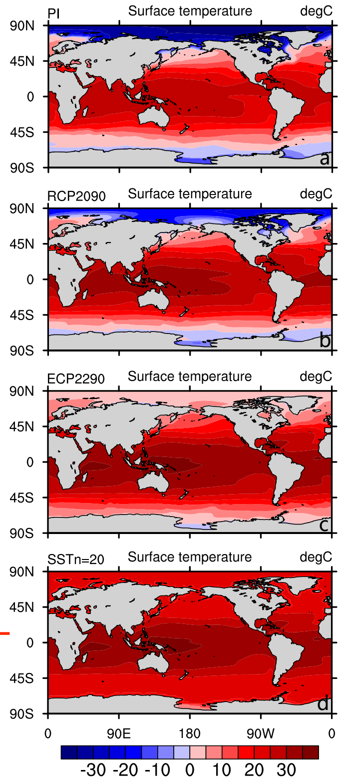

coldest 2m T for PI

coldest 2m T for warm SST

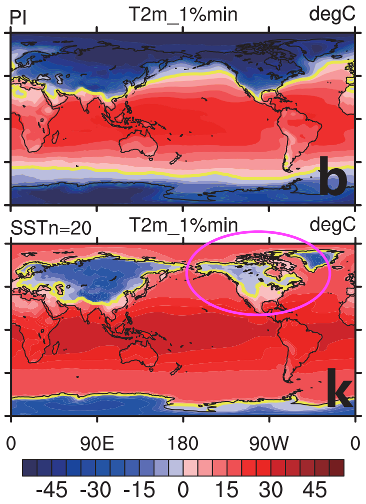

low clouds increase over land

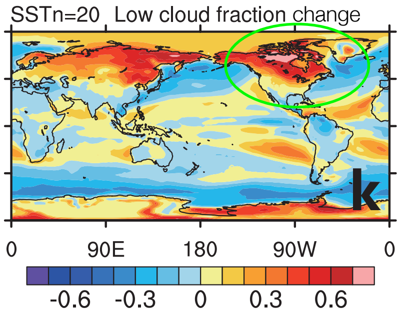

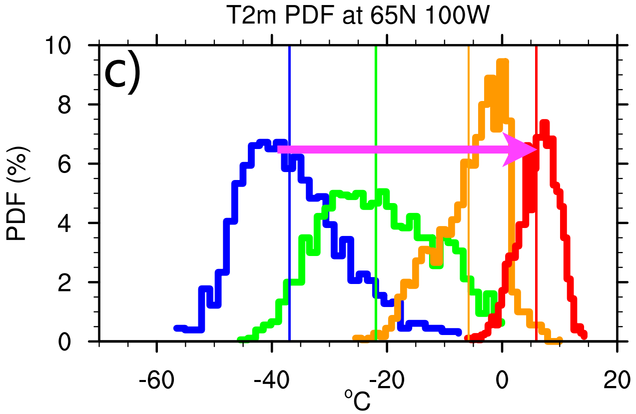

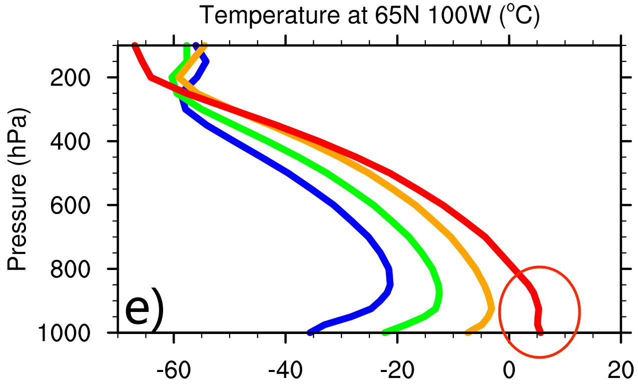

Coldest temperatures warm (mean&pdf),

more low clouds over land,

T profile without inversion - all consistent w/ Arctic air suppression

Hu, Cronin, Tziperman, 2018

Arctic convective cloud feedback

wintertime deep Arctic convection

→ high cloud emissivity/ greenhouse effect → Warmer winter Arctic

(6)

Abbot & Tziperman 2008

Arctic convective cloud feedback: idea & outline

Idea:

- In a warm climate, deep convection—which today occurs mostly in the tropics—may occur in the Arctic during polar night (😳)
- Convective cloud greenhouse effect keeps winter Arctic ice-free.
- Warmer Arctic warms temperature minima at nearby continents.

Arctic convective cloud feedback: idea & outline

Idea:

- In a warm climate, deep convection—which today occurs mostly in the tropics—may occur in the Arctic during polar night (😳)
- Convective cloud greenhouse effect keeps winter Arctic ice-free.
- Warmer Arctic warms temperature minima at nearby continents.

Outline:

1. Moist Static Energy, calculating MSE conserving T profile.
2. Moist convection: Lift Condensation Level, Level of Free Convection, Level of Neutral Buoyancy.
3. Condition on stability to convection between the surface ($z=0$) and a height z based on MSE_S vs $\mathrm{MSE}^*(z)$.
4. 2-level model formulation.
5. The solution, multiple equilibria, and hysteresis.
6. GCM verification.

Moist convection and cloud formation

Moist static energy (MSE), the energy per unit mass of a moist air parcel, is conserved when the parcel is lifted adiabatically in the atmosphere,

$$MSE(z) = c_p T(z) + gz + Lq(z)$$

c_p: specific heat, J/(kg K); L: latent heat of condensation J/kg;

$q(z)$: specific humidity (kg water vapor/kg air)

Moist convection and cloud formation

Moist static energy (MSE), the energy per unit mass of a moist air parcel, is conserved when the parcel is lifted adiabatically in the atmosphere,

$$MSE(z) = c_p T(z) + gz + Lq(z)$$

c_p: specific heat, J/(kg K); L: latent heat of condensation J/kg;

$q(z)$: specific humidity (kg water vapor/kg air)

Parcel starts at surface, with $MSE_s = c_p T_s + L q_s$. Initially, the rising air parcel is not saturated & there is no condensation, $q(z) = q_s$ so that the conservation may be written in terms of the *Dry Static Energy* as: $DSE(z) = c_p T(z) + gz = c_p T_s$

Moist convection and cloud formation

Moist static energy (MSE), the energy per unit mass of a moist air parcel, is conserved when the parcel is lifted adiabatically in the atmosphere,

$$MSE(z) = c_p T(z) + gz + Lq(z)$$

c_p: specific heat, J/(kg K); L: latent heat of condensation J/kg;

$q(z)$: specific humidity (kg water vapor/kg air)

Parcel starts at surface, with $MSE_s = c_p T_s + Lq_s$. Initially, the rising air parcel is not saturated & there is no condensation, $q(z) = q_s$ so that the conservation may be written in terms of the *Dry Static Energy* as: $DSE(z) = c_p T(z) + gz = c_p T_s$

This leads to a solution for the temperature profile and lapse rate,

$$T(z) = T_s - gz/c_p, \qquad dT/dz = -g/c_p = -9.8\ \mathrm{K/km}$$

Moist convection and cloud formation

The parcel keeps rising & cooling, until the saturation moisture is smaller than the parcel's moisture & condensation occurs, $q(z) = q^*(T(z), p(z))$. The conservation law is $c_p T(z) + L q^*(T(z), p(z)) + gz = MSE_s$ which may be solved graphically for $T(z)$.

Moist convection and cloud formation

The parcel keeps rising & cooling, until the saturation moisture is smaller than the parcel's moisture & condensation occurs, $q(z) = q^*(T(z), p(z))$. The conservation law is $c_p T(z) + Lq^*(T(z), p(z)) + gz = MSE_s$ which may be solved graphically for $T(z)$.

Both the initial unsaturated & the later saturated MSE conservation of the air-parcel ascent may be written as

$$MSE_s = c_p T(z) + gz + L\min(q_s, q^*(T(z), p(z))$$

Moist convection and cloud formation

The parcel keeps rising & cooling, until the saturation moisture is smaller than the parcel's moisture & condensation occurs, $q(z) = q^*(T(z), p(z))$. The conservation law is $c_p T(z) + Lq^*(T(z), p(z)) + gz = MSE_s$ which may be solved graphically for $T(z)$.

Both the initial unsaturated & the later saturated MSE conservation of the air-parcel ascent may be written as

$$MSE_s = c_p T(z) + gz + L\min(q_s, q^*(T(z), p(z))$$

To solve, need to find $p(z)$ from the vertical momentum (hydrostatic) balance for an air parcel: $dp/dz = -\rho g$. Using $\rho = p/(RT)$ this becomes $dp/dz = -pg/RT$, or $d\ln p = -(g/RT)\,dz$.

Integrating, we find $\ln p(z) - \ln p_s = -gz/R\overline{T}$,

so that $p(z) = p_s e^{-gz/R\overline{T}}$

➨ pressure is exponential in height.

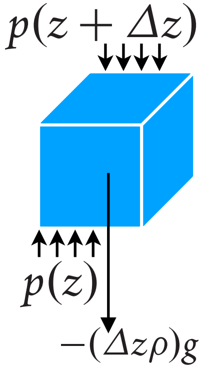

Calculating T from MSE conservation

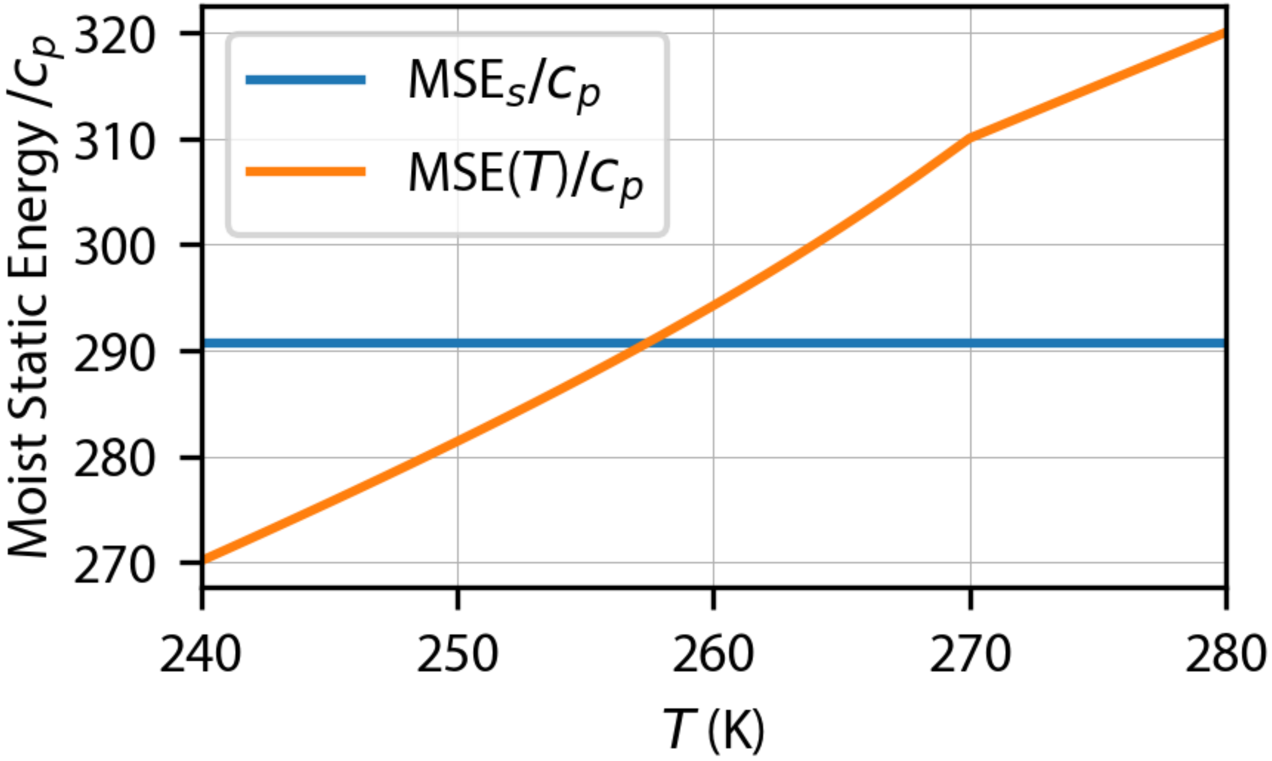

Moist Convection: LCL, LFC, LNB

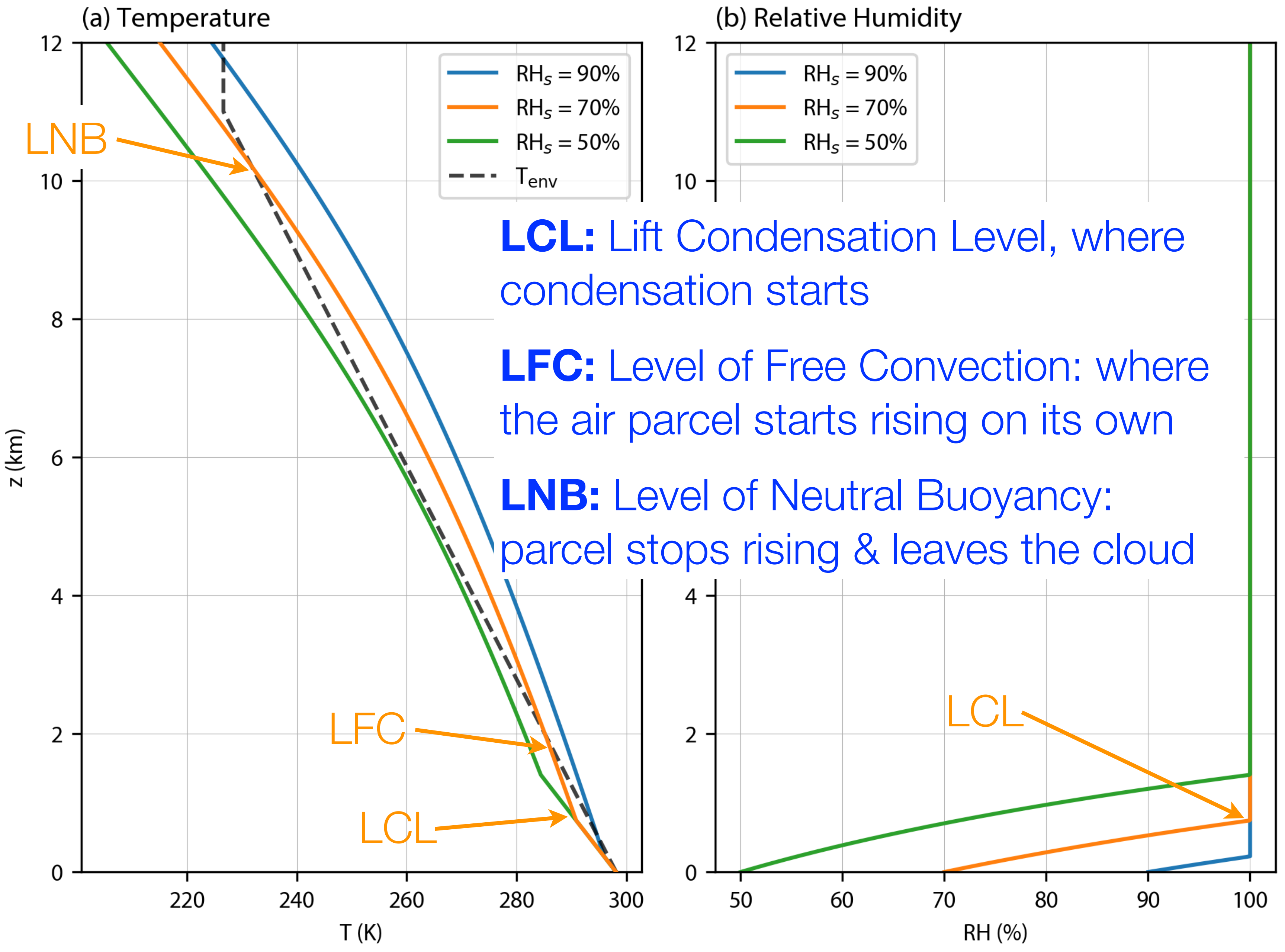

LCL: Lift Condensation Level, where condensation starts

LFC: Level of Free Convection: where the air parcel starts rising on its own

LNB: Level of Neutral Buoyancy: parcel stops rising & leaves the cloud

Condition for convection to occur between surface & *z*

Condition for convection to occur between surface & z

If z is high enough, we expect a parcel starting at the surface to be saturated there:

$$MSE^{parcel}(z) = MSE^{*,parcel}(z).$$

MSE conservation for the parcel also implies:

$$MSE^{parcel}(0) = MSE^{parcel}(z) = MSE^{*,parcel}(z)$$

A parcel brought to z will be unstable if

$$T^{parcel}(z) \geq T^{env}(z)$$

Because $MSE*$ is only a function of temperature, this can be written as

$$MSE^{*,parcel}(z) \geq MSE^{*,env}$$

Given above conservation for parcel, condition for convection becomes

$$MSE_s \geq MSE^{*,env}$$

Multiple equilibria due to convective cloud feedback

(Abbot & Tziperman 2009)

A 2-level energy balance model with convective heat flux:

$$C_s dT_s/dt = F_s - F_c + \epsilon\sigma T_a^4 - \sigma T_s^4,$$
$$C_a dT_a/dt = F_a + F_c + \epsilon\sigma(T_s^4 - 2T_a^4).$$

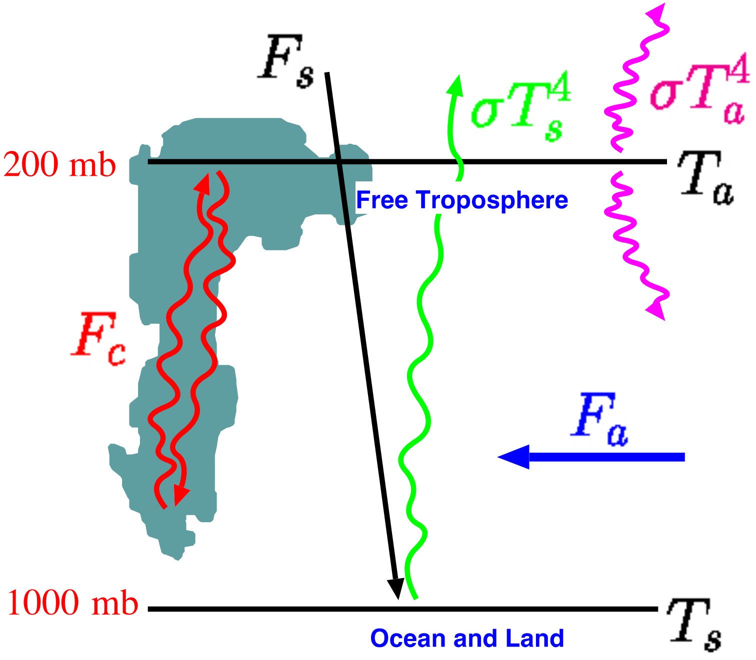

Multiple equilibria due to convective cloud feedback

(Abbot & Tziperman 2009)

A 2-level energy balance model with convective heat flux:

$$C_s dT_s/dt = F_s - F_c + \epsilon\sigma T_a^4 - \sigma T_s^4,$$

$$C_a dT_a/dt = F_a + F_c + \epsilon\sigma(T_s^4 - 2T_a^4).$$

convection occurs when moist static

Energy (MSE) satisfies

$$MSE_s = C_p T_s + g z_s + L r_s$$

$$MSE_a^* = C_p T_a + g z_a + L r_a^*$$

$$MSE_s > MSE_a^*$$

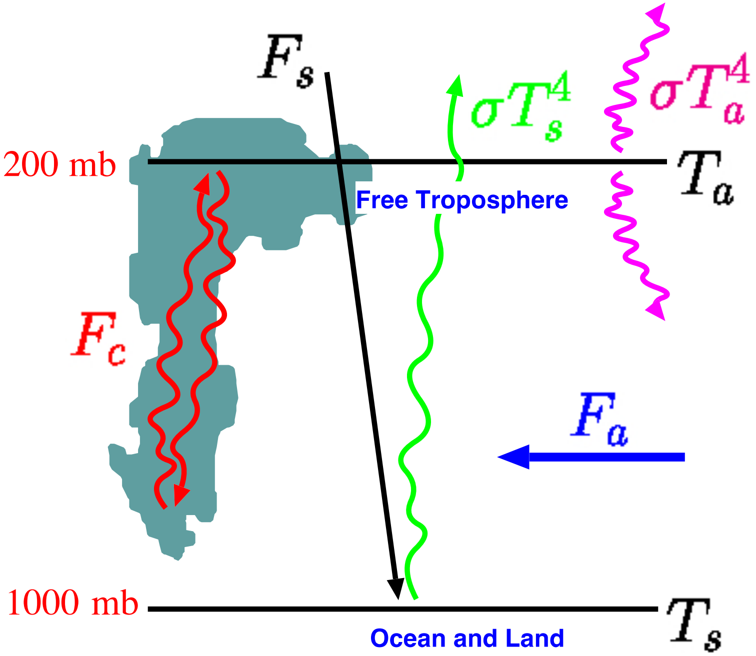

Multiple equilibria due to convective cloud feedback

(Abbot & Tziperman 2009)

A 2-level energy balance model with convective heat flux:

$$C_s dT_s/dt = F_s - F_c + \epsilon\sigma T_a^4 - \sigma T_s^4,$$
$$C_a dT_a/dt = F_a + F_c + \epsilon\sigma(T_s^4 - 2T_a^4).$$

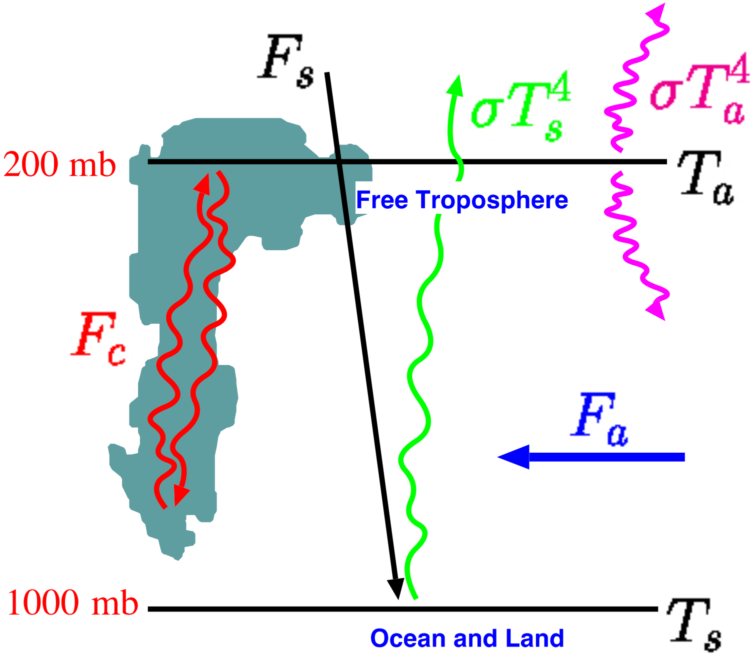

convection occurs when moist static Energy (MSE) satisfies

$$MSE_s = C_p T_s + g z_s + L r_s$$
$$MSE_a^* = C_p T_a + g z_a + L r_a^*$$
$$MSE_s > MSE_a^*$$

Without convection, find two temperatures from:

$$0 = F_s + \epsilon\sigma T_{a2}^4 - \sigma T_{s2}^4,$$
$$0 = F_a + \epsilon\sigma(T_{s2}^4 - 2T_{a2}^4),$$

Multiple equilibria due to convective cloud feedback

(Abbot & Tziperman 2009)

A 2-level energy balance model with convective heat flux:

$$C_s dT_s/dt = F_s - F_c + \epsilon\sigma T_a^4 - \sigma T_s^4,$$

$$C_a dT_a/dt = F_a + F_c + \epsilon\sigma (T_s^4 - 2T_a^4).$$

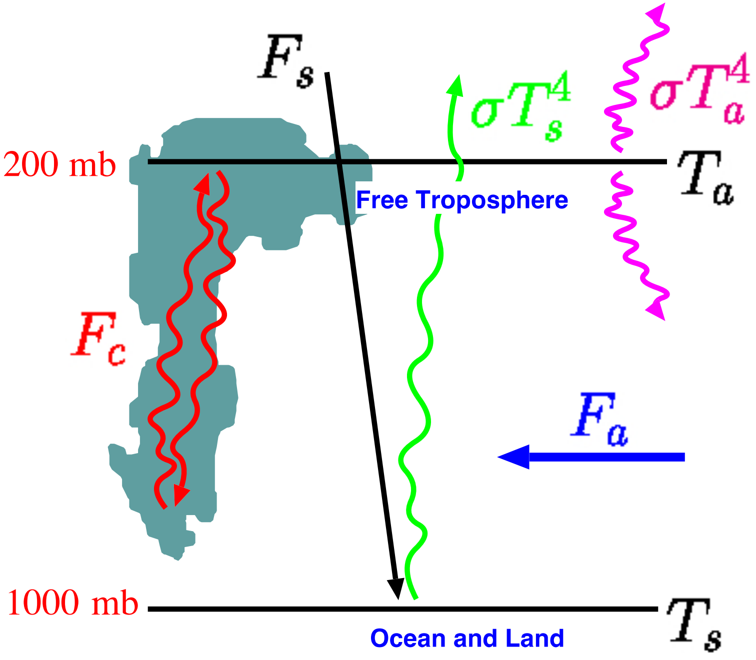

convection occurs when moist static Energy (MSE) satisfies

$$MSE_s = C_p T_s + g z_s + L r_s$$

$$MSE_a^* = C_p T_a + g z_a + L r_a^*$$

$$MSE_s > MSE_a^*$$

Without convection, find two temperatures from:

$$0 = F_s + \epsilon\sigma T_{a2}^4 - \sigma T_{s2}^4,$$

$$0 = F_a + \epsilon\sigma (T_{s2}^4 - 2T_{a2}^4),$$

With convection: cloud emissivity increases: & found from

$$\tilde{\epsilon} = \epsilon_0 + \Delta\epsilon \quad F_c, T_a, T_s$$

$$0 = F_s - F_c + \tilde{\epsilon}\sigma T_{a2}^4 - \sigma T_{s2}^4,$$

$$0 = F_a + F_c + \tilde{\epsilon}\sigma (T_{s2}^4 - 2T_{a2}^4),$$

$$C_p T_{s2} + L r_{s2} = C_p T_{a2} + L r_{a2}^* + g z_a$$

Multiple equilibria due to convective cloud feedback

(Abbot & Tziperman 2009)

Results for surface temperature: multiple equilibria!

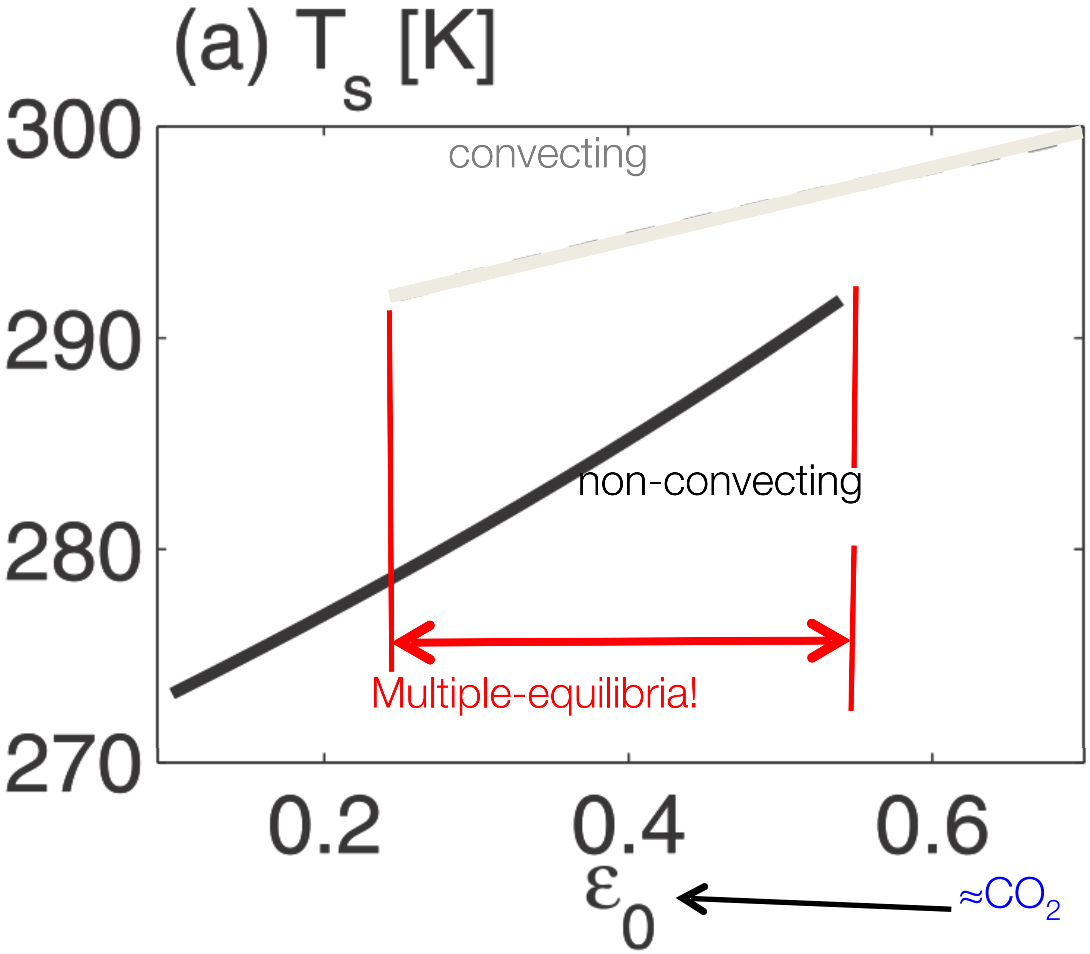

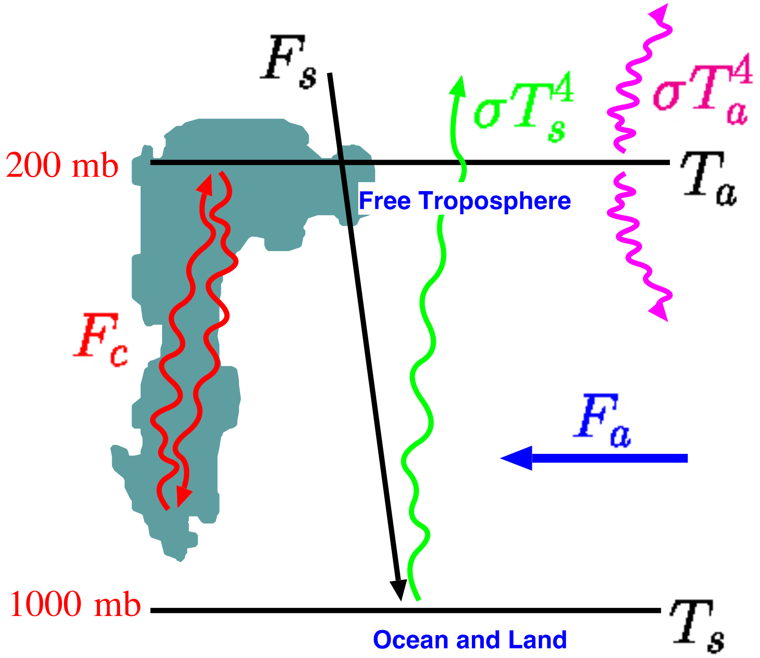

Note: must check self-consistency of sol’n with/without convection

Multiple equilibria due to convective cloud feedback

(Abbot & Tziperman 2009)

Reviews & then the following slide with GCM results supporting this mechanism

Back to the future

Enticing 3D IPCC Model Simulations

Consider the NCAR & GFDL 3d coupled ocean-atmosphere state-of-the-art (2009…) models, at x4 CO_2; anomaly from pre-industrial

Enticing 3D IPCC Model Simulations

Consider the NCAR & GFDL 3d coupled ocean-atmosphere state-of-the-art (2009…) models, at x4 CO_2; anomaly from pre-industrial

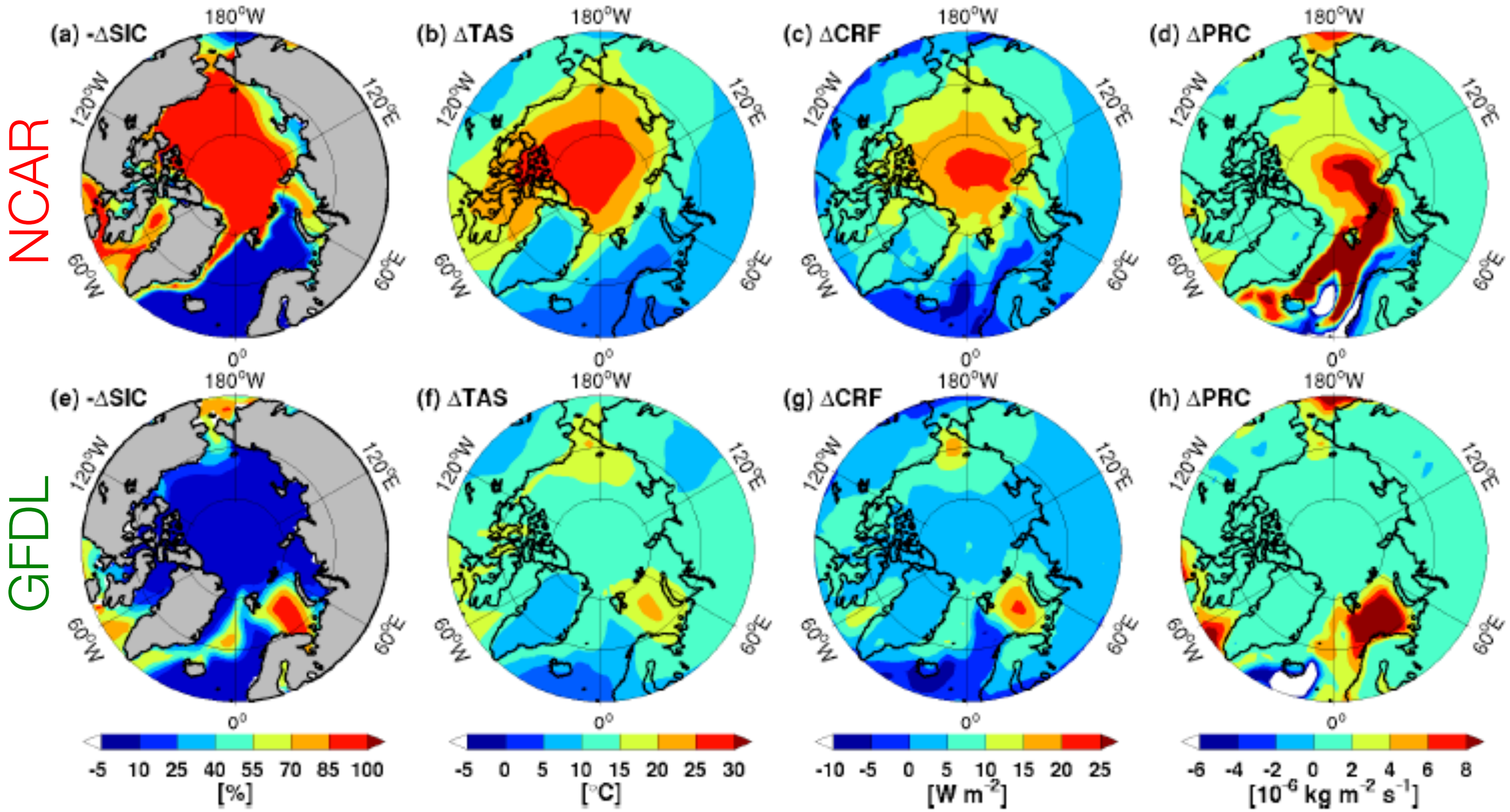

Enticing 3D IPCC Model Simulations

Consider the NCAR & GFDL 3d coupled ocean-atmosphere state-of-the-art (2009…) models, at x4 CO_2; anomaly from pre-industrial

NCAR

GFDL

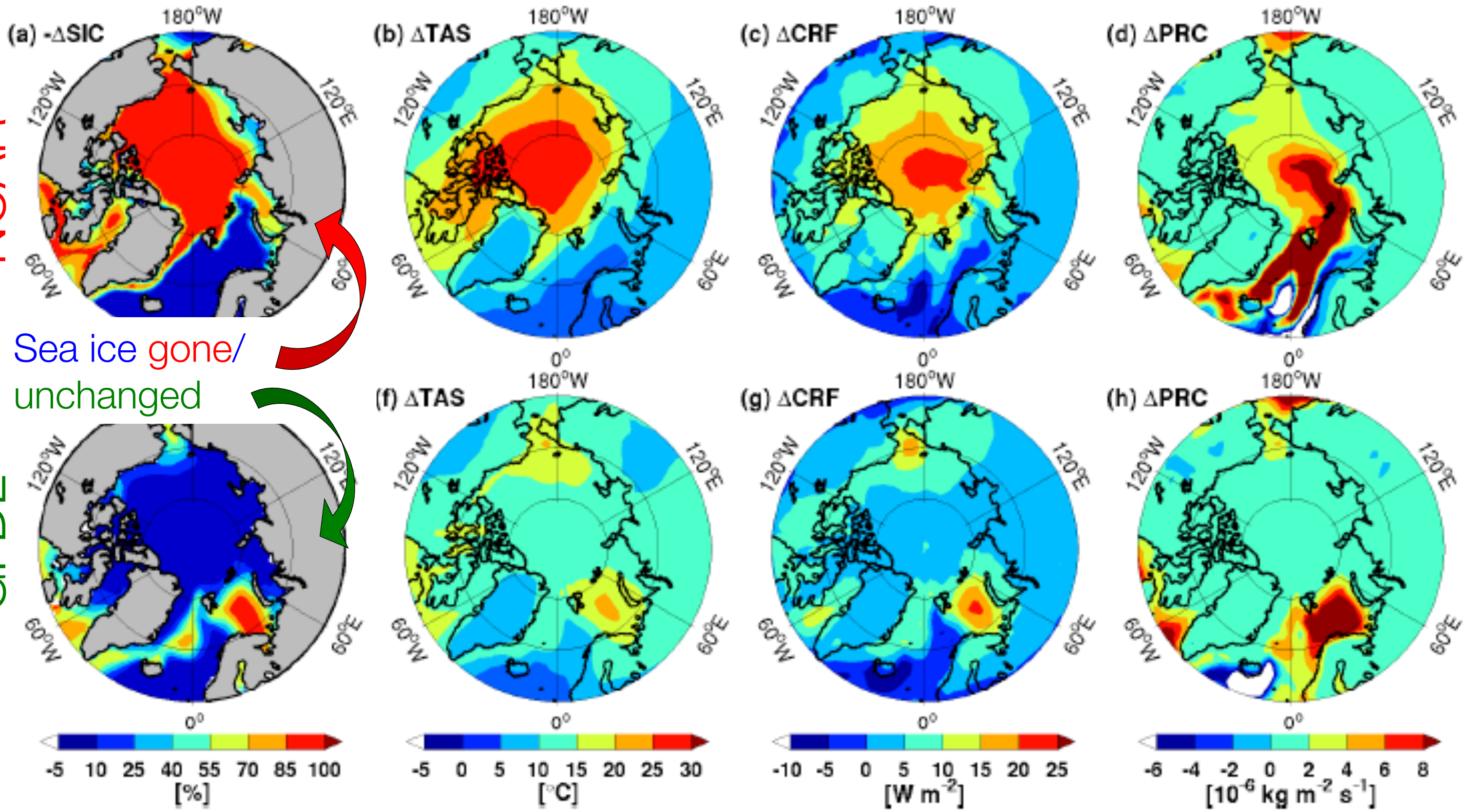

Sea ice gone/
unchanged

Enticing 3D IPCC Model Simulations

Consider the NCAR & GFDL 3d coupled ocean-atmosphere state-of-the-art (2009…) models, at x4 CO_2; anomaly from pre-industrial

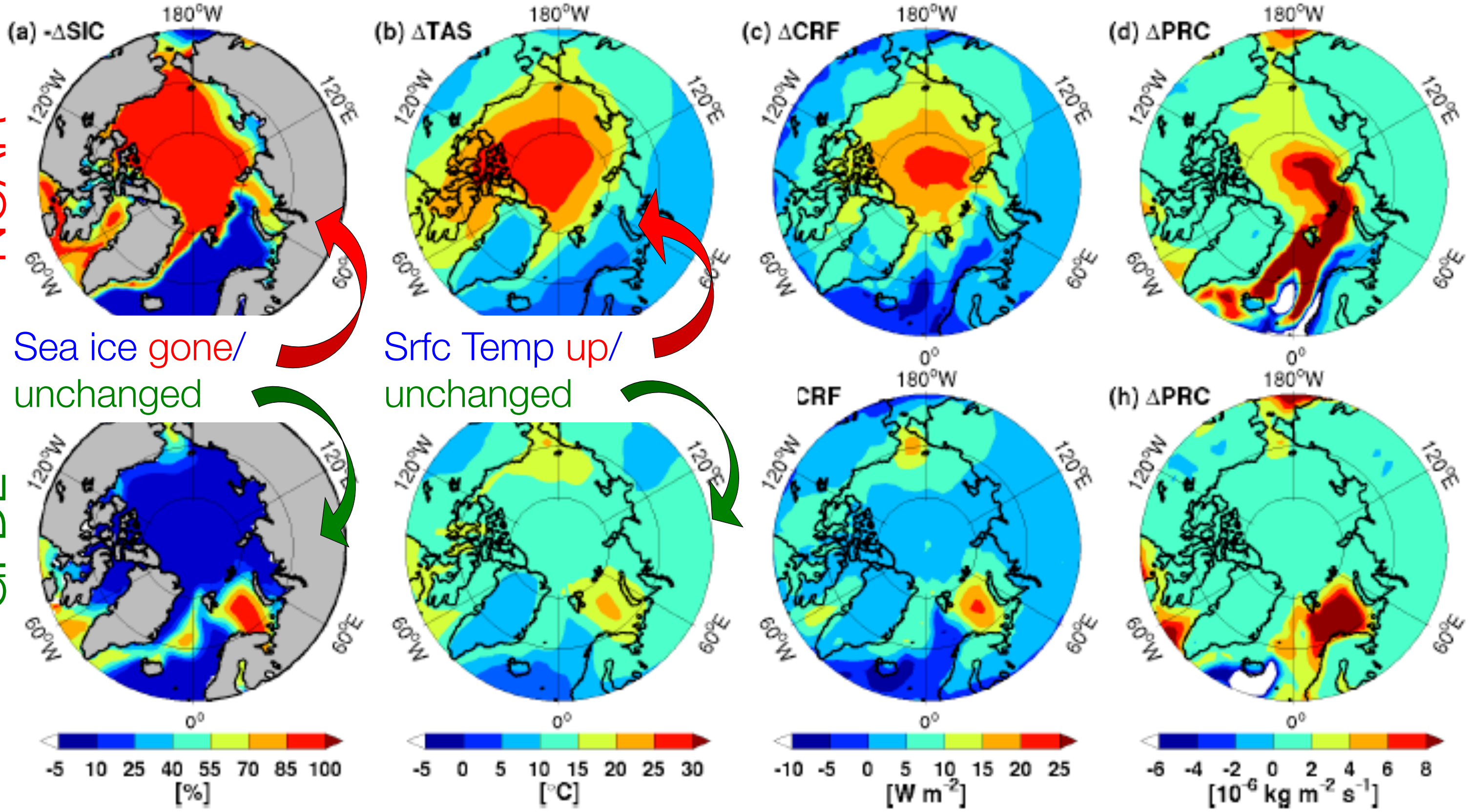

NCAR

GFDL

Sea ice gone/ unchanged

Srfc Temp up/ unchanged

Enticing 3D IPCC Model Simulations

Consider the NCAR & GFDL 3d coupled ocean-atmosphere state-of-the-art (2009…) models, at x4 CO_2; anomaly from pre-industrial

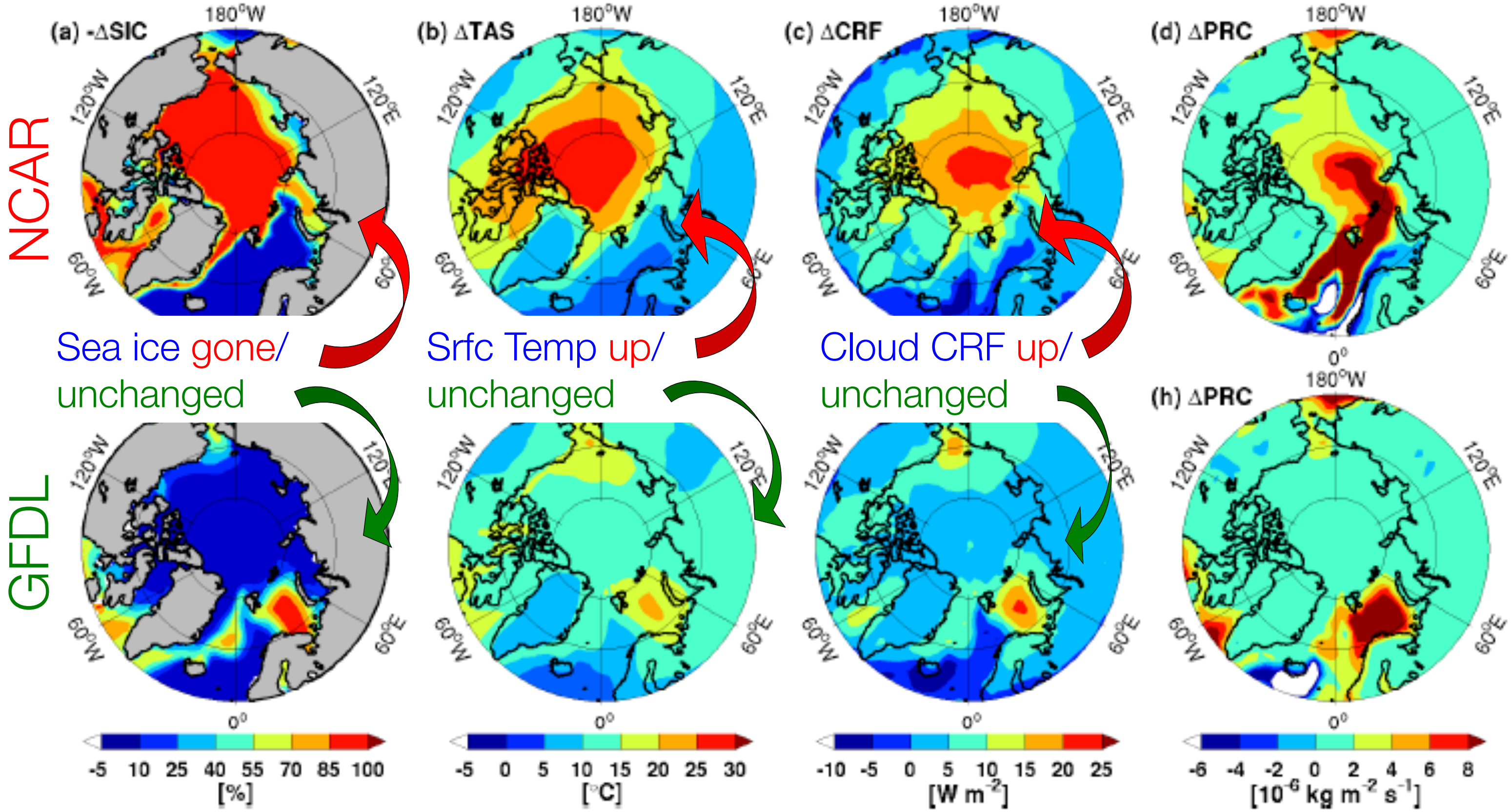

NCAR

GFDL

Sea ice gone/ unchanged

Srfc Temp up/ unchanged

Cloud CRF up/ unchanged

Enticing 3D IPCC Model Simulations

Consider the NCAR & GFDL 3d coupled ocean-atmosphere state-of-the-art (2009…) models, at x4 CO_2; anomaly from pre-industrial

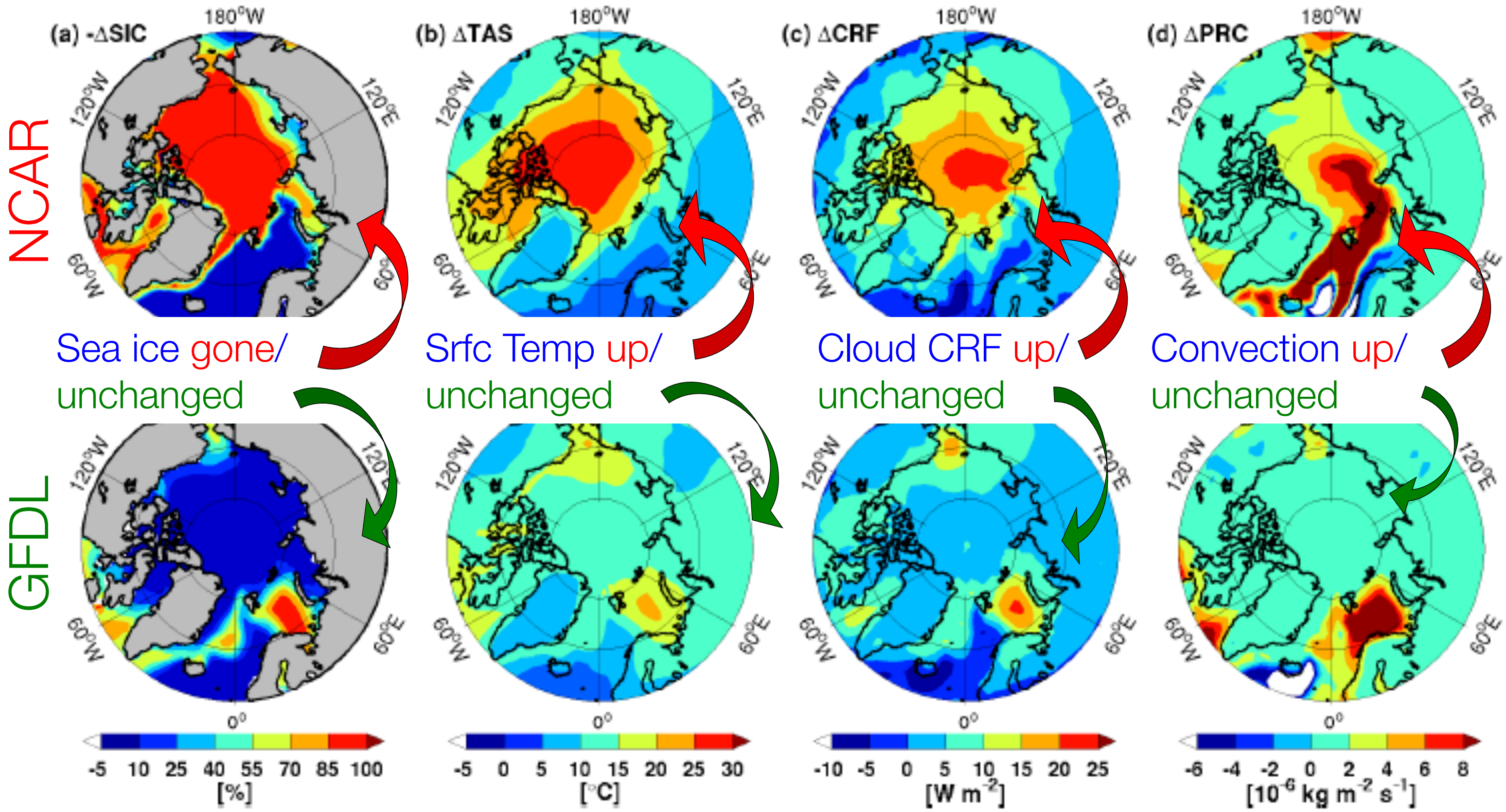

Sea ice gone/ unchanged

Srfc Temp up/ unchanged

Cloud CRF up/ unchanged

Convection up/ unchanged

Enticing 3D IPCC Model Simulations

Consider the NCAR & GFDL 3d coupled ocean-atmosphere state-of-the-art (2009…) models, at x4 CO_2; anomaly from pre-industrial

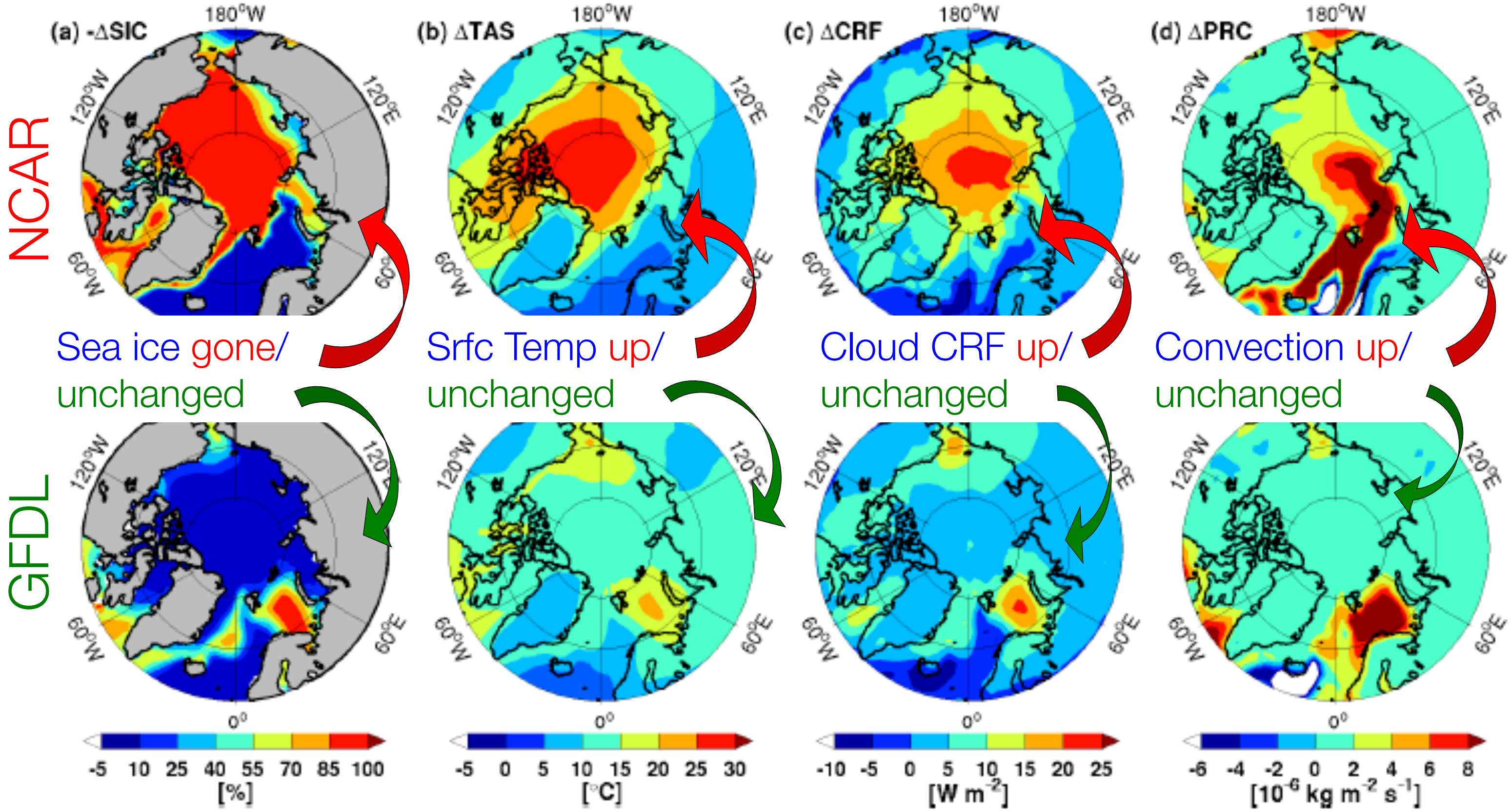
NCAR

GFDL

Sea ice gone/
unchanged

Srfc Temp up/
unchanged

Cloud CRF up/
unchanged

Convection up/
unchanged

➔ IPCC NCAR 3d model behaves like toy model!!

Enticing 3D IPCC Model Simulations

Consider the NCAR & GFDL 3d coupled ocean-atmosphere state-of-the-art (2009…) models, at x4 CO$_2$; anomaly from pre-industrial

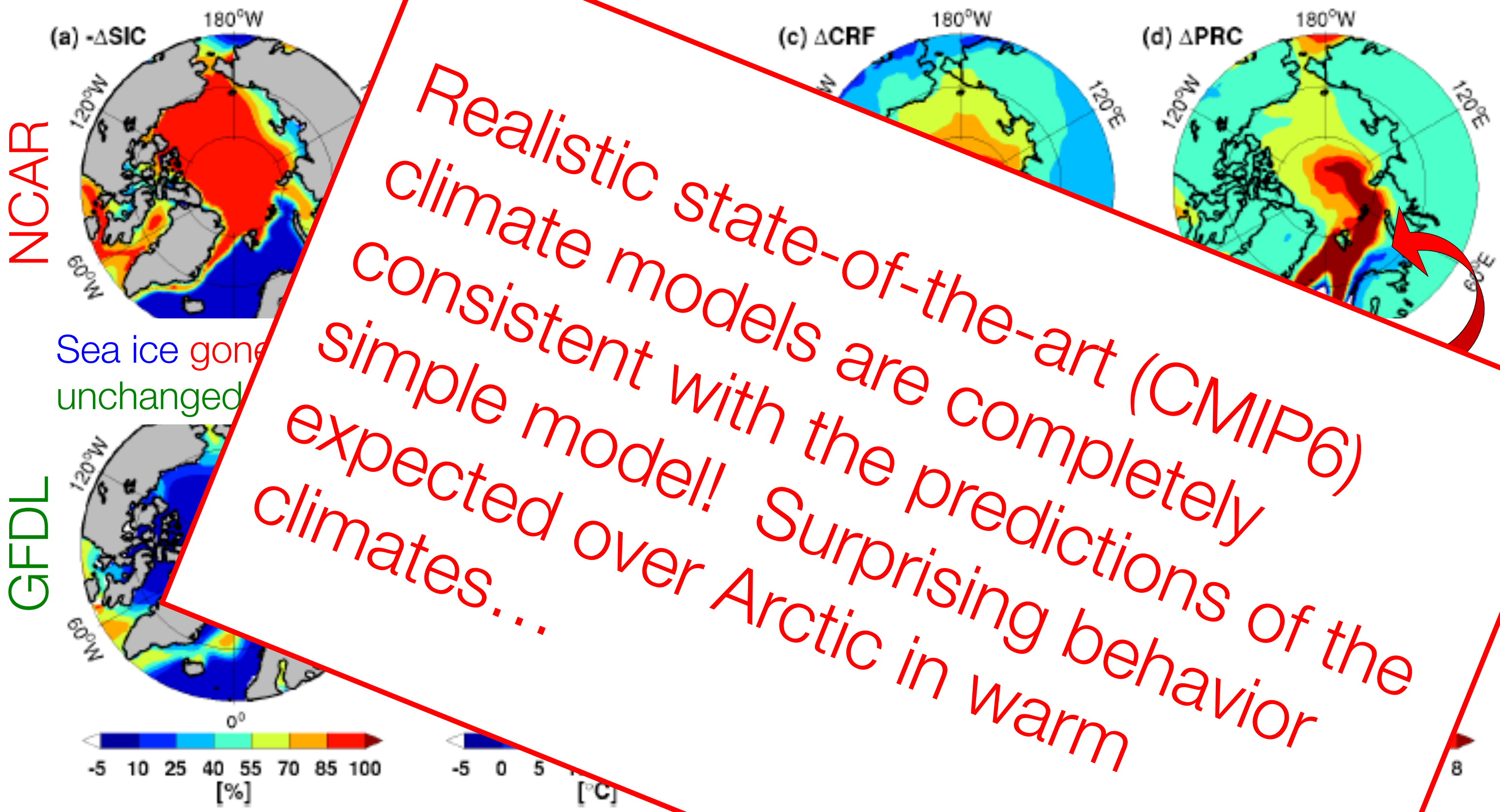

Sea ice gone
unchanged

Realistic state-of-the-art (CMIP6) climate models are completely consistent with the predictions of the simple model! Surprising behavior expected over Arctic in warm climates…

➔ IPCC NCAR 3d model behav del!!

In-class workshop

For each of the six mechanisms covered:

- What did we learn about the natural climate system regardless of the warm climate behavior?
- Come up with a one-minute summary of (two for polar stratospheric clouds, for the two versions there),
- Come up with a one-sentence summary of the weakness(es) of the proposed mechanism.

Equable climate summary

back to two initial overview slides with 6 mechanisms

The End